

BIOLOGICAL-PHYSICAL INTERACTIONS IN PACIFIC
CORAL REEF ECOSYSTEMS

A DISSERTATION SUBMITTED TO THE GRADUATE DIVISION OF THE UNIVERSITY
OF HAWAI'I AT MĀNOA IN PARTIAL FULFILLMENT OF THE REQUIREMENTS FOR
THE DEGREE OF

DOCTOR OF PHILOSOPHY

IN

OCEANOGRAPHY

DECEMBER 2013

By

Jamison M. Gove

Dissertation Committee:

Margaret A. McManus, Co-chairperson

Jeffrey C. Drazen, Co-chairperson

Craig R. Smith

Mark A. Merrifield

Alan M. Friedlander

ACKNOWLEDGEMENTS

I would like to express the utmost gratitude to Margaret McManus for the tremendous amount of advice, supervision, and assistance she gave me throughout this research. Her wisdom will stay with me for the rest of my life. I would like to thank my dissertation committee – Jeff Drazen, Mark Merrifield, Craig Smith and Alan Friedlander – for their invaluable scientific input and guidance. I would also like to thank Rusty Brainard for 12 years of support and for providing me with the amazing opportunity to dive throughout the Pacific researching some of the world's most incredible coral reef ecosystems.

In addition, I would like to thank the many individuals who contributed greatly to this research. Thank you to Gareth Williams who served as an important mentor, collaborator, and friend. Thanks to Oliver Vetter, Chip Young, Danny Merritt, and Ron Hoeke for not only being my closest friends in life, but for putting in ridiculously long hours in the field to help with data collection. Finally, thanks to Dave Foley, my original mentor who taught me so much about satellite oceanography.

I am especially thankful and indebted to my family who has given me a substantial amount of support and love. Particularly I would like to thank my mother, father, sister, and grandmother for being such a solid foundation throughout my life and for their invaluable advice and constant encouragement.

Lastly, I would like to thank my friends, who have played a crucial role in my happiness throughout this research and my life here in Hawai'i.

ABSTRACT

Coral reefs are some of the most diverse and productive marine ecosystems on earth. They are also among the most threatened by human disturbance. On a local scale, many of these systems are subject to over-fishing and land-based pollution, and on a global scale, these systems are impacted by climate change and ocean acidification: human activities clearly influence the structure of coral reef communities. However, before considering anthropogenic influence, it is necessary to consider the influence of local and regional environmental forcings on these ecosystems.

In this research, I investigate natural environmental and anthropogenic drivers of benthic community organization in 41 coral reef ecosystems across the Pacific (14.2°S – 28.4°N, 144.8°E – 155.4°W). These systems have been the focus of a long-term, multi-disciplinary NOAA-led monitoring effort. I present a new methodological approach to spatially constrain environmental forcings at the scale of individual islands and atolls. The results indicate considerable spatial heterogeneity in environmental forcings, namely sea surface temperature, waves, chlorophyll-a concentration (a proxy for phytoplankton biomass) and irradiance. Further examination of long-term (10-year) chlorophyll-a concentrations revealed sustained increased phytoplankton biomass just offshore of reefs compared to surrounding oceanic waters around a majority (91%) of islands and atolls, providing widespread evidence of the occurrence and scale of the “island mass effect”. Additionally, significant differences in horizontal gradients in chlorophyll-a between island and atoll systems were observed. Variations in reef area, bathymetric slope, geomorphic type (e.g. atoll *versus* island), and human population were identified as important drivers of increased phytoplankton biomass, together explaining 77% of the variability observed. In order to investigate biological-physical relationships at a smaller

spatial scale, I focused on one oceanic atoll with a history of minimal human influence, Palmyra Atoll (5.8°N, 162.1°W). At intra-island scales, wave forcing and reef geomorphology were important drivers of benthic community organization. Model performance improved when hard coral cover was modeled in distinct morphological groups (encrusting, plating, branching), highlighting the response of coral reef communities to extrinsic physical forcings. Superimposed on natural variations in coral reef benthic community organization are the effects of anthropogenic disturbance.

TABLE OF CONTENTS

Acknowledgements.....	ii
Abstract.....	iii
List of Tables.....	vi
List of Figures.....	vii
Chapter I: Introduction.....	1
Chapter II: Quantifying Climatological Ranges and Anomalies for Pacific Coral Reef Ecosystems.....	5
Chapter III: The Island Mass Effect: Explaining Enhanced Phytoplankton Biomass for Island Ecosystems Across the Pacific.....	42
Chapter IV: Intra-island Gradients in Physical Forcings Drive Spatial Patterning in Coral Reef Benthic Communities.....	72
Chapter V: Conclusions.....	115
References.....	121

LIST OF TABLES

2.1	General information for the 41 Pacific island and atoll coral reef ecosystems.....	30
3.1	General information on the islands and atolls used to study the island mass effect.....	60
3.2	List of biogeophysical drivers of increased phytoplankton biomass.....	61
3.3	Best-fit generalized linear model results for the island mass effect.....	61
4.1	Information on the physical environmental data collected from Palmyra Atoll.....	100
4.2	Summary of cold-pulses by mooring location around Palmyra Atoll.....	101
4.3	Significant drivers of benthic community structure around Palmyra Atoll.....	101

LIST OF FIGURES

2.1	Map highlighting the coral reef ecosystems of the U.S. Pacific.....	32
2.2	Spatially constrained chlorophyll-a at Pearl and Hermes Reef.....	33
2.3	Long-term mean of chlorophyll-a by data inclusion zone at Pearl and Hermes Reef.....	34
2.4	Map of long-term means in environmental forcings across the U.S. Pacific.....	35
2.5	Climatological ranges and anomalies for U.S. Pacific coral reef ecosystems.....	36
2.6	Principle component analysis of environmental forcings.....	37
3.1	Map of long term mean chlorophyll-a across the U.S Pacific.....	63
3.2	Spatially constrained long-term mean chlorophyll-a from Midway Atoll.....	63
3.3	Long-term mean of chlorophyll-a by data inclusion zone at Midway Atoll.....	64
3.4	Gradients in chlorophyll-a and biogeophysical predictors of the island mass effect.....	65
3.5	Long-term mean and <i>in situ</i> chlorophyll-a in the Hawaiian Archipelago.....	66
4.1	Map Palmyra Atoll in the northern Line Islands.....	103
4.2	Climatological and time series information for Palmyra Atoll.....	104
4.3	Current ellipses and dominant tidal frequencies at Palmyra Atoll.....	105
4.4	In situ temperature time series obtained from six locations at Palmyra Atoll.....	106
4.5	In situ temperature and current data highlighting an observed internal wave.....	107
4.6	Numerical wave model results representing maximum annual wave forcing.....	108
4.7	Spatial variability in benthic structure and environmental forcings around Palmyra.....	109
4.8	Partial dependency plots from ecological modeling of benthic functional groups.....	110

CHAPTER I

INTRODUCTION

Coral reefs are among the most diverse and productive marine ecosystems on earth. They provide economic benefits to millions of people as sources of food, employment, natural products, coastal protection and recreation (Knowlton 2001). Coral reef ecosystems are also among the most threatened by human disturbance, both at local scales due to over-fishing and land-based pollution, and on local to global scales owing to climate change and ocean acidification (Hughes et al. 2003; Knowlton and Jackson 2008). Despite the societal importance and susceptibility of reef systems to human impacts, until these contributions the intrinsic natural biological-physical relationships in coral reef ecosystems have not been well explored. Now, more than any other time in our history, effective ecosystem-based management and successful strategies to mitigate anthropogenic impacts to coral reef ecosystems require a fundamental understanding of the underlying abiotic-biotic interactions determining coral reef ecosystem function and health.

Coral reef ecosystems are influenced by a suite of physical, chemical and biological environmental forcings that are highly variable across time and space (Brown 1997; Done 1999). Over time, coral reefs have adapted to exist within an envelope of environmental forcings that is region-specific and governed in part by a reef's geographic location (Done 1999; Kleypas et al. 1999). Regional variation (hundreds to thousands of kilometers) in long-term environmental conditions drive spatial differences in coral reef communities (Brown 1997; Kleypas et al. 1999). Therefore, long-term gradients in environmental forcings should lead to clear spatial patterning in the benthic community as it organizes to adapt to local conditions (Hughes et al. 2012).

Human activity can also profoundly influence coral reef ecosystems (Knowlton 2001). Urbanization, coastal development and land-use can result in increased sedimentation and nutrient enrichment, resulting in reef degradation and coral mortality (Fabricius et al. 2005; Wooldridge 2009). Overfishing, particularly the depletion of herbivorous fishes, can alter competitive interactions within coral reef benthic communities (McCook et al. 2001) and lead to alternate benthic regimes (Hughes 1994; Nyström et al. 2000) as well as a loss of ecosystem structure and function (Done 1992; Jackson et al. 2001). Exacerbating the effects of local human impacts are global-scale changes that include ocean warming (Donner et al. 2007), ocean acidification (Caldeira and Wickett 2003), sea-level rise (Church and White 2006), and increased intensity of tropical cyclones (Emanuel 2005), each of which have considerable implications for the future of coral reef ecosystems (Donner 2009; Hoegh-Guldberg 2011; Knowlton and Jackson 2008). As one example, coral bleaching events – the loss of corals’ photosynthetic symbionts induced by thermal stress – are expected to increase with rising ocean temperatures (Hoegh-Guldberg et al. 2007). More frequent and severe bleaching events will result in lowered coral growth rates and reproductive output and compromise corals’ competitive abilities (Hoegh-Guldberg 1999). Human disturbance can fundamentally alter intrinsic biological-physical relationships in coral reef ecosystems, making it challenging to distinguish the ultimate drivers of shifts in community organization.

In this research, I seek to understand the biological-physical interactions in Pacific coral reef ecosystems, with emphases on environmental drivers of benthic community organization. Forty-one coral reef ecosystems in the Pacific, which are the focus the long-term Pacific Reef Assessment and Monitoring Program (Pacific-RAMP) led by NOAA’s Coral Reef Ecosystem Division (CRED), were studied. Pacific-RAMP surveys coral reefs that reside in disparate

oceanographic regimes and are exposed to varying levels of potential human impact. The study locations include the heavily populated and urbanized islands of Oahu, Guam, and Saipan, as well as some of the most isolated and functionally intact ecosystems in the Pacific, such as Kingman, Palmyra, Howland, Baker, and Jarvis. In total, CRED surveys over 41 island- and atoll-reef ecosystems that provide a unique opportunity to examine intrinsic biological-physical relationships in coral reef ecosystems – with and without human habitation.

In this dissertation, I first present a unique methodological approach to characterize environmental forcings at the scale of individual islands and atolls (Chapter II; Quantifying Climatological Ranges and Anomalies for Pacific Coral Reef Ecosystems). Specifically, I incorporate the following remotely sensed and modeled parameters; sea surface temperature (SST), wave energy, chlorophyll-*a* (proxy for phytoplankton biomass) and irradiance. Previous research has shown these parameters to be among the primary environmental drivers for spatiotemporal differences in coral reef communities (Done 1999; Freeman et al. 2012; Hughes and Connell 1999; Kleypas et al. 1999; Wooldridge 2009). Novel island- and atoll-scale environmental metrics are presented, enabling a comprehensive assessment of environmental forcings across 41 island and atoll Pacific coral reef ecosystems relative to each other.

Building upon these findings, I then explore spatial gradients in chlorophyll-*a* concentrations at each of the island- and atoll-reef ecosystems within our study region (Chapter III; The Island Mass Effect: Explaining Enhanced Phytoplankton Biomass for Island Ecosystems Across the Pacific). In particular, I investigate the ‘island mass effect’ – the enhancement in phytoplankton biomass near oceanic islands and atolls compared to surrounding waters (Doty and Oguri 1956). I utilized long-term (10-year) averages of satellite derived chlorophyll-*a* to evaluate the extent and persistence of increased phytoplankton biomass near study locations, and

investigated a suite of biogeophysical parameters to identify the proximate drivers of chlorophyll-*a* gradients between locations.

Finally, to examine intrinsic biological-physical relationships within an atoll-system, I focused on a single atoll – Palmyra – a remote, steep-sided, oceanic atoll that has been exposed to minimal human influence over the last half century (Chapter IV; Intra-island Gradients in Physical Forcings Drive Spatial Patterning in Coral Reef Benthic Communities). I assess the effects of key physical forcings on coral reef benthic community organization in the absence of confounding local human impacts. To address this overall goal, I quantified intra-island gradients in oceanographic conditions (currents, temperature, and waves) and spatial distributions of five benthic functional groups (hard coral, crustose coralline algae (CCA), macroalgae, turf algae, soft coral). I then examined the relationships between the benthic response variables (e.g. coral cover) and the environmental predictors, specifically wave forcing (i.e. bed shear stress) and reef geomorphological characteristics (i.e. reef slope, slope of slope, bathymetric position index).

Ascertaining the effects of both local- and regional-scale gradients in environmental forcings on coral reef communities is critically important. Understanding intrinsic biological-physical interactions in coral reef ecosystems will help contextualize coral reef community changes across space and through time. With increased understanding of both human and natural drivers of benthic community regimes, the scientific community can better predict how coral reef communities may change as a consequence of increased human population. Moreover, this information will aid in the prediction of potential changes in coral reef ecology owing to a changing climate, an indisputable aspect of future reef ecosystem dynamics.

CHAPTER II

**QUANTIFYING CLIMATOLOGICAL RANGES AND ANOMALIES FOR PACIFIC
CORAL REEF ECOSYSTEMS**

Jamison M. Gove^{1,2*}, Gareth J. Williams³, Margaret A. McManus⁴, Scott F. Heron^{5,6}, Stuart A. Sandin³, Oliver J. Vetter^{1,2}, David G. Foley^{1,7}

¹Joint Institute for Marine and Atmospheric Research, University of Hawai`i at Mānoa, Honolulu, Hawai`i, United States of America

²Coral Reef Ecosystem Division, NOAA Pacific Islands Fisheries Science Center, Honolulu, Hawai`i, United States of America

³Scripps Institution of Oceanography, University of California San Diego, San Diego, California, United States of America

⁴School of Ocean and Earth Science and Technology, University of Hawai`i at Mānoa, Honolulu, Hawai`i, United States of America

⁵Coral Reef Watch, NOAA National Environmental and Satellite, Data, and Information Service, Silver Spring, Maryland, United States of America

⁶Marine Geophysical Laboratory, Physics Department, School of Engineering and Physical Sciences, James Cook University, Townsville, Queensland, Australia

⁷Environmental Research Division, NOAA Southwest Fisheries Science Center, Pacific Grove, California, United States of America

Abstract

Coral reef ecosystems are exposed to a range of environmental forcings that vary on daily to decadal time scales and across spatial scales spanning from reefs to archipelagos.

Environmental variability is a major determinant of reef ecosystem structure and function, including coral reef extent and growth rates, and the abundance, diversity, and morphology of reef organisms. Proper characterization of environmental forcings on coral reef ecosystems is critical if we are to understand the dynamics and implications of abiotic–biotic interactions on reef ecosystems. This study combines high-resolution bathymetric information with remotely sensed sea surface temperature, chlorophyll-*a* and irradiance data, and modeled wave data to quantify environmental forcings on coral reefs. We present a methodological approach to develop spatially constrained, island- and atoll-scale metrics that quantify climatological range limits and anomalous environmental forcings across U.S. Pacific coral reef ecosystems. Our results indicate considerable spatial heterogeneity in climatological ranges and anomalies across 41 islands and atolls, with emergent spatial patterns specific to each environmental forcing. For example, wave energy was greatest at northern latitudes and generally decreased with latitude. In contrast, chlorophyll-*a* was greatest at reef ecosystems proximate to the equator and northernmost locations, showing little synchrony with latitude. In addition, we find that the reef ecosystems with the highest chlorophyll-*a* concentrations; Jarvis, Howland, Baker, Palmyra and Kingman, are each uninhabited and are characterized by high hard coral cover and large numbers of predatory fishes. Finally, we find that scaling environmental data to the spatial footprint of individual islands and atolls is more likely to capture local environmental forcings, as chlorophyll-*a* concentrations decreased at relatively short distances (>7 km) from 85% of our study locations. These metrics will help identify reef ecosystems most exposed to environmental

stress as well as systems that may be more resistant or resilient to future climate change.

Introduction

Coral reef ecosystems are exposed to a suite of physical, chemical and biological environmental forcings that are highly variable across time and space (Brown 1997; Done 1999). Environmental forcings influence coral reef ecosystem process and function, including coral reef extent and growth rates and the abundance, diversity, and morphology of reef organisms (Brown 1997). Over time, coral reefs have adapted to exist within a particular climatological range; an envelope of environmental forcings that is region-specific and governed by a reef's geographic location (Done 1999; Kleypas et al. 1999). Regional variation (hundreds to thousands of kilometers) in the climatological range is a major determinant of spatial differences in coral reef communities (Brown 1997) and how they respond to environmental forcings (McClanahan et al. 2007). Anomalous environmental forcings exceed the climatological range limits and are considered beyond a reef ecosystem's 'normal' or adapted range of environmental conditions (Kleypas et al. 1999). Anomalous environmental forcings have caused mass coral mortality and shifts in reef community structure (Barton and Casey 2005; Hoegh-Guldberg et al. 2005; Hughes and Connell 1999), even in the most remote parts of the world (Obura and Mangubhai 2011; Sheppard et al. 2008; Williams et al. 2010).

Previous research has focused on the characterization of environmental forcings that influence coral reef ecosystems across broad geographic areas (Couce et al. 2012; Freeman et al. 2012; Kleypas et al. 1999; Maina et al. 2011; Maina et al. 2008). Such studies have been important for establishing environmental limits to coral reef development (Kleypas et al. 1999), identifying broad geographic patterns in environmental habitats in which coral reefs reside

(Freeman et al. 2012; Lough 2012), and assessing the susceptibility of coral reefs to anomalies in environmental forcings on a global scale (Maina et al. 2011; Maina et al. 2008; Teneva et al. 2012). In many previous studies, (Couce et al. 2012; Freeman et al. 2012; Kleypas et al. 1999) environmental data were synthesized at $1 \times 1^\circ$ ($12,100 \text{ km}^2$); a coarse resolution when compared to the size of many of the islands and atolls in the Pacific. Research has shown environmental conditions such as productivity (Doty and Oguri 1956; Karnauskas and Cohen 2012) and temperature (Gove et al. 2006; Hendry and Wunsch 1973) proximate to islands can be distinct from regional conditions. Hence, downscaling is needed to better assess environmental forcings at the scale of individual island- and atoll-reef ecosystems.

Work to date that focused on the characterization of environmental conditions in which coral reefs reside has included a broad suite of environmental forcings (i.e. temperature, irradiance, chlorophyll-*a*, nutrients, aragonite saturation state, wind, currents, and sedimentation). However, wave energy, a major environmental forcing determining coral reef community patterns (Dollar 1982; Grigg 1983; Kilar 1989; Madin et al. 2006; Storlazzi et al. 2005), has been conspicuously absent. Gradients in wave energy and associated flow produce different levels of disturbance which, in turn, lead to changes in benthic community composition and coral morphology (Bradbury and Young 1981; Brown 1997; Madin et al. 2006; Reidenbach et al. 2006; Storlazzi et al. 2005). Wave energy can also mix the upper water column, reducing temperatures during warming events (Mcclanahan et al. 2005) and potentially enhancing surface nutrient availability (Wolanski and Delesalle 1995). Although larger, highly episodic wave events (i.e., generated by tropical cyclones) are also of great ecological relevance (Hughes and Connell 1999; Rogers 1993), including the prevailing wave climate would more thoroughly characterize the environmental conditions of coral reef ecosystems (Monismith 2007).

In recent decades it has become clear that coral reef communities are not only structured by natural environmental forcings, but also by human activities (Knowlton and Jackson 2008; Sandin et al. 2008). Global-scale forcing associated with human activity is driving ocean warming (Donner et al. 2007), ocean acidification (Caldeira and Wickett 2003), sea-level rise (Church and White 2006), and increased intensity of tropical cyclones (Emanuel 2005), each of which have profound implications for the future of coral reef ecosystems (Done 1999; Donner 2009; Donner et al. 2005; Hoegh-Guldberg 1999; Hoegh-Guldberg 2011; Hoegh-Guldberg et al. 2007; Knowlton and Jackson 2008). The resiliency of corals and their ability to adapt to future environmental conditions may be, in part, linked to their historical environmental climate (Carilli et al. 2012; Castillo et al. 2012; Donner 2011; Teneva et al. 2012; Williams et al. 2010). For example, Castillo et al., 2012 (Castillo et al. 2012) showed differences in coral growth based on oceanographic habitat, concluding that corals in more thermally variable environments may be better acclimatized and/or adapted to thermal stress than corals inhabiting more thermally stable environments. Such inductive reasoning may not apply to all environmental forcings. However, assessing a reef ecosystem's environmental setting as well as shorter-term environmental variability will provide insight into how these ecosystems may respond to future climate scenarios.

In this research, we build upon previous studies and present a unique methodological approach to characterize environmental forcings at the scale of individual islands and atolls. We incorporate the following remotely sensed and modeled parameters; sea surface temperature (SST), wave energy, chlorophyll-*a* (proxy for phytoplankton biomass) and irradiance. Previous research has shown these parameters to be among the primary environmental drivers for spatiotemporal differences in coral reef communities (Brown 1997; Done 1999; Fabricius 2005;

Freeman et al. 2012; Hughes and Connell 1999; Kleypas et al. 1999; Storlazzi et al. 2005; Wooldridge 2009). There are inherent limits to satellite-derived and modeled information (Eakin et al. 2010; Mumby et al. 2004); therefore, additional environmental forcings pertinent to coral reef communities (e.g. nutrients, aragonite saturation state, salinity, etc.) are presently unavailable at the resolution (spatial and/or temporal) required to calculate a robust island- and atoll-scale environmental setting for these properties.

Here, we target the U.S.-owned and affiliated reef ecosystems in the Pacific that are the focus of a long-term coral reef ecosystem monitoring program, NOAA's Pacific Reef Assessment and Monitoring Program (Pacific RAMP). Pacific RAMP surveys coral reefs that reside in disparate oceanographic regimes and that are exposed to varying levels of potential human impact. Locations include the heavily populated and urbanized islands of Oahu, Guam, and Saipan, as well as some of the most isolated and pristine reef ecosystems in the Pacific, such as Kingman, Palmyra, Howland, Baker, and Jarvis.

Using high-resolution bathymetric data, we spatially constrain and quality control environmental data across 41 islands and atolls that comprise the coral reef ecosystems of the U.S. Pacific (Figs. 1 – 3; Table 1). We then derive island- and atoll-scale metrics that quantify climatological range limits and the occurrence and magnitude of anomalous events (events that fall outside of the climatologic range) for each environmental forcing at each study location (Tables S1 – S6). We then present these metrics from a univariate perspective, to compare the latitudinal differences in climatological ranges and anomalies at all locations (Figs. 4 – 5, S1 – S4), and from a multivariate perspective, to more comprehensively assess environmental conditions of reef ecosystems relative to each other (Fig. 6).

Materials and Methods

Satellite-derived observations and model output of SST, wave height and period, chlorophyll-*a* and irradiance were used to develop time series data sets and quantify long-term means (Figs. 4, 6B; Table S1) climatological range limits (Figs. 5, 6A, 6C, S1 – S2; Tables S1, S3 – S6) and the magnitude and occurrence of anomalous events (Figs. 5, S3 – S4; Tables S2 – S6). The following describes the methodological approach to spatially constrain and quality control these data to characterize island and atoll (henceforth referred to as island for both) specific environmental forcing. Additional information pertaining to the quality control of each environmental data set is found in Appendix S1.

SST: Derived from the Pathfinder v5.0 dataset (<http://pathfinder.nodc.noaa.gov>, (Casey et al. 2010)), we quantified SST using a 0.0439° (hereafter 4-km) resolution weekly product for the 1985 – 2009 period (Heron et al. 2010). This product uses only night-time retrievals, consistent with NOAA’s Coral Reef Watch (CRW) thermal stress products. Data were excluded if deemed of poor quality (quality value < 4, (Kilpatrick et al. 2001)) or if individual pixels were masked as land. Missing data were filled with temporal interpolation for gaps of 3 weeks or less, beyond which gap filling may produce unrealistic temperature values based on the time-dependent variability of oceanic processes. Remaining gaps were filled by comparing ambient temperatures in adjacent pixels with the spatial pattern of climatological temperatures, setting the gap-value to match this identified pattern.

Island-specific SST time series data were produced by spatially averaging the individual 4-km pixels that were intersected by or contained within the 30-m bathymetric contour for each island. Several metrics were then derived to quantify thermal variability on coral reefs. Monthly climatological means were first calculated for each location from the weekly data. The maximum

monthly mean (the warmest of the 12 monthly values) served as the upper climatological range limit for each island, while the minimum monthly mean (the coldest of the 12 monthly values) provided the lower climatological range limit. Long-term mean SST was calculated by averaging all weekly data over the 25-year time series.

The *HotSpot* metric, developed by CRW, quantified the occurrence and magnitude of positive SST anomalies; i.e., SST values that exceeded the upper climatological range limit. The *ColdSpot* metric, developed here as an analogue to the HotSpot metric, quantified negative SST anomalies; i.e., SST values that were below the lower climatological range limit.

Waves: NOAA's Wave Watch III (WWIII; <http://polar.ncep.noaa.gov/waves>) is a global, full spectral wave model. We used WWIII one-degree spatial resolution, 3-hour output of mean significant wave height, dominant period, and direction from 1997 to 2010. Wave data were extracted from the one-degree grid cell in which each island location was located. Wave energy flux in kilowatts per meter (kW m^{-1}) was calculated for each time step for the full time series. Wave energy flux (henceforth referred to as wave energy) is shown in the following equation:

$$E_f = \frac{\rho g}{64\pi} H_s^2 T_p$$

where ρ is the density of seawater (1024 kg m^{-3}), g is the acceleration of gravity (9.8 m s^{-2}), H_s is mean significant wave height, and T_p is the dominant wave period. Although wave height is frequently used in ecological research and is often easier to contextualize, wave energy (given its dependence on wave period and wave height) is a more realistic estimate of wave forcing, and, therefore, a more ecologically relevant parameter with which to quantify wave impact (Storlazzi et al. 2003; Storlazzi et al. 2005).

Several wave metrics were developed to encapsulate the spatial and temporal patterns in wave forcing. Using the native 3-hour WWIII output, daily maximum and minimum wave

energy values were calculated for each island over the entire time series. Climatological values were then calculated by taking the maximum and minimum values over a 5-day temporal window, and then averaging these values (separately) for the same 5-day period over all years. A 5-day temporal window was chosen for these calculations because it captures the episodic nature of wave events and avoids averaging out the signal of potentially heterogeneous data. Upper and lower climatological range limits were obtained by taking the highest and lowest values from the maximum and minimum wave energy data sets, respectively. Long-term mean wave energy was calculated by averaging all 3-hour output values over the 14-year time series.

To quantify when wave forcing fell outside the climatological range, a novel *wave anomaly value (WAV)* metric was calculated by identifying all days that were above or below the upper and lower climatological range limits from the respective daily time series. Analogous to the HotSpot and ColdSpot metrics previously defined, the WAV metric quantified the occurrence and magnitude of anomalous wave events at each island.

Chlorophyll-a and Irradiance: Remotely sensed ocean color algorithms are calibrated for optically-deep waters, where the signal received by the satellite sensor originates from the water column without any bottom contribution. In our study region, optically-deep waters are typically deeper than 15 – 30 m (Mumby et al. 2004). In optically-shallow waters such as lagoons, regions within atolls, and most coral reef environments, bottom substrate properties and sediment suspension may affect light propagation, which increases marine reflectance and data quality issues when quantifying in-water constituents, such as chlorophyll-*a* (Boss and Zaneveld 2003).

Satellite-derived irradiance, specifically photosynthetically available radiation (PAR; defined as downwelling irradiance between 400 and 700 nm), is subject to similar data quality concerns. The data production algorithm (Carder 2003), in addition to a number of other quality

control steps, incorporates irradiance attenuation in the overall calculation of irradiance. Attenuation sources in the atmosphere include the absorption and scattering of irradiance as a result of concentrations of ozone, water vapor, and aerosols. Attenuation sources at the air-sea interface include reflection, associated with surface properties such as sea-surface roughness and levels of sea foam (Carder 2003). Optically-shallow areas are often wrongly interpreted as irradiance attenuation sources, thereby leading to spuriously low irradiance values (Carder 2003).

Eight-day, 0.0417° (hereafter 4-km) spatial resolution time series of chlorophyll-*a* (mg m^{-3}) and irradiance ($\text{Einsteins m}^{-2} \text{d}^{-1}$; henceforth $\text{E m}^{-2} \text{d}^{-1}$) products derived from Moderate Resolution Imaging Spectroradiometer (MODIS; <http://modis.gsfc.nasa.gov/>) were obtained for the July 2002 – May 2011 period. Taking into account the data-quality concerns described above, we developed a multistep masking routine to remove contaminated data pixels. Following Maina et al., 2011 (Maina et al. 2011), we used the 30-m contour as the cutoff for pixel inclusion; all pixels inshore of the 30-m isobath were identified (Fig. 2A) and removed from the data set prior to analysis (Fig. 2B). This step, however, is not sufficient to ensure error-free chlorophyll-*a* and irradiance data sets, because pixels outside the 30-m isobath may still contain biased information associated with optically-shallow waters. This occurs because data pixels are box-like in shape and are georeferenced at their center point; thus, information contributing to any single pixel value is collected up to one-half a pixel diagonal distance away. To address this, we created a data exclusion zone of one-half a pixel diagonal in length (0.0295° or $\sim 3.27 \text{ km}$) everywhere perpendicular to the 30-m isobath, with all pixels on or within this zone also removed from the data set (Fig. 2C).

To determine the spatial domain that best represented island-scale chlorophyll-*a*, a series

of spatially expanding, non-overlapping data inclusion zones were created for each island, with the width of each zone set at half the pixel diagonal. At all island locations, chlorophyll-*a* concentrations were compared between zones by taking the long-term mean for each pixel and calculating the average (\pm standard error) of all pixels within a given zone. In total, 6 zones were analyzed at each island representing distances 3.27 – 6.54 km to 19.62 – 22.89 km away from the 30-m bathymetric contour (see Fig. 3 for example). At 35 of the 41 locations, the zone most proximate to the island (zone one: 3.27 – 6.54 km from the 30-m contour) showed the highest concentration of chlorophyll-*a*, thereby capturing the signal most indicative of the island. These same pixels were used to represent the irradiance data set.

A series of metrics were derived using the masked, spatially constrained, and quality controlled chlorophyll-*a* and irradiance time series data sets. Eight-day climatological values were calculated by averaging all same 8-day time periods from each year over all years. The maximum and minimum island-specific climatological values were used as the upper and lower climatological range limits of chlorophyll-*a* and irradiance. Long-term mean chlorophyll-*a* and irradiance values were calculated by averaging all data over the entire time series from July 2002 to May 2011 for each location.

Analogous to the thermal and wave energy metrics previously described, we quantified the magnitude and occurrence of chlorophyll-*a* and irradiance values above and below their respective climatological range limits. This created *chlorophyll-a anomaly value (CAV)* and *irradiance anomaly value (IAV)* metrics.

Bathymetry: Gridded multi-beam bathymetric data were collected during Pacific RAMP surveys and provided by the Pacific Islands Benthic Habitat Mapping Center (<http://www.soest.hawaii.edu/pibhm>).

Data Manipulation and Statistical Analysis

Wave, chlorophyll-*a*, and irradiance data were analyzed and manipulated using Matlab R2010a (<http://www.mathworks.com>). SST data were analyzed using IDL v8.0 (<http://www.exelisvis.com/language/en-US/ProductsServices/IDL.aspx>). Thirty-meter depth contours were derived using ArcGIS 9.3. A one-way analysis of variance (ANOVA) with a post-hoc Tukey comparison test was used to test the difference in long-term means, climatological range limits and average annual anomalies for all regions and pair-wise for each of the 10-pair combinations. Principle Component Analysis (PCA) of normalized data was used to explore similarities in environmental forcings across all islands and regions. Similarity Profile (SIMPROF) analysis (Clarke et al. 2008) was used to test the presence of island groupings within each of the environmental metrics used in the PCA. The SIMPROF analyses were based on 9999 permutations at the 1% significance level, resulting in a significance of $p < 0.0001$. ANOVA and Tukey comparisons tests were conducted in Matlab. PCA and SIMPROF analyses were conducted in PRIMER V6 (Clarke and Gorley 2006).

Results

Climatological range limits and long-term means for SST, wave energy, chlorophyll-*a*, and irradiance along with associated metrics quantifying the magnitude and occurrence of anomalous events; HotSpot & ColdSpot, WAV, CAV and IAV, respectively, are shown for all islands from the Northwestern Hawaiian, Hawai'i, Mariana, Equatorial and Samoa regions (Figs. 4 – 6, S1– S4; Tables S1 – S6). Anomaly metrics were calculated as an annual average and are presented as a percentage of time above (positive anomaly) or below (negative anomaly) the

upper and lower climatological range limit (Figs. 5, S3 – S4). For example, at Kure Atoll, the lower climatological range limit in SST is 18.98 °C. In an average year (over the 25-year record), SST at Kure Atoll was anomalously cold (colder than 18.98 °C) 6% of the year, or roughly 3 weeks a year.

To effectively compare latitudinal changes in climatological range limits and anomalies, Figure 5 presents islands in decreasing latitude (from north to south) from left to right. Hawai'i Island, and Johnston and Wake Atolls, however, are oriented according to geographic proximity to a region as opposed to strict latitudinal orientation. Hawai'i Island is relatively close (48 km) to Maui, while Johnston Atoll is located 1,300 km southwest of Oahu; both locations are geographically aligned with the Hawaiian Archipelago. Wake Atoll is most proximate to the Mariana region and is therefore placed after Johnston Atoll and before Farallon de Pajaros. There is less than a 4° latitudinal deviation between the geographic based island sequence in Figure 5 and the actual latitudinal sequence of islands (see Table 1 for specific geographic coordinates).

Climatological Ranges and Anomalies

SST: Long-term mean SST was significantly different among regions ($F_{4,36} = 122.2$, $p < 0.00001$) except when comparing each of the Mariana, Samoa and Equatorial regions ($p < 0.05$; Fig. 4A; Table S1). The Northwestern Hawaiian region was characterized by relatively low long-term mean SST (mean \pm se: 24.25°C \pm 0.25), particularly at northern-most latitudes, while the Samoa region had the highest long-term SST (28.42°C \pm 0.11).

Upper climatological range limits of SST differed between regions ($F_{4,36} = 161.82$, $p < 0.00001$). Most regions were different from each other ($p < 0.05$) with the exception of the Northwestern Hawaiian and Hawai'i regions, and when comparing each of the Mariana, Samoa

and Equatorial regions (Figs. 5A, S1; Tables S1, S3). Across all regions, a Pacific-wide dichotomous pattern in upper climatological range limits was observed; the Northwestern Hawaiian and Hawai'i regions had similar upper limits ($26.64^{\circ}\text{C} \pm 0.05$ and $26.71^{\circ}\text{C} \pm 0.13$, respectively), as did the Mariana, Equatorial, and Samoa regions ($28.79^{\circ}\text{C} \pm 0.03$, $28.48^{\circ}\text{C} \pm 0.21$, $28.93^{\circ}\text{C} \pm 0.06$, respectively). Jarvis Island (Equatorial region), an obvious outlier in the observed split pattern, showed an upper limit that was 0.82°C colder than the region mean. Lower climatological range limits also differed between regions ($F_{4,36} = 67.3$, $p < 0.0001$), with all regions differing ($p < 0.05$) except comparisons between the Mariana, Samoa, and Equatorial regions. Lower climatological range limits were coldest in the Northwestern Hawaii region ($21.24^{\circ}\text{C} \pm 0.52$) and increased with each subsequent region from Hawai'i ($24.01^{\circ}\text{C} \pm 0.16$), to Mariana ($26.18^{\circ}\text{C} \pm 0.16$), to Equatorial ($27.19^{\circ}\text{C} \pm 0.17$), to Samoa ($27.24^{\circ}\text{C} \pm 0.17$).

When comparing the climatological range across all islands, a narrowing pattern was observed from Kure ($\Delta 7.46^{\circ}\text{C}$) to Jarvis ($\Delta 1.14^{\circ}\text{C}$), and then a slight broadening pattern from Swains ($\Delta 1.18^{\circ}\text{C}$) to Rose Atoll ($\Delta 1.89^{\circ}\text{C}$). The observed variations in the climatological range were principally a result of variability in the lower climatological range limit.

Average annual HotSpots (positive SST anomalies) were significantly differently between regions ($F_{4,36} = 21.57$, $p < 0.00001$), with the same regions having distinct average annual anomalies as had distinct upper climatological range limits in SST ($p < 0.05$; Figs. 5A, S3; Tables S2 – S3). The Equatorial region had the greatest average annual HotSpots ($29.24\% \pm 5.03$), followed by the Samoa ($29.10\% \pm 1.13$) and Mariana ($28.75\% \pm 1.16$) regions. HotSpots in the Northwestern Hawaiian ($15.64\% \pm 0.39$) and Hawai'i ($14.37\% \pm 0.45$) regions did not differ from each other but had much lower values (approximately half) and were significantly ($p < 0.05$) different from HotSpots in the Equatorial, Mariana, and Samoa regions. Average annual

ColdSpots (negative SST anomalies) also differed between regions ($F_{4,36} = 75.25$, $p < 0.0001$) and were greatest in the Equatorial region ($25.25\% \pm 2.47$; $p < 0.05$; Figs. 5A, S4; Tables S2 – S3). All other regions experienced comparatively low average annual ColdSpots ($< 11\%$ of the year).

Wave Energy: Long-term mean wave energy was significantly different between regions ($F_{4,36} = 68.93$, $p < 0.0001$) except between the Hawai'i and Equatorial regions, and when comparing Samoa with the Mariana and Equatorial regions ($p < 0.05$; Fig. 4B; Table S1). The Northwestern Hawaiian region was characterized by the highest long-term wave energy ($41.97 \text{ kW m}^{-1} \pm 1.08$), while the Mariana region had the lowest long-term wave energy ($19.84 \text{ kW m}^{-1} \pm 0.77$).

Upper climatological range limits in wave energy were significantly different between regions ($F_{4,36} = 105.23$, $p < 0.0001$), with the greatest upper limits observed in the Northwestern Hawaiian region ($309.36 \text{ kW m}^{-1} \pm 16.16$; $p < 0.05$; Fig. 4b; Tables S1, S4). The northern three islands within the Northwestern Hawaiian region; Kure ($370.18 \text{ kW m}^{-1} \pm 73.48$), Midway ($367.42 \text{ kW m}^{-1} \pm 71.74$) and Pearl and Hermes Reef ($364.45 \text{ kW m}^{-1} \pm 68.37$), had the greatest upper climatological range limits; ~ 2.5 times greater than islands within the Hawai'i region (e.g., Oahu $151.12 \text{ kW m}^{-1} \pm 21.43$) and 5 – 7 times greater than all other islands in this study. It should be noted, however, that the Mariana and Samoa regions are located in areas of the Pacific that experienced tropical cyclones on an annual to interannual basis, which generated positive WAV values that were 10 times greater or more than the regional average. Lower climatological range limits in wave energy were also significantly different between regions ($F_{4,36} = 80.59$, $p < 0.0001$), with all regions differing from each other ($p < 0.05$) with the exception of the Northwestern Hawaiian and Hawai'i regions, and the Equatorial and Samoa regions.

Average annual positive WAVs (positive wave anomalies) were significantly different between regions ($F_{4,36} = 38.39$, $p < 0.0001$) but were generally low across all regions ($< 5\%$; Fig. 4b; Tables S2, S4). Average annual negative WAVs (negative wave anomalies) were also significantly different between regions ($F_{4,36} = 21.42$, $p < 0.0001$) and were generally greater (5 – 11% of the year at all locations) than positive WAVs (Figs. 5B, S4). Thus, in an average year, there were more days with anomalously low wave energy than days with anomalously high wave energy.

Chlorophyll-a: Long-term mean chlorophyll-*a* was significantly different between regions ($F_{4,36} = 59.55$, $p < 0.0001$) with the exception of the Mariana and Samoa regions and when comparing Hawai'i with the Northwestern Hawaiian and Samoa regions ($p < 0.05$; Fig. 4C; Table S1). Long-term mean chlorophyll-*a* was greatest in the Equatorial region ($0.1672 \text{ mg m}^{-3} \pm 0.0175$); between 1.8 – 3.4 times greater than long-term chlorophyll-*a* in each of the other regions.

Upper climatological range limits in chlorophyll-*a* were also significantly different between regions ($F_{4,36} = 50.01$, $p < 0.0001$). Most regions differed from each other ($p < 0.05$) with the exception of Hawai'i and Samoa, and Mariana and Samoa (Figs. 5C, S1; Tables S1, S5). The Equatorial region had the greatest upper climatological range limit ($0.2350 \text{ mg m}^{-3} \pm 0.0175$, $p < 0.05$), with Jarvis ($0.2913 \text{ mg m}^{-3} \pm 0.0757$), Howland ($0.2432 \text{ mg m}^{-3} \pm 0.0213$), and Baker ($0.2410 \text{ mg m}^{-3} \pm 0.0493$) characterized by the greatest upper climatological range limits of all study locations. Kure Atoll ($0.206 \text{ mg m}^{-3} \pm 0.0362$), the northern-most island of the study, had an upper climatological range limit approximately equal to the upper limit at Palmyra Atoll ($0.186 \text{ mg m}^{-3} \pm 0.0083 \text{ mg m}^{-3}$) and Kingman Reef ($0.213 \text{ mg m}^{-3} \pm 0.005$), despite the 22° of latitude or $\sim 2,420$ km separating Kure (28.42°N , -178.33°W) from Palmyra (5.88°N , -

162.09°W) and Kingman (6.39°N, -162.38°W). Lower climatological range limits were also significantly different between regions ($F_{4,36} = 19.32, p < 0.0001$), with most regions differing ($p < 0.05$) with the exception of Northwestern Hawaiian and Hawai'i, and Samoa when compared to the Hawai'i and Mariana regions. The Equatorial region not only had the greatest upper climatological limit in chlorophyll-*a*, but also had the greatest lower climatological limit ($0.1120 \text{ mg m}^{-3} \pm 0.0237 \text{ mg m}^{-3}, p < 0.05$). The islands in this region therefore experience relatively high annual productivity when compared to the other study locations.

Average annual positive CAVs (positive chlorophyll-*a* anomalies) were not significantly different ($F_{4,36} = 0.94, p = 0.45$; Fig. 4c; Tables S2, S5) and were low across all regions (5.50 – 9.12%). Average annual negative CAVs (negative chlorophyll-*a* anomalies) were generally greater (7.58 – 15.29%) and were significantly different between regions ($F_{4,36} = 5.06, p = 0.0024$), with the Hawai'i and Samoa regions differing, and the Equatorial region differing from all regions except the Northwestern Hawaiian region ($p < 0.05$).

Irradiance: Long-term mean irradiance values differed between regions ($F_{4,36} = 2.96, p = 0.0325$), although the only paired-wise comparison that differed was between the Northwestern Hawaiian and Equatorial region ($p < 0.05$; Fig. 4D; Table S1). Both across and within the regions, long-term mean irradiance showed little spatial heterogeneity with the exception of the Equatorial region, which had both the highest ($50.1 \text{ E m}^{-2} \text{ d}^{-1}$) and lowest ($39.05 \text{ E m}^{-2} \text{ d}^{-1}$) island mean irradiance values.

Upper ($F_{4,36} = 14.11, p < 0.0001$) and lower ($F_{4,36} = 19.71, p < 0.0001$) climatological range limits in irradiance were significantly different between regions (Figs. 5D, S1, S2; Tables S1, S6). Across all islands in the Northwestern Hawaiian, Hawai'i and Mariana regions, the climatological range exhibited a narrowing pattern with latitude, ranging from $\Delta 33.75 \text{ E m}^{-2} \text{ d}^{-1}$

at Kure to $\Delta 18.08 \text{ E m}^{-2} \text{ d}^{-1}$ at Guam. In addition, the Equatorial region contained islands with the lowest upper climatological limits (Kingman, $45.11 \text{ m}^{-2} \text{ d}^{-1} \pm 1.08$; Palmyra, $46.72 \text{ m}^{-2} \text{ d}^{-1} \pm 1.03$) as well as islands with the highest lower climatological range limits (Jarvis, $42.36 \text{ E m}^{-2} \text{ d}^{-1} \pm 0.94$; Howland, $43.12 \text{ E m}^{-2} \text{ d}^{-1} \pm 2.04$; Baker, $44.20 \text{ E m}^{-2} \text{ d}^{-1} \pm 2.69$) when compared to all other islands in each of the regions.

Average annual positive and negative IAVs (positive and negative irradiance anomalies, respectively) were significantly different between regions ($F_{4,36} = 19.88, p < 0.0001$ and $F_{4,36} = 11.51, p < 0.0001$, respectively; Figs. 5D, S3 – S4; Tables S1, S6). Average annual positive IAVs increased with each subsequent region from Northwestern Hawaiian to Samoa; however, only the Northwestern Hawaiian, Hawai'i and Mariana regions when each compared to the Equatorial and Samoa regions were significantly different, with the former regions greater than the latter ($p < 0.05$). When comparing islands across all regions, a majority (85%) of islands had higher average annual positive IAVs than negative IAVs.

PCA and SIMPROF Results

PCA on upper climatological range limits indicated wave energy and SST as the major loadings of PC1 (59.3% of variation explained) and chlorophyll-*a* and irradiance as the major loadings of PC2 (26.2% of variation explained; Fig. 6A). PCA of upper limits resulted in islands clustering by region, with little overlap of islands among different regions. However, the SIMPROF analyses overlaid on the PCA (dashed lines) resulted in four distinct groupings ($p < 0.0001$). Pearl and Hermes, Midway and Kure of the Northwestern Hawaiian region formed a unique group, whereas the remaining islands within the Northwestern Hawaiian region (Maro, Lisianski, Laysan, French Frigate Shoals, Necker and Nihoa) grouped with much of the Hawai'i

region (Niihau, Kauai, Oahu, Molokai, Lanai, and Oahu). Hawai'i Island and Johnston Atoll grouped with islands from the Samoa and Mariana regions. All islands within the Equatorial region grouped together, the only geographic region to be statistically grouped together.

PCA of long-term mean values also indicated wave energy and SST as the major loadings of PC1 (53.8% variation explained) and chlorophyll-*a* and irradiance as the major loadings of PC2 (33.8% variation explained; Fig.6B). PCA of means clustered the Mariana and Samoa regions together, while islands from Hawai'i and Northwestern Hawaiian regions were less clustered, primarily separating along PC1. Jarvis, Howland and Baker clustered together, well removed from other islands. Kingman and Palmyra were clustered in proximity to islands within the Hawai'i region. The SIMPROF analysis indicated greater complexity of island clustering than inferred from the PCA, with a total of 7 distinct groups ($p < 0.0001$). The Samoa and Mariana (save Wake) regions formed a group, as did islands from the Hawai'i region along with Wake and Nihoa, Necker, and French Frigate Shoals of the Northwestern Hawaiian region. Distinct groups also included: Howland, Baker and Jarvis (Equatorial); Kingman and Palmyra (Equatorial); Laysan, Lisianski, and Maro (Northwestern Hawaiian); Midway and Kure (Northwestern Hawaiian); and Pearl and Hermes (Northwestern Hawaiian).

Unlike the PCA results from upper climatological range limits and long-term means, a PCA based on the lower climatological range limits indicated irradiance and SST as the major loadings of PC1 (49.8% of variation explained) and chlorophyll-*a*, SST and wave energy as the primary loadings of PC2 (30.3% of variation explained; Fig. 6C). PCA of lower limits resulted in islands from different regions clustering in close proximity to each other. For example, Kingman, Palmyra and Johnston clustered with the Samoa region, while much of the Hawai'i region clustered with the Northwestern Hawaiian region. Jarvis, Howland, and Baker islands clustered

well apart from all other islands, as did Pearl and Hermes, Kure and Midway Atolls. The SIMPROF analysis resulted in seven distinct groups ($p < 0.0001$). The Mariana region was divided into three separate groups: islands geographically located from Guam to Sarigan; from Guguan to Farallon de Pajaros; and Wake Atoll. Islands from the Samoa region were grouped with Johnston (Hawai'i) and Kingman and Palmyra (Equatorial). Other lower limit groupings were: Jarvis, Howland and Baker (Equatorial); Pearl and Hermes, Midway and Kure (Northwestern Hawaiian); and Laysan, Lisianski, Maro, French Frigate Shoals, Necker, and Nihoa (Northwestern Hawaiian) with islands from the Hawai'i region (save Johnston).

Discussion

Our analyses suggest considerable spatial heterogeneity in climatological ranges across U.S. Pacific coral reef ecosystems (Figs. 4 – 6, S1 – S2; Tables S1 – S6). The emergent spatial patterns and the degree of variability in upper and lower climatological range limits of SST, wave energy, chlorophyll-*a* and irradiance were unique for each environmental forcing, with no obvious or clear common spatial patterns across forcings. For example, upper climatological range limits in wave energy followed an overall trend with latitude; islands located farther north (i.e., Kure and Midway) showed higher upper limits of wave energy compared to islands located farther south (i.e., Swains and Tutuila), with the change in wave energy between island locations reducing with decreasing latitude (Figs. 5B, S1). In contrast, the upper climatological range limit for chlorophyll-*a* concentration exhibited a complex spatial pattern that appeared to be influenced by a combination of region and island specific environmental forcings (Figs. 5C, S1). For example, Jarvis, Howland and Baker Islands are located on the equator and had the highest upper climatological range limits of all the islands examined. The upper climatological range

limit at Jarvis Island, and presumably at Howland and Baker Islands, is driven by regional thermocline variability and by a unique localized upwelling phenomenon created by island-current interactions (Gove et al. 2006) that increase nutrient availability and enhance local productivity (Miller et al. 2008). Kure Atoll was also characterized by a relatively high upper climatological range limit of chlorophyll-*a*, though this atoll is located 28° (3,080 km) to the north of Jarvis Island. Kure Atoll is likely influenced by local conditions, but also by proximity to the Transition Zone Chlorophyll Front (TZCF); a basin-wide chlorophyll front located at the boundary between the subtropical and subpolar gyres that migrates southward in the winter months to the latitude of the atoll (Polovina et al. 2001). Hence, the spatial patterns are unique for each environmental forcing.

The PCA and SIMPROF analyses revealed two important findings when comparing the environmental setting across the study region (Fig. 6). First, different environmental metrics can lead to differences in the environmental setting. For example, when comparing upper climatological range limits, Palmyra and Kingman Atolls had a similar environmental setting when compared to Jarvis, Howland, and Baker Islands (Fig. 6A). However, when comparing long-term means (Fig. 6B) and lower climatological range limits (Fig. 6C), Palmyra and Kingman grouped either independently or with islands from a different region entirely. Hence, careful consideration of the appropriate environmental metric must be made, as the choice of metric can have considerable bearing on interpretation of the environmental setting at individual island and atoll reef ecosystems. Second, geographic proximity was not a prerequisite for similarities in the environmental setting. When comparing long-term means (Fig. 6B), environmental conditions at geographically separate locations were found to be similar. For example, all locations within the Samoa region grouped with the Mariana region despite a

~6,000 km distance between the 2 archipelagos. Conversely, environmental conditions at geographically proximate locations were found to be different. For example, in the SIMPROF analysis, Midway and Pearl and Hermes Reef grouped separately despite being separated by only ~150 km.

We also find that the spatial scale in which environmental data are synthesized can substantially affect the quantification of environmental forcings. Previous research synthesized data on a $1 \times 1^\circ$ (~12,100 km²) spatial grid (Couce et al. 2012; Freeman et al. 2012; Kleypas et al. 1999) and/or grouped numerous islands across large ocean provinces (Freeman et al. 2012; Maina et al. 2011). Our study encompassed 41 islands and atolls, many of which are completely isolated and are 1.13 – 8254 times smaller in area (land + reef area; Table 1) than a 12,100 km² grid cell. When comparing expanding spatial footprints of data inclusion, we found that chlorophyll-*a* concentrations decreased at relatively short distances (>7 km; Fig. 3) from 85% of our study locations. Hence, proportionally scaling environmental data to the study location (as opposed to using large, spatial grids) is more likely to capture local environmental forcings that may be pertinent to coral reef ecosystem dynamics.

The spatial patterns in chlorophyll-*a* concentration observed here have important implications for coral reef research. Chlorophyll-*a* has been used as an indicator of stress inducing environmental conditions to coral reefs (Maina et al. 2011), serving as a proxy for eutrophic conditions, which can affect the thermal tolerance of corals (Wooldridge 2009), and as a proxy for increased turbidity and sedimentation, which can result in coral mortality (Fabricius 2005). In general, these studies are geographically specific and associate high levels of chlorophyll-*a* with poor water quality, attributable to anthropogenic influences. In this study, the islands with the highest chlorophyll-*a* concentrations; Jarvis, Howland, Baker, Palmyra and

Kingman, are each uninhabited and are characterized by high hard coral cover and large numbers of predatory fishes (Sandin et al. 2008; Vroom et al. 2010; Williams et al. 2011). Thus, natural elevated levels of chlorophyll-*a* may serve to positively influence coral reef ecosystems, possibly through increased food availability (i.e., phytoplankton) for primary consumers (Leichter et al. 1998), or through enhanced nutrient levels, important for sessile benthic organisms such as corals and algae (Leichter and Genovese 2006; Leichter et al. 2007; Leichter et al. 2003; Smith et al. 2004).

Assessing climatological conditions and the history of anomalies may provide insight into coral reef ecosystem response to future climate scenarios. For example, history of exposure to positive SST anomalies may serve to enhance physiological tolerance (i.e., acclimation) of corals to resist future bleaching (Castillo et al. 2012; Donner 2011; Teneva et al. 2012) or possibly increase survival of corals through natural selection (i.e., adaptation) (Smith-Keune and Van Oppen 2006; Visram and Douglas 2007). Island and atoll reef ecosystems influenced by enhanced upwelling could possibly serve as refugia for coral reef ecosystems by mitigating the extent of future increases in ocean temperatures (Karnauskas and Cohen 2012). Also, reef ecosystems subject to a high annual wave energy may have increased susceptibility to coral breakage in the future (Erez et al. 2011), given projected changes in ocean chemistry and associated impacts to coral calcification (Hoegh-Guldberg et al. 2007).

Despite the broad applicability of the environmental forcing metrics presented here, we acknowledge that there are some limitations. First, environmental forcing can have considerable spatial heterogeneity on intra-island scales (Monismith 2007). This intra-island variability is not captured in these mesoscale analyses. ‘Tuning’ these metrics to the intra-island scale is the focus of our subsequent research. Second, despite our attempts to produce metrics that are

representative of environmental conditions on coral reefs, satellite-derived environmental data can differ from in-situ, reef level measurements (Sheppard 2009). Third, although we feel the use of deep-water wave information is a good, first-order approximation of wave forcing on coral reefs (Storlazzi et al. 2001), waves are highly complex as a result of refraction, dissipation, and other wave-bathymetry interactions (Storlazzi et al. 2005), leading to potential differences between nearshore wave forcing and the wave metrics presented in this research. Fourth, this research is limited to locations with bathymetric data at the resolution needed to clearly identify the 30-m contour. Future work will explore the feasibility of using remotely sensed, depth-flagged grid cells (Maina et al. 2011) to include a greater number of coral reef ecosystems throughout the Pacific. A final limitation pertains to climatological range calculations, as the data set lengths for irradiance, chlorophyll-*a* and waves are temporally limited (< 15 years), hindering the calculation at time-scales that are likely relevant to biological adaptation.

Despite these limitations, this research provides an important environmental context for which to compare coral reef communities across the U.S. Pacific coral reef ecosystems. It is our hope that the results of this study will help to elucidate the differential importance of environmental forcings to coral reef communities in this region, fostering more targeted ecosystem research and aiding in the formulation of effective ecosystem-based management practices. It is also our hope this research will aid in the prediction of potential changes in coral reef ecology owing to a changing climate, an indisputable aspect of future reef system dynamics.

Acknowledgments

We would like to thank the following individuals for their important contributions to this work: Rusty Brainard, Alan Friedlander, Jeff Drazen, Mark Merrifield, Craig Smith, Eric

Franklin, Lucas Moxey, and Rachel Morrison. We also thank the two anonymous reviewers and the Academic Editor, Christopher Fulton, for comments that greatly improved this manuscript. The contents of this manuscript are solely the opinions of the authors and do not constitute a statement of policy, decision, or position on behalf of NOAA or the U.S. Government.

Tables and Figures

Table 1. Table of information for each of the 41 islands and atolls that comprise the coral reef ecosystems of the U.S. Pacific. All locations are grouped by regions, indicated in bold. *Island Name* is the name of the island or atoll. *Island* is the three-letter code used in Figures 1, 5 and 6. *Island Type* is based on primary geological make-up. Closed atoll designation is where a majority of the atoll is enclosed by emergent or semi-emergent reef. *Latitude* and *Longitude* are in degrees north and east, respectively, based on the center point of each island and atoll. *Land Area* and *Reef Area* are shown in square kilometers. *Reef Area* is calculated from the shoreline to the 30-m isobath.

Island Name	Island	Island Type	Latitude	Longitude	Land Area	Reef Area
Northwestern Hawaiian Region						
Kure	KUR	Closed atoll	28.42	-178.33	0.92	83.15
Midway	MID	Closed atoll	28.23	-177.38	5.98	101.52
Pearl & Hermes Reef	PHR	Closed atoll	27.86	-175.85	0.50	467.27
Lisianski	LIS	Open atoll	26.01	-173.95	1.50	1004.27
Laysan	LAY	Carbonate island	25.78	-171.73	3.53	488.13
Maro Reef	MAR	Open atoll	25.41	-170.58	0.00	1075.44
French Frigate Shoals	FFS	Open atoll	23.79	-166.21	0.20	677.96
Necker	NEC	Basalt island	23.58	-164.70	0.12	1028.32
Nihoa	NIH	Basalt island	23.06	-161.93	0.72	0.74
Hawai'i Region						
Kauai	KAU	Basalt/Carbonate island	22.09	-159.57	1436.70	241.70
Niihau	NII	Basalt/Carbonate island	21.90	-160.15	186.82	108.06
Oahu	OAH	Basalt/Carbonate island	21.49	-158.00	1548.99	422.72
Molokai	MOL	Basalt/Carbonate island	21.14	-157.09	670.22	198.51
Lanai	LAN	Basalt island	20.82	-156.92	365.37	55.49
Maui	MAI	Basalt island	20.82	-156.40	1886.32	196.84
Hawaii	HAW	Basalt island	19.53	-155.42	10441.51	201.67
Johnston	JOH	Open atoll	16.74	-169.52	2.63	194.01
Mariana Region						
Wake	WAK	Closed atoll	19.30	166.62	6.97	19.18
Farallon de Pajaros	FDP	Basalt island	20.55	144.89	2.25	1.38
Maug	MAU	Basalt island	20.02	145.22	2.14	3.17
Asuncion	ASC	Basalt island	19.69	145.40	7.86	2.54
Agrihan	AGR	Basalt island	18.76	145.66	44.05	9.50
Pagan	PAG	Basalt island	18.11	145.76	47.75	16.29
Alamagan	ALA	Basalt island	17.60	145.83	12.96	4.28
Guguan	GUG	Basalt island	17.31	145.84	4.24	2.00
Sarigan	SAR	Basalt island	16.71	145.78	4.47	2.00
Saipan	SAI	Basalt/Carbonate island	15.19	145.75	118.98	73.04
Tinian	TIN	Basalt/Carbonate island	14.99	145.63	101.21	16.20
Aguijan	AGU	Basalt/Carbonate island	14.85	145.55	7.01	5.91
Rota	ROT	Basalt/Carbonate island	14.16	145.21	85.13	16.03
Guam	GUA	Basalt/Carbonate island	13.46	144.79	544.34	94.85
Equatorial Region						
Kingman	KIN	Open atoll	6.40	-162.38	0.76	47.63
Palmyra	PAL	Closed atoll	5.88	-162.09	2.23	52.50
Howland	HOW	Carbonate island	0.80	-176.62	1.80	2.57
Baker	BAK	Carbonate island	0.20	-176.48	1.60	4.43
Jarvis	JAR	Carbonate island	-0.37	-160.00	4.43	4.32

Samoa Region						
Swains	SWA	Carbonate island	-11.06	-171.08	2.38	2.82
Ofu & Olosega	OFU	Basalt island	-14.17	-169.65	12.61	12.03
Tau	TAU	Basalt island	-14.24	-169.47	45.09	10.38
Tutuila	TUT	Basalt island	-14.30	-170.70	137.45	50.89
Rose	ROS	Closed atoll	-14.55	-168.16	0.09	7.80

Figure Legends

Figure 1. Map highlighting the 41 islands and atolls that comprise the coral reef ecosystems of the U.S. Pacific. Individual locations are color-coded by region. Regions include Northwestern Hawaiian, Hawai'i, Mariana, Equatorial and Samoa. Table 1 provides additional information pertaining to each location, including the location name for each of the location codes.

Figure 2. Monthly composite of chlorophyll-*a* concentrations at Pearl and Hermes Reef in the Northwestern Hawaiian Region for September 2003. A) Unfiltered data with contaminated information associated with shallow-water bottom reflectance; B) data filtered using the 30-m bathymetric contour (black line), although contaminated information still remains as a result of bottom reflectance; C) fully cleaned data set using an additional data removal filter (gray line) that is everywhere perpendicular to the 30-m contour, removing all contaminated data associated with bottom reflectance.

Figure 3. Chlorophyll-*a* concentrations ($\text{mg m}^{-3} \pm \text{standard error}$) by data inclusion zone from the error-free data set (Fig. 2) at Pearl and Hermes Reef. Values for each data inclusion zone were calculated by taking the long-term mean of each pixel from July 2002 to May 2011, and then averaging over all pixels within each zone. The numbers on the x-axis are associated with sequentially expanding data inclusion zone, separated by 0.0295° (~ 3.27 km). The data inclusion zones are exclusive and nonoverlapping, and color-coded and numbered based on the inset of Pearl and Hermes Reef. The black line represents the 30-m isobath and the gray line represents the additional data removal filter.

Figure 4. Map of long-term means in A) SST, B) wave energy, C) chlorophyll-*a* and D) irradiance across each of the regions that comprise the coral reef ecosystems of the U.S. Pacific. Regions indicated in panel A are the same for panels B –D. Please see Fig. 1 as a reference for individual island and atoll locations.

Figure 5. Climatological ranges and average annual anomalies for U.S. Pacific coral reef ecosystems. Island- and atoll-scale metrics for A) SST, B) wave energy, C) chlorophyll-*a* and D) irradiance. In each of the panels (A – D), the black bar represents the climatological range, with the top and bottom of the bar representing the upper and lower climatological range limits, respectively. The yellow and blue bars signify average annual positive and negative anomalies, respectively, represented here as the average annual percentage of time above (positive) the upper climatological range limit and below (negative) the lower climatological range limit. Islands and atoll names are presented as a three-letter code (see Table 1 for full location names), grouped and color-coded by region (see Fig. 1 for map of locations), and oriented by decreasing latitude from left to right (see Table 1 for specific positions). The asterisks represent the islands that are oriented based on geographic proximity to other islands and atolls, as opposed to strict latitudinal orientation. See Tables S1 – S6 for climatology and anomaly values presented in this figure.

Figure 6. Principle component analysis (PCA) of the A) upper climatological range limit, B) long-term mean and C) lower climatological range limit for all environmental forcings: SST, wave energy, chlorophyll-*a*, irradiance. Island and atoll names are presented as a three-letter code (see Table 1 for full location names) and grouped and color-coded by region (see Fig. 1 for map of locations). The direction of loading for each of the parameters is indicated by the black line, with the direction of the line pointed towards increasing values. Similarity Profile (SIMPROF) results are represented by dashed lines and indicate islands with similar environmental forcings ($p < 0.0001$) with respect to each of the metrics. See Table S1 for climatological range limit and long-term mean values presented in this figure.

Fig. 1

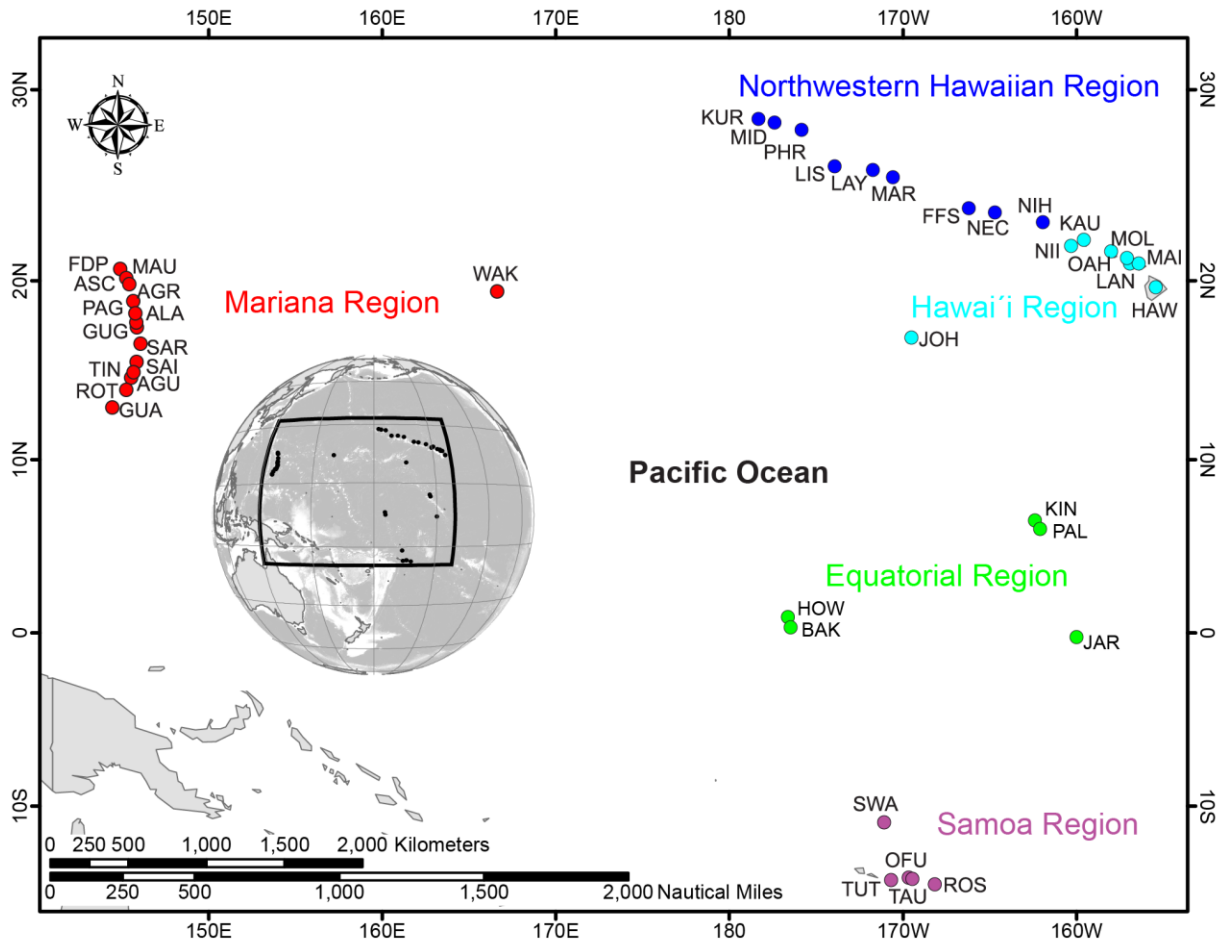


Fig. 2

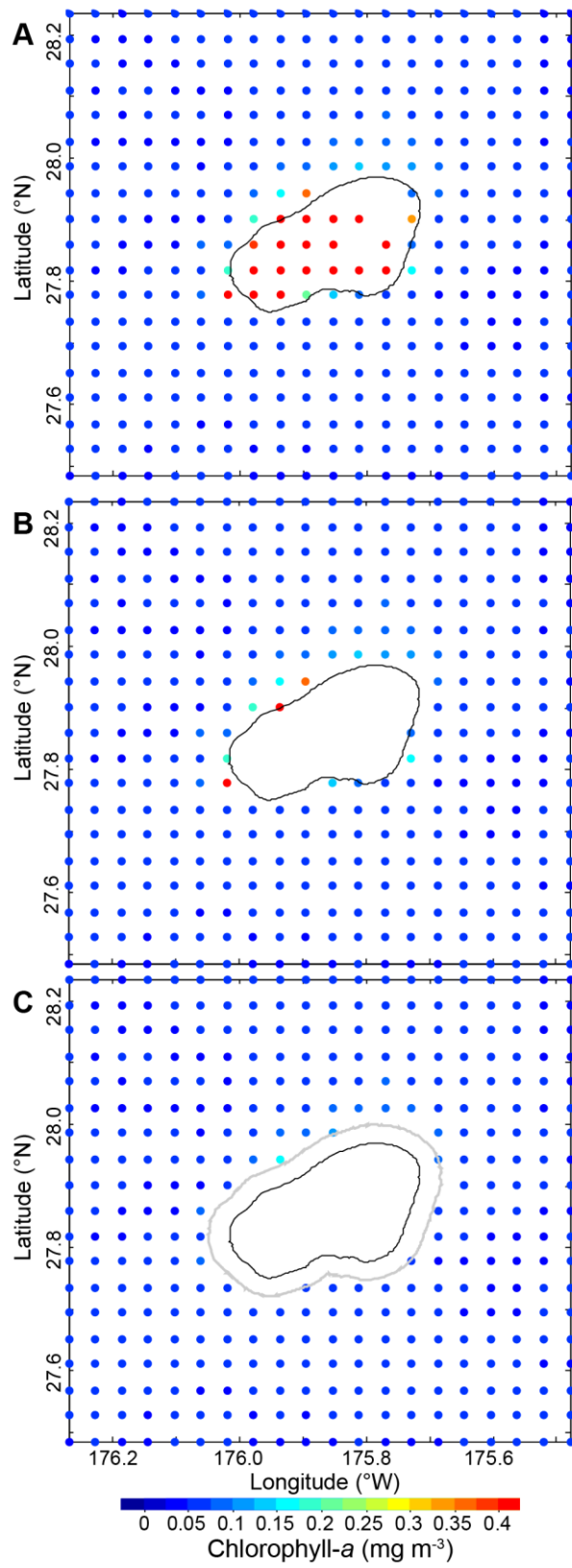


Fig. 3

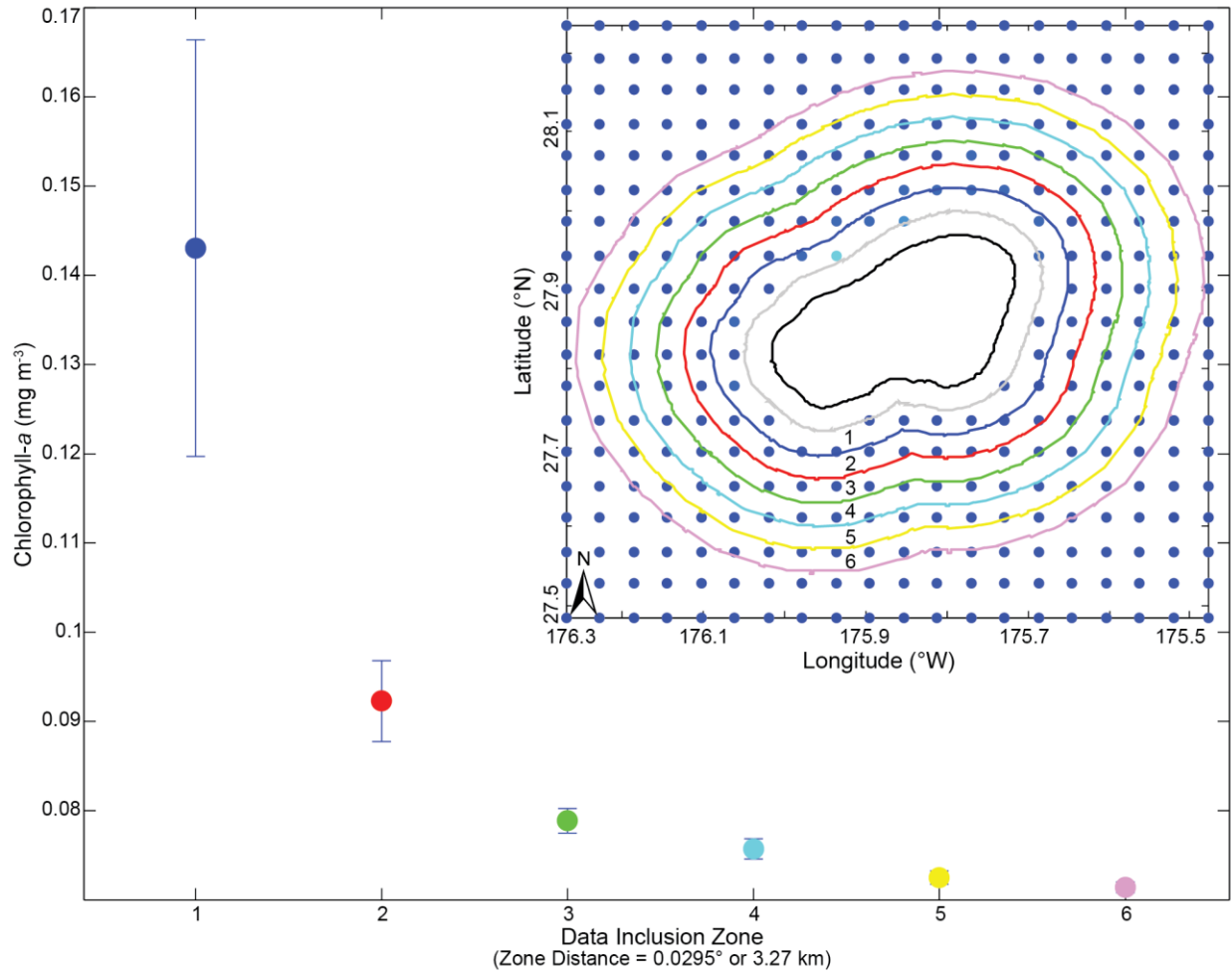


Fig. 4

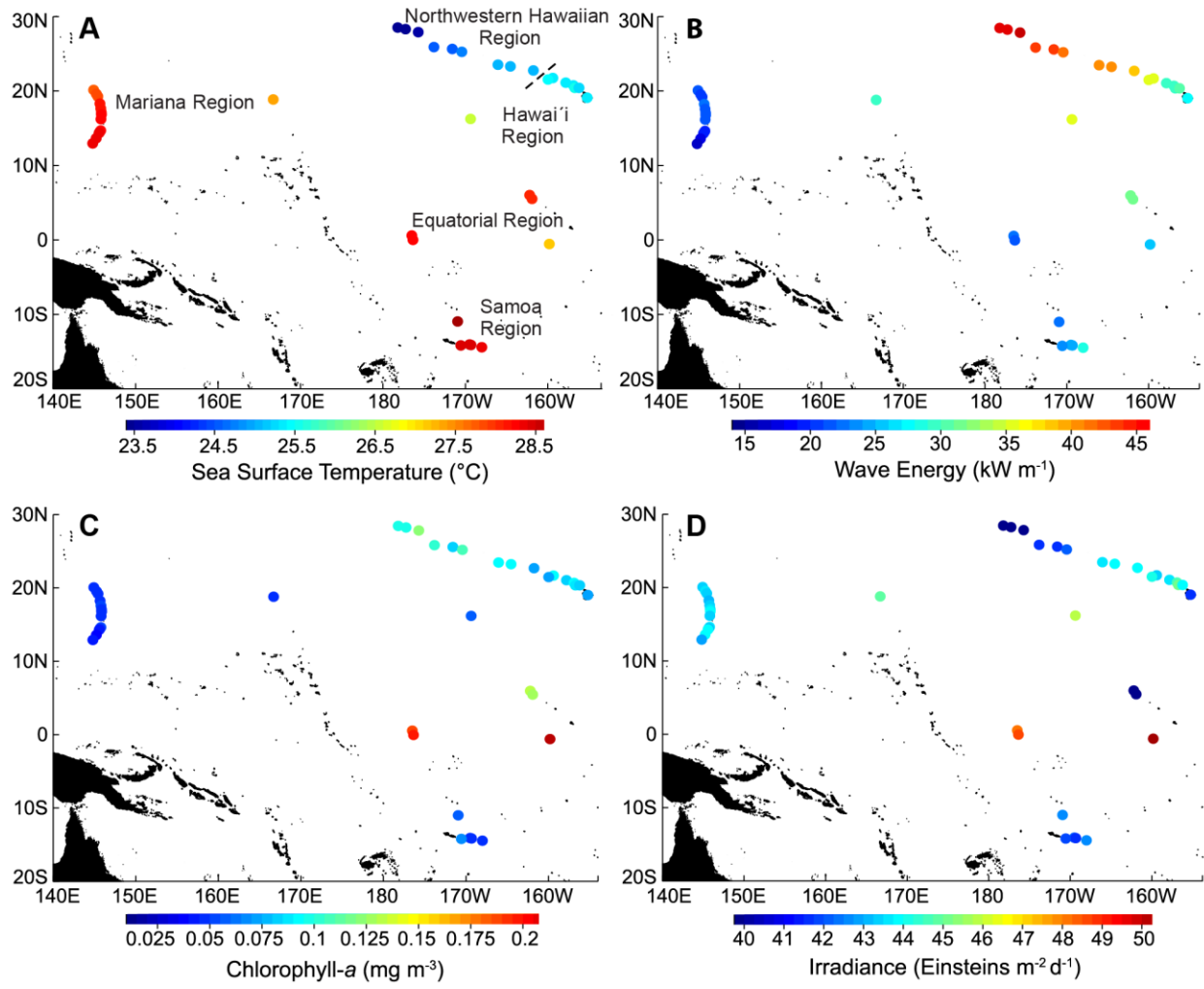


Fig. 5

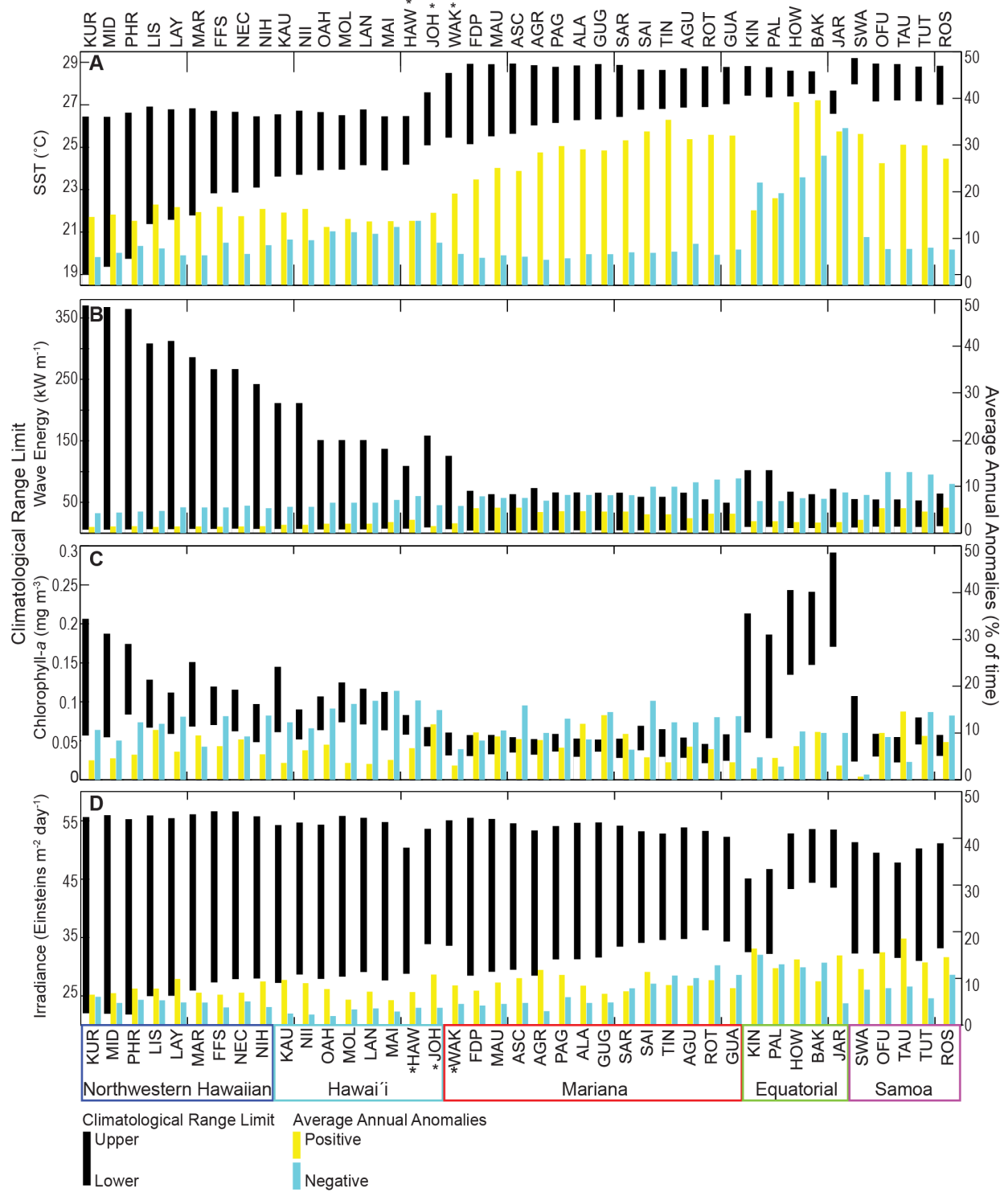
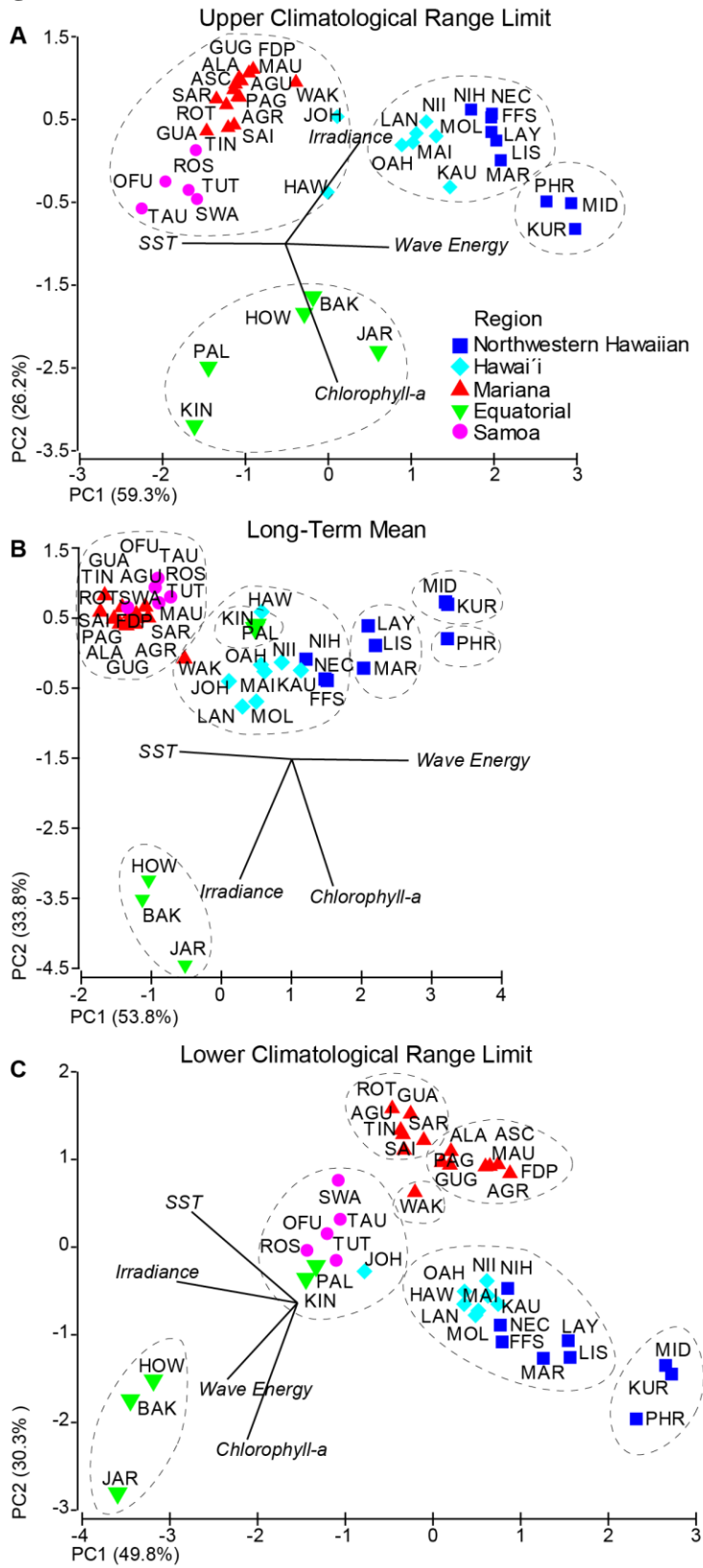


Fig. 6



References

- Barton, A. D., and K. S. Casey. 2005. Climatological context for large-scale coral bleaching. *Coral Reefs* **24**: 536-554.
- Boss, E., and J. R. V. Zaneveld. 2003. The effect of bottom substrate on inherent optical properties: Evidence of biogeochemical processes. *Limnol Oceanogr* **48**: 346-354.
- Bradbury, R. H., and P. C. Young. 1981. The Effects of a Major Forcing Function, Wave Energy, on a Coral-Reef Ecosystem. *Mar Ecol-Prog Ser* **5**: 229-241.
- Brown, B. E. 1997. Adaptations of Reef Corals to Physical Environmental Stress, p. 221-299. *In* J. H. S. Blaxter and A. J. Southward [eds.], *Advances in Marine Biology*. Academic Press.
- Caldeira, K., and M. E. Wickett. 2003. Anthropogenic carbon and ocean pH. *Nature* **425**: 365-365.
- Carder, K. L., Chen, R.F., Hawes, S.K. 2003. Instantaneous Photosynthetically Available Radiation and Absorbed Radiation by Phytoplankton: Algorithm Theoretical Basis Document *In* M. O. S. Team [ed.]. National Aeronautics and Space Administration.
- Carilli, J., S. D. Donner, and A. C. Hartmann. 2012. Historical Temperature Variability Affects Coral Response to Heat Stress. *Plos One* **7**: e34418.
- Casey, K., T. Brandon, P. Cornillon, and R. Evans. 2010. The past, present and future of the AVHRR Pathfinder SST program. *Oceanography from space: Revisited*.
- Castillo, K. D., J. B. Ries, J. M. Weiss, and F. P. Lima. 2012. Decline of forereef corals in response to recent warming linked to history of thermal exposure. *Nature Clim. Change* **2**: 756-760.
- Church, J. A., and N. J. White. 2006. A 20th century acceleration in global sea-level rise. *Geophys. Res. Lett.* **33**: L01602.
- Clarke, K., and R. Gorley. 2006. *PRIMER-E User Manual and Tutorial*.
- Clarke, K. R., P. J. Somerfield, and R. N. Gorley. 2008. Testing of null hypotheses in exploratory community analyses: similarity profiles and biota-environment linkage. *J Exp Mar Biol Ecol* **366**: 56-69.
- Couce, E., A. Ridgwell, and E. J. Hendy. 2012. Environmental controls on the global distribution of shallow-water coral reefs. *J Biogeogr* **39**: 1508-1523.
- Dollar, S. J. 1982. Wave stress and coral community structure in Hawaii. *Coral Reefs* **1**: 71-81.
- Done, T. J. 1999. Coral community adaptability to environmental change at the scales of regions, reefs and reef zones. *American Zoologist* **39**: 66-79.
- Donner, S. D. 2009. Coping with Commitment: Projected Thermal Stress on Coral Reefs under Different Future Scenarios. *Plos One* **4**: e5712.
- . 2011. An evaluation of the effect of recent temperature variability on the prediction of coral bleaching events. *Ecol Appl* **21**: 1718-1730.
- Donner, S. D., T. R. Knutson, and M. Oppenheimer. 2007. Model-based assessment of the role of human-induced climate change in the 2005 Caribbean coral bleaching event. *Proceedings of the National Academy of Sciences* **104**: 5483-5488.
- Donner, S. D., W. J. Skirving, C. M. Little, M. Oppenheimer, and O. Hoegh-Guldberg. 2005. Global assessment of coral bleaching and required rates of adaptation under climate change. *Global Change Biol* **11**: 2251-2265.
- Doty, M. S., and M. Oguri. 1956. The Island Mass Effect. *Journal du Conseil* **22**: 33-37.

- Eakin, C. M. and others 2010. Monitoring Coral Reefs from Space. *Oceanography* **23**: 118-133.
- Emanuel, K. 2005. Increasing destructiveness of tropical cyclones over the past 30 years. *Nature* **436**: 686-688.
- Erez, J., S. Reynaud, J. Silverman, K. Schneider, and D. Allemand. 2011. Coral Calcification Under Ocean Acidification and Global Change, p. 151-176. *In* Z. Dubinsky and N. Stambler [eds.], *Coral Reefs: An Ecosystem in Transition*. Springer Netherlands.
- Fabricius, K. E. 2005. Effects of terrestrial runoff on the ecology of corals and coral reefs: review and synthesis. *Mar Pollut Bull* **50**: 125-146.
- Freeman, L. A., A. J. Miller, R. D. Norris, and J. E. Smith. 2012. Classification of remote Pacific coral reefs by physical oceanographic environment. *J. Geophys. Res.* **117**: C02007.
- Gove, J. M., M. A. Merrifield, and R. E. Brainard. 2006. Temporal variability of current-driven upwelling at Jarvis Island. *Journal of Geophysical Research-Oceans* **111**.
- Grigg, R. W. 1983. Community Structure, Succession and Development of Coral Reefs in Hawaii. *Mar Ecol-Prog Ser* **11**: 1-14.
- Hendry, R., and C. Wunsch. 1973. High Reynolds number flow past an equatorial island. *J Fluid Mech* **58**: 97-114.
- Heron, S. F., B. L. Willis, W. J. Skirving, C. M. Eakin, C. A. Page, and I. R. Miller. 2010. Summer Hot Snaps and Winter Conditions: Modelling White Syndrome Outbreaks on Great Barrier Reef Corals. *Plos One* **5**:e12210.
- Hoegh-Guldberg, O. 1999. Climate change, coral bleaching and the future of the world's coral reefs. *Marine and Freshwater Research* **50**: 839-866.
- Hoegh-Guldberg, O. 2011. The Impact of Climate Change on Coral Reef Ecosystems *Coral Reefs: An Ecosystem in Transition*, p. 391-403. *In* Z. Dubinsky and N. Stambler [eds.]. Springer Netherlands.
- Hoegh-Guldberg, O., M. Fine, W. Skirving, R. Johnstone, S. Dove, and A. Strong. 2005. Coral bleaching following wintry weather. *Limnol Oceanogr* **50**: 265-271.
- Hoegh-Guldberg, O. and others 2007. Coral reefs under rapid climate change and ocean acidification. *Science* **318**: 1737.
- Hughes, T. P., and J. H. Connell. 1999. Multiple stressors on coral reefs: A long-term perspective. *Limnol Oceanogr* **44**: 932-940.
- Karnauskas, K. B., and A. L. Cohen. 2012. Equatorial refuge amid tropical warming. *Nature Clim. Change* **advance online publication**.
- Kilar, J. A., Mclachlan, J. 1989. Effects of wave exposure on the community structure of a plant-dominated, fringing-reef platform: intermediate disturbance and disturbance mediated competition. *Mar Ecol-Prog Ser* **54**: 265-276.
- Kilpatrick, K. A., G. P. Podesta, and R. Evans. 2001. Overview of the NOAA/NASA advanced very high resolution radiometer Pathfinder algorithm for sea surface temperature and associated matchup database. *J Geophys Res-Oceans* **106**: 9179-9197.
- Kleypas, J. A., J. W. Mcmanus, and L. a. B. Menez. 1999. Environmental Limits to Coral Reef Development: Where Do We Draw the Line? *American Zoologist* **39**: 146-159.
- Knowlton, N., and J. B. C. Jackson. 2008. Shifting baselines, local impacts, and global change on coral reefs. *Plos Biology* **6**: 215-220.
- Leichter, J. J., and S. J. Genovese. 2006. Intermittent upwelling and subsidized growth of the scleractinian coral *Madracis mirabilis* on the deep fore-reef slope of Discovery Bay, Jamaica. *Marine Ecology Progress Series* **316**: 95-103.

- Leichter, J. J., A. Paytan, S. Wankel, K. Hanson, S. Miller, and M. A. Altabet. 2007. Nitrogen and oxygen isotopic signatures of subsurface nitrate seaward of the Florida Keys reef tract. *Limnol Oceanogr*: 1258-1267.
- Leichter, J. J., G. Shellenbarger, S. J. Genovese, and S. R. Wing. 1998. Breaking internal waves on a Florida (USA) coral reef: a plankton pump at work? *Marine Ecology Progress Series* **166**: 83-97.
- Leichter, J. J., H. L. Stewart, and S. L. Miller. 2003. Episodic nutrient transport to Florida coral reefs. *Limnol Oceanogr*: 1394-1407.
- Lough, J. M. 2012. Small change, big difference: Sea surface temperature distributions for tropical coral reef ecosystems, 1950-2011. *J. Geophys. Res.* **117**: C09018.
- Madin, J., K. Black, and S. Connolly. 2006. Scaling water motion on coral reefs: from regional to organismal scales. *Coral Reefs* **25**: 635-644.
- Maina, J., T. R. Mcclanahan, V. Venus, M. Ateweberhan, and J. Madin. 2011. Global Gradients of Coral Exposure to Environmental Stresses and Implications for Local Management. *Plos One* **6**.
- Maina, J., V. Venus, M. R. Mcclanahan, and M. Ateweberhan. 2008. Modelling susceptibility of coral reefs to environmental stress using remote sensing data and GIS models. *Ecol Model* **212**: 180-199.
- Mcclanahan, T. R. and others 2007. Western Indian Ocean coral communities: bleaching responses and susceptibility to extinction. *Marine Ecology Progress Series* **337**: 1-13.
- Mcclanahan, T. R., J. Maina, R. Moothien-Pillay, and A. C. Baker. 2005. Effects of geography, taxa, water flow, and temperature variation on coral bleaching intensity in Mauritius. *Marine Ecology Progress Series* **298**: 131-142.
- Miller, J. and others 2008. The state of coral reef ecosystems of the Pacific Remote Island Areas. The state of coral reef ecosystems of the United States and Pacific Freely Associated States: 354-386.
- Monismith, S. G. 2007. Hydrodynamics of coral reefs. *Annu Rev Fluid Mech* **39**: 37-55.
- Mumby, P. J. and others 2004. Remote sensing of coral reefs and their physical environment. *Mar Pollut Bull* **48**: 219-228.
- Obura, D., and S. Mangubhai. 2011. Coral mortality associated with thermal fluctuations in the Phoenix Islands, 2002-2005. *Coral Reefs* **30**: 607-619.
- Polovina, J. J., E. Howell, D. R. Kobayashi, and M. P. Seki. 2001. The transition zone chlorophyll front, a dynamic global feature defining migration and forage habitat for marine resources. *Prog Oceanogr* **49**: 469-483.
- Reidenbach, M. A., J. R. Koseff, S. G. Monismith, J. V. Steinback, and A. Genin. 2006. The effects of waves and morphology on mass transfer within branched reef corals. *Limnol Oceanogr*: 1134-1141.
- Rogers, C. S. 1993. Hurricanes and coral reefs: The intermediate disturbance hypothesis revisited. *Coral Reefs* **12**: 127-137.
- Sandin, S. A. and others 2008. Baselines and Degradation of Coral Reefs in the Northern Line Islands. *Plos One* **3**: e1548
- Sheppard, C. 2009. Large temperature plunges recorded by data loggers at different depths on an Indian Ocean atoll: comparison with satellite data and relevance to coral refuges. *Coral Reefs* **28**: 399-403.

- Sheppard, C. R. C., A. Harris, and A. L. S. Sheppard. 2008. Archipelago-wide coral recovery patterns since 1998 in the Chagos Archipelago, central Indian Ocean. *Marine Ecology Progress Series* **362**: 109-117.
- Smith-Keune, C., and M. Van Oppen. 2006. Genetic structure of a reef-building coral from thermally distinct environments on the Great Barrier Reef. *Coral Reefs* **25**: 493-502.
- Smith, J. E., C. M. Smith, P. S. Vroom, K. L. Beach, and S. Miller. 2004. Nutrient and growth dynamics of *Halimeda* tuna on Conch Reef, Florida Keys: Possible influence of internal tides on nutrient status and physiology. *Limnol Oceanogr*: 1923-1936.
- Storlazzi, C., J. Logan, and M. Field. 2003. Quantitative morphology of a fringing reef tract from high-resolution laser bathymetry: Southern Molokai, Hawaii. *Geological Society of America Bulletin* **115**: 1344-1355.
- Storlazzi, C. D., E. K. Brown, M. E. Field, K. Rodgers, and P. L. Jokiel. 2005. A model for wave control on coral breakage and species distribution in the Hawaiian Islands. *Coral Reefs* **24**: 43-55.
- Storlazzi, C. D., M. E. Field, J. D. Dykes, P. L. Jokiel, and E. K. Brown. 2001. Wave Control on Reef Morphology and Coral Distribution: Molokai, Hawaii, p. 784-793. *Waves Conference, American Society of Civil Engineers*
- Teneva, L., M. Karneckas, C. Logan, L. Bianucci, J. Currie, and J. Kleypas. 2012. Predicting coral bleaching hotspots: the role of regional variability in thermal stress and potential adaptation rates. *Coral Reefs* **31**: 1-12.
- Visram, S., and A. E. Douglas. 2007. Resilience and acclimation to bleaching stressors in the scleractinian coral *Porites cylindrica*. *J Exp Mar Biol Ecol* **349**: 35-44.
- Vroom, P., C. Musburger, S. Cooper, J. Maragos, K. Page-Albins, and M. V. Timmers. 2010. Marine biological community baselines in unimpacted tropical ecosystems: spatial and temporal analysis of reefs at Howland and Baker Islands. *Biodivers Conserv* **19**: 797-812.
- Williams, G. J., I. S. Knapp, J. E. Maragos, and S. K. Davy. 2010. Modeling patterns of coral bleaching at a remote Central Pacific atoll. *Mar Pollut Bull* **60**: 1467-1476.
- Williams, I. D. and others 2011. Differences in Reef Fish Assemblages between Populated and Remote Reefs Spanning Multiple Archipelagos Across the Central and Western Pacific. *Journal of Marine Biology* **2011**.
- Wolanski, E., and B. Delesalle. 1995. Upwelling by internal waves, Tahiti, French Polynesia. *Cont Shelf Res* **15**: 357-368.
- Wooldridge, S. A. 2009. Water quality and coral bleaching thresholds: Formalising the linkage for the inshore reefs of the Great Barrier Reef, Australia. *Mar Pollut Bull* **58**: 745-751.

CHAPTER III

THE ISLAND MASS EFFECT: EXPLAINING ENHANCED PHYTOPLANKTON BIOMASS FOR ISLAND ECOSYSTEMS ACROSS THE PACIFIC

Jamison M. Gove^{1,2}, Margaret A. McManus³, Anna B. Neuhemier³, Julia S. Ehses^{1,2}, Jeffrey C. Drazen, Craig R. Smith³, Mark A. Merrifield³

¹Joint Institute for Marine and Atmospheric Research, University of Hawai`i at Mānoa, Honolulu, Hawai`i, United States of America

²Coral Reef Ecosystem Division, NOAA Pacific Islands Fisheries Science Center, Honolulu, Hawai`i, United States of America

³School of Ocean and Earth Science and Technology, University of Hawai`i at Mānoa, Honolulu, Hawai`i, United States of America

Abstract

Primary production in surface ocean waters provides essential energy to marine ecosystems. This is particularly relevant for island- and atoll-reef ecosystems where the surrounding oceanic environment typically displays very low new production. Past research has found evidence of enhanced phytoplankton biomass near islands and atolls (i.e., the ‘island mass effect’) with a broad-scale investigation evaluating the extent and forcings of phytoplankton increases yet to be performed. Here we use a ten-year record of satellite-derived chlorophyll-a (a proxy for phytoplankton biomass) to evaluate horizontal gradients in long-term (2002 through 2012) phytoplankton biomass near 35 Pacific island- and atoll-reef ecosystems. We show a sustained increase in phytoplankton biomass compared to surrounding oceanic waters among the majority (91%) of our study locations. Furthermore, we find the rate of increase in phytoplankton biomass with decreased distance to shore was significantly different between locations. Generalized linear modeling indicated a subset of biogeophysical parameters, namely reef area, bathymetric slope, geomorphic type (e.g. atoll *versus* island) and the presence of human habitation, are the primary drivers of increased phytoplankton biomass, together explaining 77% of the variability observed. *In situ* observations within the Hawaiian Archipelago contextualize satellite-derived information, demonstrating that short-term (1 – 3 day) spatial patterns in time-specific phytoplankton biomass may not reflect long-term trends.

Introduction

Phytoplankton primary production is an essential source of energy in the marine environment (Duarte and Cebrian 1996; Jennings et al. 2008). The extent and availability of primary producers drives marine ecosystem trophic-structure (Iverson 1990), including the

distribution and production of the world's fisheries (Brander 2007; Chassot et al. 2010; Pauly and Christensen 1995). Near oceanic island and atoll coral reef ecosystems, processes that enhance phytoplankton biomass are particularly important to food-web dynamics and total ecosystem productivity (Hernández-León 1991; Sander and Steven 1973; Wolanski and Hamner 1988) as the surrounding environment is often nutrient limited and lacking new production (Hamner and Hauri 1981).

The enhancement in phytoplankton biomass near oceanic islands and atolls compared to surrounding waters – the 'island mass effect' – may be the result of several mechanisms. Current-bathymetric interactions can force vertical transport of subsurface, nutrient-rich waters, either through current impingement and positive uplift of isotherms on the upstream side of an island (Gierach et al. 2013; Gove et al. 2006; Hamner and Hauri 1981), through turbulent mixing, lee eddy, and wake effects on the downstream side (Coutis and Middleton 1999; Hernández-León 1991), or through the generation of internal waves (Leichter et al. 1998; Sander 1981). Outflow from rivers, land-based run-off, and other terrigenous input can also stimulate phytoplankton production near islands (Bucciarelli et al. 2001; Dandonneau and Charpy 1985). Likewise, an island's geochemical make-up may provide essential limiting micronutrients (e.g. iron), further influencing phytoplankton production (Palacios 2002; Signorini et al. 1999). Human habitation and associated land use, agricultural run-off and wastewater input can dramatically increase nearshore productivity (Anderson et al. 2002; Smith et al. 1999), often resulting in negative impacts to local biological communities (Caperon et al. 1971; Fabricius 2005; Pastorok and Bilyard 1985). Nutrients may also become available through intrinsic coral reef ecosystem processes (Doty and Oguri 1956; Sander 1981) and in particular, through consumer-derived sources such as fishes and microbes (Burkepile et al. 2013; Pernthaler 2005).

Research on the island mass effect has traditionally been limited to a small spatial (i.e. single or small number of locations) and temporal (i.e. multiple days to a few years) scale, limiting our ability to identify the proximate factors driving increased phytoplankton. The degree to which physical versus anthropogenic factors are controlling the enhancement of nearshore production are still unknown. Here, we provide a broad-scale investigation of both the nature and prevalence of the island mass effect. We assess horizontal spatial gradients in chlorophyll-*a* concentrations (a proxy for phytoplankton biomass) at 35 island- and atoll-reef ecosystems across the Pacific Ocean (Fig. 1). Our study locations span 43° of latitude and 60° of longitude and cross multiple gradients in oceanographic conditions (Gove et al. 2013), geophysical attributes (Table 1), local human impact (Williams et al. 2011) and biological community organization (Schils et al. 2013; Williams et al. 2013; Williams et al. 2011). We utilized long-term (10 year) averages of satellite derived chlorophyll-*a* to evaluate the extent and persistence of increased phytoplankton biomass near study locations, and investigated a suite of biogeophysical parameters to identify the proximate drivers of chlorophyll-*a* gradients between locations. *In situ* chlorophyll-*a* measurements available for several coral reef ecosystems are presented to provide context to long-term observations.

Methods

Study region – We investigate 35 coral reef ecosystems across the Pacific (14°S – 29°N, 144°E – 155°W) that are the focus of the long-term Pacific Reef Assessment and Monitoring Program (Pacific-RAMP) led by NOAA’s Coral Reef Ecosystem Division (CRED). Pacific-RAMP surveys coral reefs that reside in disparate oceanographic regimes exposed to varying levels of potential human impact. Locations included the heavily populated and urbanized

islands of Oahu, Guam, and Saipan, as well as some of the most remote and functionally intact coral reef ecosystems in the Pacific, such as Kingman Reef, Palmyra Atoll, and Jarvis Island in the Line Islands and Howland and Baker Islands in the Phoenix Islands (Table 1 and Fig. 1).

Satellite chlorophyll-a – Remotely sensed ocean color algorithms are calibrated for optically-deep waters (>30 m; Carder 2003). In optically-shallow waters, such as regions within atolls and coral reef environments, bottom substrate properties and sediment suspension affect light propagation and increase marine reflectance, resulting in data quality issues for ocean color constituents, such as chlorophyll-*a* (Boss and Zaneveld 2003). Until future algorithms are developed for shallow water environments, analysis of remotely sensed chlorophyll-*a* near islands and atolls are constrained to offshore waters (i.e. >30 m; Gove et al. 2013; Maina et al. 2011; Mumby et al. 2004).

Eight-day, 0.0417° (hereafter 4 km) spatial resolution time series of chlorophyll-*a* (mg m^{-3}) were obtained from Moderate Resolution Imaging Spectroradiometer (MODIS). At the time of data analysis, errors were reported by NASA in the MODIS data set beyond 1 August 2012. We therefore calculated the long-term mean in chlorophyll-*a* for each data pixel over a 10 year period, from July 2002 (beginning of MODIS data set) through June 2012. Following Gove et al. (2013), a multistep masking routine was applied to remove optically shallow data and quantify long-term chlorophyll-*a* concentrations at fixed, equally spaced distances away from each location. All pixels inshore of the 30-m isobath were identified and removed (Fig. 2A). Because pixels are box-like in shape and georeferenced at their center point, information contributing to any single pixel value is collected up to one-half a pixel diagonal distance away (0.0295° or ~ 3.27 km). As such, pixels outside the 30-m isobath may still contain biased information associated with optically-shallow waters (Fig. 2B). To address this, all pixels up to 0.0295° off-

shore of the 30-m isobath were also removed (Fig. 2C).

A series of spatially expanding, non-overlapping data inclusion zones set 0.0295° apart were developed for each island and atoll (sensu Gove et al. 2013). In total, 8 zones were developed at each island at equidistance locations from $0.0295 - 0.0590^\circ$ to $0.2360 - 0.2655^\circ$ (approximately 3.27 – 6.54 km to 26.16 – 29.43 km) offshore from the 30-m bathymetric contour (Fig. 3A). For ease of interpretation, zone distances are presented as the average distance of each zone from the 30-m contour (4.9 – 27.79 km; Fig. 3B). Where island or atoll proximity resulted in zones from different locations containing common data pixels, pixels were identified and removed prior to zone averaging to avoid potential biases associated with the chlorophyll-*a* signal from one island influencing another's. In the event island or atoll proximity resulted in a large proportion of pixels in common (> 50%) between two locations, bathymetry was combined and zones recalculated for the larger formed island-complex. Specifically, Molokai, Maui, Lanai and Kahoolawe were combined to form Maui Nui; Saipan, Tinian and Agujan were combined to form Sai-Tin-Agu; Ofu, Olosega and Tau were combined to form Manua (Table 1). Maui Nui and Manua are pre-established name identifiers for their respective group of islands.

Biogeophysical drivers – We incorporated a series of biogeophysical parameters that are potential drivers of increased phytoplankton biomass near oceanic island- and atoll-reef ecosystems. The following were quantified for each location: latitude, geomorphic type (atoll *versus* island), reef area, land area, bathymetric slope, elevation, population status (remote *versus* populated) and the long-term mean and standard deviation for: sea surface temperature (SST), precipitation and ocean currents (Table 2).

Latitude ($^\circ$) represented the center point of each location. Geomorphic type was either 'atoll' or 'island'. Reef area (km^2) was calculated from the shore-line to the 30-m isobath and

land area (km²) was calculated for all emergent land. Bathymetric slope (°) was derived from bathymetric grids in ArcGIS v10.1 using the Spatial Analyst *slope* function, calculated between 30 – 300 m depth and then averaged across the entire location. A detailed description of these factors (latitude, geomorphic type, reef area and land area) can be obtained from Gove et al. (2013).

Elevation (m) was obtained from a variety of sources, including the U.S. Central Intelligence Agency (<https://www.cia.gov>), NOAA's Coral Reef Information System (<http://www.coris.noaa.gov>), and the U.S. Fish and Wildlife Service (www.fws.gov). Population status was either 'remote' or 'populated' following Williams et al. (2011). Locations were considered populated with a human habitation of >160 people.

Island- and atoll-scale SST (°C) was obtained for all locations from Gove et al. (2013). SST was quantified using the 0.0439° (hereafter 4-km) resolution weekly product from the Pathfinder v5.0 dataset (<http://pathfinder.nodc.noaa.gov>). Data were excluded if deemed of poor quality (quality value < 4, Kilpatrick et al. (2001)) or if individual pixels were masked as land. Island- and atoll-specific SST data were produced by spatially averaging the individual 4-km pixels that were intersected by or contained within the 30-m bathymetric contour for each location (Gove et al. 2013).

Precipitation data was obtained from the Global Precipitation Climatology Project v2.2; a global, 2.5° spatial resolution, monthly data set that merges remotely-sensed (microwave and infrared) and surface rain gauge observations (Adler et al. 2003).

Ocean current data were obtained from NOAA's OSCAR (Ocean Surface Current Analysis – Real time); a global, 1° spatial resolution, monthly ocean current data set derived from satellite altimetry (sea-level) and scatterometer (wind). The magnitude of current was

calculated from the zonal (u) and meridional (v) components of flow for each time step. Grid cells for precipitation and ocean currents were chosen based on the center point of each island or atoll.

The long-term mean and the standard deviation were calculated for SST, precipitation and ocean currents for each location over the 10 year time period concurrent with the long-term chlorophyll-*a* values (July 2002 – June 2012). Where locations were combined to form a larger island-complex (i.e. Maui Nui, Manua and Sai-Tin-Agu), time series data among islands were averaged for each time step prior to long-term mean and standard deviation calculations while remaining biogeophysical metrics were summed (land area, reef area), averaged (slope, latitude), or the maximum value was obtained (elevation).

Underlying bathymetry data for all locations were provided by the Pacific Islands Benthic Habitat Mapping Center (PIBHMC), Hawaii Mapping Research Group (HMRG), National Geophysical Data Center (NGDC), and satellite-derived global topography (Becker et al. 2009; Smith and Sandwell 1997).

In situ chlorophyll-a – As part of Pacific RAMP, *in situ* chlorophyll-*a* samples were obtained from August – September 2013 at 8 islands and atolls throughout the Hawaiian Archipelago. Specifically, Hawaii, Maui Nui, Oahu, Kauai and Niihau were sampled over a 2 – 4 day period from August 5 – 25, 2013. French Frigate Shoals, Lisianski and Pearl and Hermes Reef were sampled over a 1– 3 day period from September 3 – 19, 2013. Water samples were collected via Niskin bottles from select depths during night-time hours. Chlorophyll-*a* was measured fluorometrically using the method outlined in Strickland and Parsons (1972) and using calibrations with a commercial standard from Turner Designs Inc. Immediately following collection, samples were filtered through Whatman GF/F glass fiber filters and maintained at -

20°C prior to being eluted with 90% acetone. This method of chlorophyll sampling provides a detection limit of 0.01 mg m⁻³ and a precision limit of 5 – 10% for concentrations ≥ 0.25 mg m⁻³. Only surface (~3 m) samples are presented in order to make direct comparisons with satellite-derived data. The total number of samples at each island and atoll varied ($n = 4 - 24$) based on weather conditions, number of days spent at each location and other logistical constraints.

Statistical analysis – The relationship between long-term chlorophyll-*a* and distance to shore was well described by a power function at all locations (e.g. Fig.s 3B). Given that a power function is equivalent to a linear fit on log-log transformed data, seamless transition can be made between nonlinear and linear fits and associated analyses. To test for differences in the relationship between long-term chlorophyll-*a* and distance to shore between locations, an analysis of covariance (ANCOVA) was performed on log-log transformed data. Two tests were performed; one test that included all islands and atolls ($n = 35$) and another that only included locations that showed significant increase in chlorophyll-*a* with decrease distance to shore ($n = 28$; $p < 0.05$).

A generalized linear model (GLM) was built to identify the proximate drivers of observed differences in long-term chlorophyll-*a* gradients between study locations. We used slope ('b') from the regression output of log-log transformed data as the response variable, enabling a standardized comparison in chlorophyll-*a* gradients between study locations. Only locations with significant negative relationships (i.e. increased chlorophyll-*a* with decreased distance to shore) were used in the model ($n = 28$; $p < 0.05$). The distribution of slope values fit a gamma distribution, requiring a positive transformation for slope values prior to model input (henceforth slope values are presented as positive). Prior to running the GLM, predictor variables were examined for co-linearity. Bathymetric slope and elevation were highly correlated ($r =$

0.98), as were the long-term mean and standard deviation of SST, precipitation and currents ($r = -0.78, 0.88, \text{ and } 0.98$, respectively). We therefore removed elevation and each of the standard deviations as predictors for the model. The GLM was run with the remaining predictors ($n = 9$; Table 2) using a stepwise selection with Akaike's information criterion ('AIC') to identify the best-fit model. All data manipulation and statistical analyses were performed using Matlab v2013b unless otherwise specified.

Results

*Long-term gradients in chlorophyll-*a** – Across the 35 locations, 32 (91%) showed an increase in long-term chlorophyll-*a* concentrations with decreased distance to shore, with 28 of 32 islands exhibiting a significant relationship ($p < 0.05$; R^2 mean = 0.87, range = 0.59 – 0.99; see Table 1 for locations). The relationship between chlorophyll-*a* and distance to shore (i.e. slope 'b' of a linear fit on log-log transformed data) was significantly different among all locations ($F_{1,35} = 24.898, p < 0.0001$) as was the comparison among the 28 locations that had significant increases in chlorophyll-*a* ($F_{1,27} = 18.998, p < 0.0001$).

*Proximate drivers of gradients in long-term chlorophyll-*a** – Differences in the relationship between chlorophyll-*a* and distance to shore across the 28 islands and atolls were best explained by a model that contained reef area, bathymetric slope, geomorphic type and population status, together explaining 77.6% of the total variation observed (Table 3). Reef area combined with bathymetric slope accounted for over one-half of the variation. Reef area explained 27.2% of the variation and was positively related to chlorophyll-*a* gradients; a stronger gradient in chlorophyll-*a* was observed at islands and atolls with more reef area (Fig. 4). Conversely, bathymetric slope explained 25.2% of the variation and was negatively related;

locations with low bathymetric slope showed stronger gradients in chlorophyll-*a* compared to steep-sloped locations (Fig. 4). Geomorphic type (atoll *versus* island) and population status (remote *versus* populated) were also significant predictors and explained 14% and 10.6% of the variability observed, respectively (Table 2). Atolls exhibited stronger gradients in chlorophyll-*a* compared with islands. Populated locations had stronger gradients in chlorophyll-*a* than those locations that were remote (Fig. 4).

In situ chlorophyll-a – Near surface *in situ* chlorophyll-*a* measurements from 8 islands and atolls within the Hawaiian Archipelago highlighted the variable nature of phytoplankton biomass (Fig. 5). The greatest concentrations of chlorophyll-*a* were observed near the populated island of Oahu, where peak concentrations were 0.154 mg m⁻³ (Fig. 5B). Similarly high chlorophyll-*a* values (>0.14 mg m⁻³) were also observed near Niihau, Kauai, as well as the remote atoll French Frigate Shoals. The island of Hawaii exhibited the lowest chlorophyll-*a* for all *in situ* stations (mean ± std; 0.048 ± 0.009 mg m⁻³); however, most island and atoll locations had similarly low values at select stations (Fig. 5B).

Differences in the relationship between *in situ* chlorophyll-*a* estimates and distance to shore between locations were also apparent (Fig. 5B). Most locations exhibited an overall increase in chlorophyll-*a* towards shore; however, this was significant only for the island of Oahu ($n = 12$, $p < 0.05$; $R^2 = 0.68$). The island of Hawaii showed no clear gradient in chlorophyll-*a* while Kauai exhibited a general decrease in surface chlorophyll-*a* towards shore.

Comparisons between long-term mean and *in situ* chlorophyll-*a* gradients show no clear uniformity (Fig. 5B). *In situ* values were both greater than and less than long-term means at select distances across most islands. Moreover, *in situ* chlorophyll-*a* collected closer to shore than satellite-derived data (< 4.9 km) was lower than long-term values at 4 of 8 locations (Kauai,

Maui Nui, Hawaii, Pearl and Hermes Reef).

Discussion

We present evidence of increased phytoplankton biomass proximate to island- and atoll-reef ecosystems over large temporal (2002 – 2012) and spatial scales (43° of latitude and 60° of longitude), spanning broad differences in oceanographic conditions, geomorphic attributes, and human impact. Characterized spatial gradients in chlorophyll-*a* differed between study locations. Locations with increased reef area exhibited stronger gradients in chlorophyll-*a* (i.e. steeper increases towards shore), supporting the hypothesis that processes intrinsic to coral reef ecosystems may favor increased phytoplankton biomass near oceanic islands and atolls (Doty and Oguri 1956; Sander 1981). Autochthonous nutrient sources include nitrogen fixation, regeneration (either through decomposition of primary producers or from sediment deposition), and recycling from other biota (Suzuki and Casareto 2011). Animal waste products, such as those derived from fishes (Burkepile et al. 2013) and mobile invertebrates (Williams and Carpenter 1988), can enhance nutrient concentrations on coral reef ecosystems. However, biogeochemical processes within coral reef ecosystems can be highly variable (Atkinson 2011), therefore the availability of nutrients for export beyond coral reef benthic communities has been poorly characterized (Suzuki and Casareto 2011).

We also find stronger gradients in chlorophyll-*a* at atolls compared to islands, possibly associated with lagoonal flushing to nearshore waters. For example, the strongest gradients in chlorophyll-*a* were observed at atolls in the Northwestern Hawaiian Islands (NWHI; e.g. Pearl and Hermes Atoll, Maro Reef, French Frigate Shoals; cf. Fig. 1 and Table 1). Many of the atolls in the NWHI are characterized by a semi-enclosed emergent barrier reef with a naturally

occurring channel open to the west or southwest direction (Rooney et al. 2008). The NWHI reside in a highly energetic wave climate (Gove et al. 2013; Grigg 1983) with swells originating from the northwest and northeast directions (Aucan et al. 2012; Rooney et al. 2008). Wave events in the NWHI can pump large amounts of water over the emergent barrier reef (Aucan et al. 2012) that flow through the atoll and eventually exit the channel. Because wave forcing is a highly efficient atoll flushing mechanism (Callaghan et al. 2006), wave pumping may advect detritus or other sources of nutrients generated via coral reef ecosystem processes (e.g. Burkepile et al. 2013) out of the atoll faster than the assimilation ability of the benthic community (Atkinson 2011), thereby fueling nearshore phytoplankton biomass.

Internal waves may enhance nearshore phytoplankton biomass (Leichter et al. 1998; Sander 1981; Wolanski and Delesalle 1995). Generated from tidal currents interacting with underlying bathymetry, internal waves can drive vertical perturbations in the background stratification that deliver cooler, nutrient-rich waters to the near surface (Leichter et al. 2003). They are a prominent feature among a variety of island- and atoll- reef ecosystems (Gove et al. 2006; Leichter and Miller 1999; Leichter et al. 2012; Mcmanus et al. 2008; Roder et al. 2010; Sevadjian et al. 2012; Wolanski and Deleersnijder 1998). In this study, we find stronger chlorophyll-*a* gradients at locations with more gradual sloping bathymetry. Moreover, we find the strongest chlorophyll-*a* gradients at islands and atolls within the Hawaiian Archipelago, a region characterized by active internal wave generation (Merrifield and Holloway 2002) and more gradual sloping bathymetry (Table 1). Because shoreward propagation of internal waves occurs more readily over gradual sloping bathymetry (Carter et al. 2006), internal waves may increase surface nutrient availability and enhance phytoplankton biomass at locations that favor cross-shore transport.

Human activities can severely alter planktonic production in marine ecosystems (Vitousek et al. 1997b). Sources of nutrients include coastal development and land use (Fabricius et al. 2005; Wooldridge 2009) as well as wastewater effluent, agricultural run-off and storm outfalls (Anderson et al. 2002; Smith et al. 1999). Human-derived nutrient input can dramatically exceed natural sources (Vitousek et al. 1997a) resulting in destructive marine ecosystem consequences, such as toxic algal blooms and hypoxia of nearshore waters (Anderson et al. 2002) and degradation of coral reef benthic communities (Caperon et al. 1971; Pastorok and Bilyard 1985). In this study, we find a positive relationship between gradients in chlorophyll-*a* and populated locations, indicating that human habitation enhances phytoplankton biomass. It should be noted that our sample number of populated to remote locations in the model differed ($n = 7$ and 21, respectively), and was restricted to islands only. Future studies would benefit from adding additional populated locations, including populated atolls, as well as more refined metrics of human habitation than used here.

In situ observations in the Hawaiian Archipelago highlight the spatially variable nature of time-specific distributions in phytoplankton biomass. The island of Hawaii, as one example, exhibited minimal variability in chlorophyll-*a* along a transect towards shore. By contrast, the island of Oahu exhibited a marked increase in nearshore chlorophyll-*a* concentrations that were ~4 times greater than offshore values (range = 0.118 mg m^{-3}). Gilmartin and Revelante (1974) found similar differences in chlorophyll-*a* distributions around Oahu as presented here, attributable to increased nutrients associated with wastewater discharge in Kaneohe Bay, east Oahu (Caperon et al. 1971). Water-quality management has since improved in Kaneohe Bay (Smith et al. 1981); however, Oahu is densely populated and associated nutrient inputs may contribute to the observed distributions in chlorophyll-*a* values.

Several factors may contribute to the observed variability and lack of coherency between short-term (*in situ* data) and long-term (a decade of satellite derived data) chlorophyll-*a* concentrations. *In situ* spatial patterning may simply reflect the time-dependency in potential biogeophysical drivers of phytoplankton biomass, as current-topographic interactions, precipitation events and associated terrigenous input, wave-driven lagoonal flushing, and other possible mechanisms can vary over hours to weeks. In addition, biogeophysical drivers often exhibit spatial heterogeneity around islands and atolls (e.g. Hernández-León 1991) resulting in a non-uniform response of phytoplankton biomass in nearshore waters. Ship-based sampling efforts therefore provide an important snap-shot of chlorophyll-*a* distribution, but are not necessarily representative of long-term spatial trends. Similarly, the spatial footprints of *in situ* and satellite-derived chlorophyll-*a* data are vastly different, and therefore may not be appropriate for comparisons. Nevertheless, *in situ* observations provide an invaluable context for which to interpret satellite-derived values, and are best utilized in concert with long-term means.

The importance of phytoplankton biomass in coastal marine ecosystems spans multiple trophic levels with clear impacts on predator-prey dynamics (Bak et al. 1998; Brander 2007; Iverson 1990; Jennings et al. 2008). The mesopelagic boundary community, for example, is a distinct community of squids, fishes, and other micronekton (Reid et al. 1991) that exhibit strong diel horizontal migration patterns, transiting long distances (>5 km) towards shore at night before returning to deeper, oceanic waters in the day (Benoit-Bird and Au 2003a; Benoit-Bird and Au 2006; Benoit-Bird et al. 2001). Mesopelagic boundary organisms can migrate at speeds well beyond current velocities (Mcmanus et al. 2008) and peak in abundance and density in waters with increased phytoplankton biomass (Benoit-Bird et al. 2001), leading researchers to postulate that horizontal migration is behaviorally mediated driven by increased food resources in

nearshore environments (Benoit-Bird and Au 2003a; Benoit-Bird and Au 2006; Benoit-Bird et al. 2001; Mcmanus et al. 2008). Pelagic predators can also exhibit spatiotemporal movements that suggest oceanic animals, such as dolphins (Baird et al. 2008; Benoit-Bird and Au 2003b) and tuna (Brill et al. 1999; Holland et al. 1990; Musyl et al. 2003) cue in on shoreward migration of mesopelagic boundary organisms, exploiting the island-associated micronekton community as a food resource. Moreover, inter-island migratory patterns in marine apex predatory fishes (i.e. Tiger sharks) appear driven by variations in phytoplankton biomass, presumably owing to net energetic gain associated with bottom-up increases in prey abundance (Papastamatiou et al. 2013).

In coral reef ecosystems, organisms that capitalize on increased phytoplankton can serve as an important energy source for benthic sessile communities (Anthony and Fabricius 2000; Bak et al. 1998; Sebens et al. 1996). For example, corals can switch their degree of autotrophy *versus* heterotrophy with conditions that limit incoming irradiance, such as increased cloud cover, water depth (via tidal oscillations), and turbidity (Anthony and Fabricius 2000; Anthony et al. 2004). Heterotrophic plasticity is particularly essential for corals under acute thermal stress. During elevated seawater temperatures and associated loss of photosynthetic endosymbionts (i.e. coral bleaching), corals can subsidize their energy requirements through particle feeding, resulting in decreased mortality rates (Grottoli et al. 2006) and increased rates and extents of recovery (Connolly et al. 2012). Additionally, increased food availability can benefit coral reef fish larvae, as locally retained larvae show enhanced growth and increased size at settlement compared with larvae dispersed through oligotrophic oceanic waters (Swearer et al. 1999).

Future changes to the world's climate will result in potential consequences to ocean productivity (Doney et al. 2012; Poloczanska et al. 2013). Global shifts in biogeochemical

cycling and ocean mixing are projected to decrease nutrient availability and primary production in the tropics and subtropics (Doney 2010), and in turn influence fisheries and compromise food security (Blanchard et al. 2012; Brander 2007). However, drivers of phytoplankton production near oceanic islands and atolls may provide a more favorable outlook. Recent research has suggested localized upwelling may increase resiliency of coral reef ecosystems to future climate change (Karnauskas and Cohen 2012; Storlazzi et al. 2013). Specifically, island-current interactions supply cold, sub-thermocline waters that may buffer island coral reef ecosystems to projected increases in surface ocean temperatures (Karnauskas and Cohen 2012). Similarly, associated nutrient input and subsequent phytoplankton increases may also enhance coral reef ecosystem resiliency. For example, the frequency and the severity of coral bleaching are projected to increase in the coming decades (Hoegh-Guldberg 1999; Pandolfi et al. 2011). Food availability for heterotrophic feeding will potentially counterbalance the more recurrent loss of autotrophic capabilities in corals (Connolly et al. 2012), provided increased resiliency to future climate change (Grottoli et al. 2006). Furthermore, enhanced phytoplankton biomass may offset projected declines in regional ocean production (Doney et al. 2012), resulting in a potentially more promising trajectory for the future of oceanic island- and atoll-reef ecosystems and the marine resource populations they support.

Acknowledgments

This work was part of an interdisciplinary effort by the NOAA Pacific Islands Fisheries Science Center's Coral Reef Ecosystem Division (CRED) to assess, understand, and monitor coral reef ecosystems of the U.S. Pacific. The authors would to thank Rusty Brainard, Principle Investigator of CRED, for his support of this research. We would also like to thank the Chip Young and the NOAA ship *Hi'ialakai* for logistic support and field assistance. Funding for

surveys (as part of the Pacific Reef Assessment and Monitoring Program, RAMP) was provided by NOAA's Coral Reef Conservation Program.

Table 1: Table of information for each of the 35 locations. Locations are oriented based the steepness of a linear fit between long-term chlorophyll-a with distance to shore (i.e. linear fit on log-log transformed chlorophyll-a and distance to shore), from strongest to weakest. *Location Name* is the name of the island(s) or atoll(s), *Location Code* is the three-letter code used in Fig. 1. *Geomorphic Type (Atoll or Island)* is based on primary geomorphological make up. *Lat (latitude)* and *Lon (longitude)* are in degrees north and east, respectively, based on the center point of each location. *Reef Area* (km²) is calculated from 0 – 30 m. *Bathymetric Slope* (°) represents the location average calculated from 30 – 300 m. *Population Status (Remote or Populated)* is based on a human population of 160 people. Locations Codes in bold represent islands and atolls that had significant (p <0.05) relationships between increased chlorophyll-a and decreased distance to shore.

Location Name	Location Code	Geomorphic Type	Lat	Lon	Reef Area	Bathymetric Slope	Population Status
Pearl & Hermes Reef	PHR	Atoll	27.86	-175.85	467.27	5.73	Remote
Maro Reef	MAR	Atoll	25.41	-170.58	1075.44	3.03	Remote
French Frigate Shoals	FFS	Atoll	23.79	-166.21	677.96	4.96	Remote
Lisianski	LIS	Atoll	26.01	-173.95	1004.27	10.21	Remote
Kauai	KAU	Island	22.09	-159.57	241.70	6.22	Populated
Necker	NEC	Island	23.58	-164.70	1028.32	8.4	Remote
Kure	KUR	Atoll	28.42	-178.33	83.15	4.87	Remote
Oahu	OAH	Island	21.49	-158.00	422.72	4.84	Populated
Maui, Lanai, Molokai, Lanai, Kahoolawe	MAUI NUI	Island	20.83	-156.75	450.84	2.68	Populated
Midway	MID	Atoll	28.23	-177.38	101.52	4.7	Remote
Johnston	JOH	Atoll	16.74	-169.52	194.01	23.73	Remote
Tutuila	TUT	Island	-14.30	-170.70	50.89	6.39	Populated
Laysan	LAY	Island	25.78	-171.73	488.13	10.36	Remote
Rose	ROS	Atoll	-14.55	-168.16	7.80	43.61	Remote
Hawaii	HAW	Island	19.53	-155.42	201.67	4.84	Populated
Kingman	KIN	Atoll	6.40	-162.38	47.63	23.88	Remote
Saipan, Tinian, Aguijan	SAI-TIN-AGU	Island	15.01	145.65	95.15	12.20	Populated
Niihau	NII	Island	21.90	-160.15	108.06	5.27	Populated
Wake	WAK	Atoll	19.30	166.62	19.18	41.4	Remote
Guam	GUA	Island	13.46	144.79	94.85	15.16	Populated
Palmyra	PAL	Atoll	5.88	-162.09	52.50	31.91	Remote
Baker	BAK	Island	0.20	-176.48	4.43	26.24	Remote
Farallon de Pajaros	FDP	Island	20.55	144.89	1.38	24.98	Remote
Pagan	PAG	Island	18.11	145.76	16.29	19.89	Remote
Maug	MAU	Island	20.02	145.22	3.17	27.28	Remote
Ofu, Olosega, Tau	MANUA	Island	-14.21	-169.56	22.42	20.53	Populated
Jarvis	JAR	Island	-0.37	-160.00	4.32	29	Remote
Swains	SWA	Island	-11.06	-171.08	2.82	51.41	Remote
Howland	HOW	Island	0.80	-176.62	2.57	26.48	Remote
Guguan	GUG	Island	17.31	145.84	2.00	21.46	Remote
Sarigan	SAR	Island	16.71	145.78	2.00	16.74	Remote
Asuncion	ASC	Island	19.69	145.40	2.54	16.32	Remote
Alamagan	ALA	Island	17.60	145.83	4.28	23.65	Remote
Rota	ROT	Island	14.16	145.21	16.03	12.34	Populated
Agrihan	AGR	Island	18.76	145.66	9.50	23.03	Remote

Table 2. List of potential biogeophysical drivers of increased phytoplankton biomass. Drivers were calculated for each island and atoll and used as predictor variables in the Generalized linear model.

Predictor	Units	Relevant Information	Source
Latitude	Degrees	Center point of each location	Gove et al., 2013
Land Area	km ²	Average area of all emergent land	Gove et al., 2013
Reef Area	km ²	Average area from 0 – 30 m	Gove et al., 2013
Bathymetric Slope	Degrees	Calculated between 30 – 300 m and averaged over the entire location	See methods
Ocean Currents	m s ⁻¹	1° spatial resolution, monthly data	NOAA’s OSCAR (Ocean Surface Current Analysis – Real time)
Precipitation	mm d ⁻¹	2.5° spatial resolution, monthly data	NOAA’s Global Precipitation Climatology Project v2.2
SST	°C	Island-specific data set derived from 4km, weekly data	Gove et al., 2013
Geomorphic Type	Atoll/Island	Based on primary geomorphological make up	Gove et al., 2013
Population Status	Remote/ Populated	Locations were considered ‘populated’ with a human population of >160 people.	Williams et al., 2011

Table 3. Best-fit generalized linear model results identifying the proximate drivers of the island mass effect across 28 U.S.-affiliated islands in the Pacific Ocean. The response variable is the rate of increase of chlorophyll-a with decreased distance the shore (i.e. slope of regression line for a log-log fit) based on average chlorophyll-a over 10-year period. The relative contribution (%) indicates the contribution of each predictor to the overall model performance (Deviance Explained). The optimal model was chosen based on Akaike Information Criteria (AIC).

Response	Predictors	t-value	p-value	Relative Contribution (%)	Deviance Explained (%)	AIC
Regression Slope	Reef Area	3.489	0.0019	27.2		
	Bathymetric Slope	-2.382	0.0258	25.7		
	Geomorphic Type (Island vs. Atoll)	5.778	<0.001	14.0		
	Populations Status (Populated vs. Remote)	3.161	0.0043	10.6	77.56	-100.90

Figure Legends

Fig. 1. Map of long-term mean (July 2002 – June 2012) chlorophyll-*a* concentrations across the Pacific Ocean. Highlighted locations represent the U.S. affiliated islands and atolls used in this study. Table 1 provides additional information pertaining to each location, including the island or atoll name for each of the three-letter location codes presented in the map.

Fig. 2. Long-term averaged (2002 – 2012) chlorophyll-*a* concentrations at Midway Atoll, located at the northwest end of the Hawaiian Archipelago (Fig. 1). 30-m contour (black line) with unfiltered, contaminated information associated with shallow-water bottom reflectance (A). Missing pixels represent islets within the atoll that have been masked prior to data download. Data filtered using the 30-m bathymetric contour (black line), although contaminated information still remains as a result of bottom reflectance (B). Fully cleaned data set using an additional data removal filter (gray area) that is everywhere perpendicular to the 30-m contour, removing all contaminated data associated with bottom reflectance (C).

Fig. 3. Long-term (2002 – 2012) averaged chlorophyll-*a* concentrations at Midway Atoll (A). Inner black line represents the 30-m contour. Gray area represents data removal filter (see Fig. 2). Expanding lines represent exclusive, non-overlapping data inclusion zones, numbered 1 – 8. Mean chlorophyll-*a* values (\pm standard error) calculated by averaging all long-term averaged pixels within each data inclusion zone (B). Significant ($p < 0.05$) nonlinear least squares regression line shown with an $R^2 = 0.95$. The numbers on the x -axis are associated with each data inclusion zone shown in panel A. Distance from shore (km) is also shown for ease of interpretation.

Fig. 4. Relationship between chlorophyll-*a* gradients (i.e. slope of a linear fit on log-log transformed chlorophyll-*a* and distance to shore) and significant predictors from the general linearized model results. Reef area (left) and bathymetric slope (right) accounted for 27.2 and 25.7 % of the variability observed in chlorophyll-*a* gradients, respectively. Islands (squares) and atolls (circles) as well as remote (open) and populated (filled) are shown due the significance of geomorphic type (14.0 %) and population status (10.6 %). No atolls in this study were populated. Significant ($p < 0.05$) nonlinear least squares regression lines are shown with R^2 values of 0.68 and 0.45 for reef area and bathymetric slope, respectively.

Fig. 5. *In situ* chlorophyll-*a* sample locations (black dots) at select islands at atolls throughout the Hawaiian Archipelago (A). Note the inset refers the islands and atolls in the Northwestern Hawaiian Islands and specifically highlights the three locations that are expanded just below; French Frigate Shoals, Lisianski and Pearl and Hermes (from right to left). Chlorophyll-*a* concentrations with distance from shore (B). *In situ* values (open circles) with best fit line (dashed red line) are overlaid long-term averages (mean \pm se; closed circles) and associated best fit line (solid red line). *In situ* data were obtained August – September, 2013. Long-term averages were derived over a 10 year period (July 2002 – June 2012) and are based on sequentially expanding independent zones, where the distance provided represents the average distance from shore for each zone. Oahu showed a significant ($p < 0.05$) increase in *in situ* chlorophyll-*a* with decreased distance to shore ($R^2 = 0.68$), the only location to do so. All fits for long-term averages were significant ($p < 0.05$) with R^2 values of 0.83 – 0.97.

Fig. 1

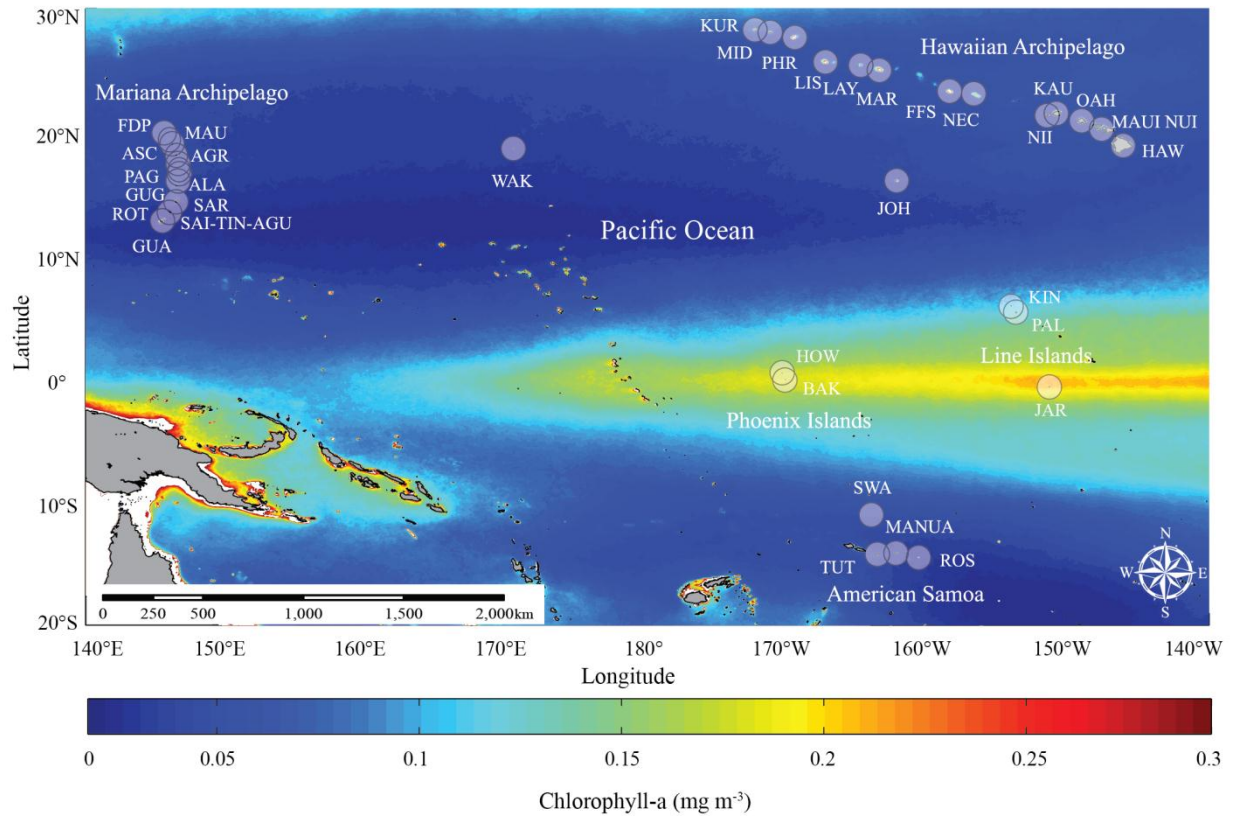


Fig. 2

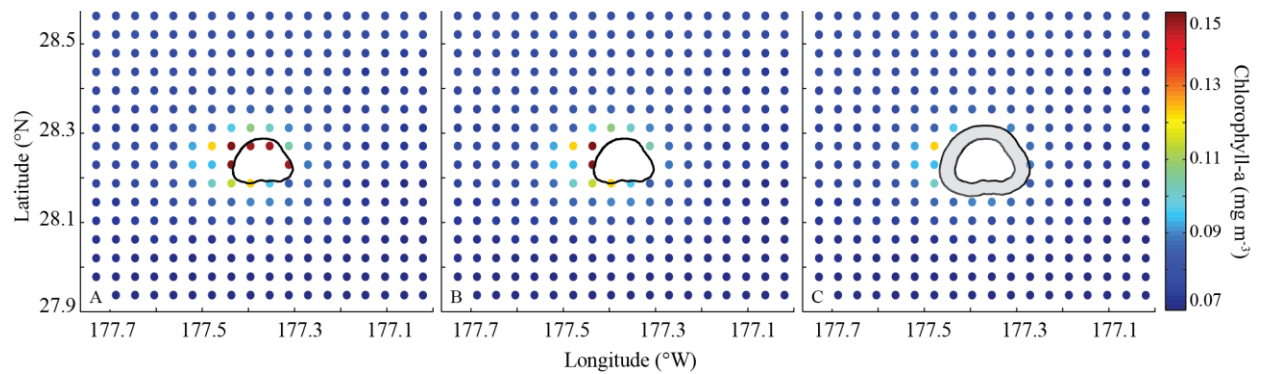


Fig. 3

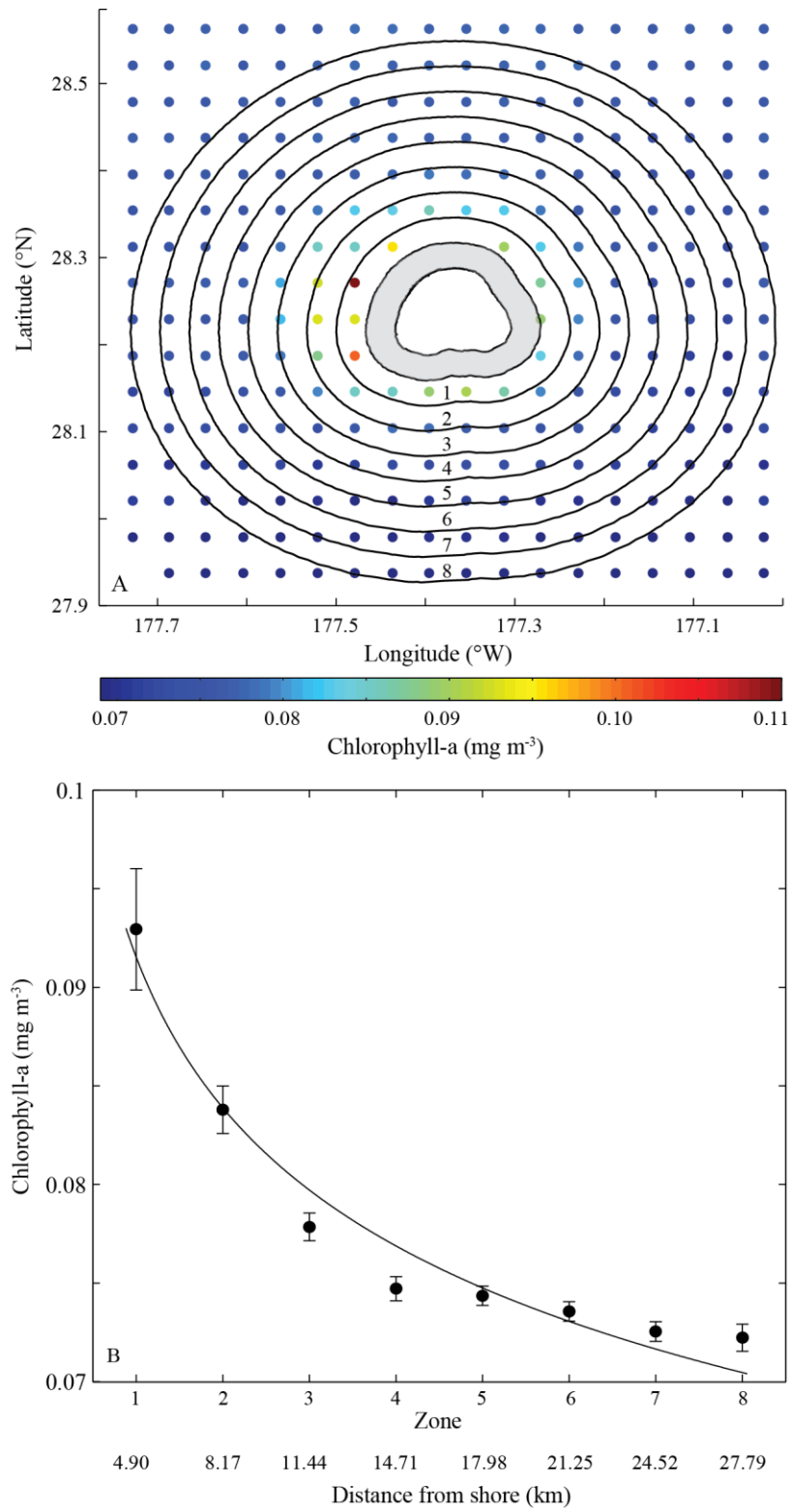


Fig. 4

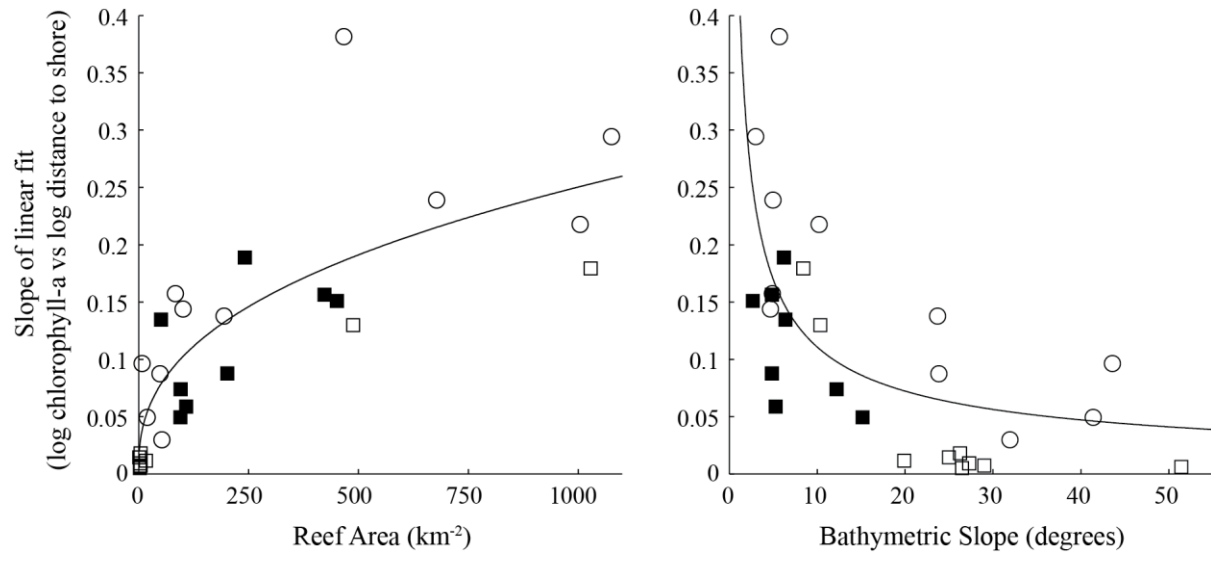
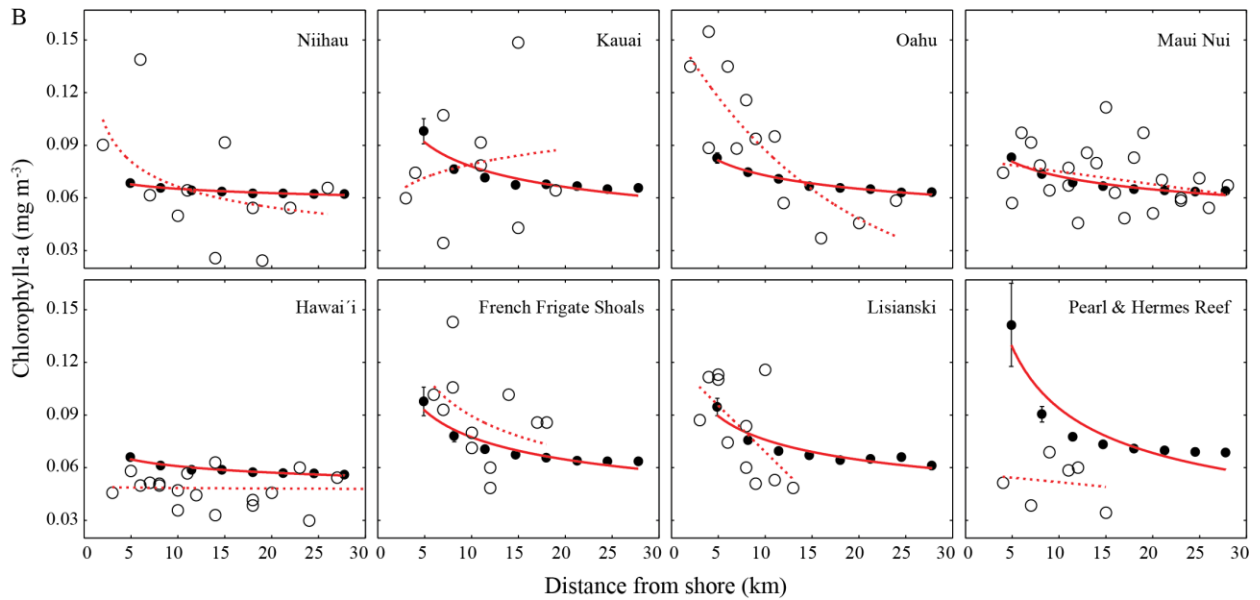
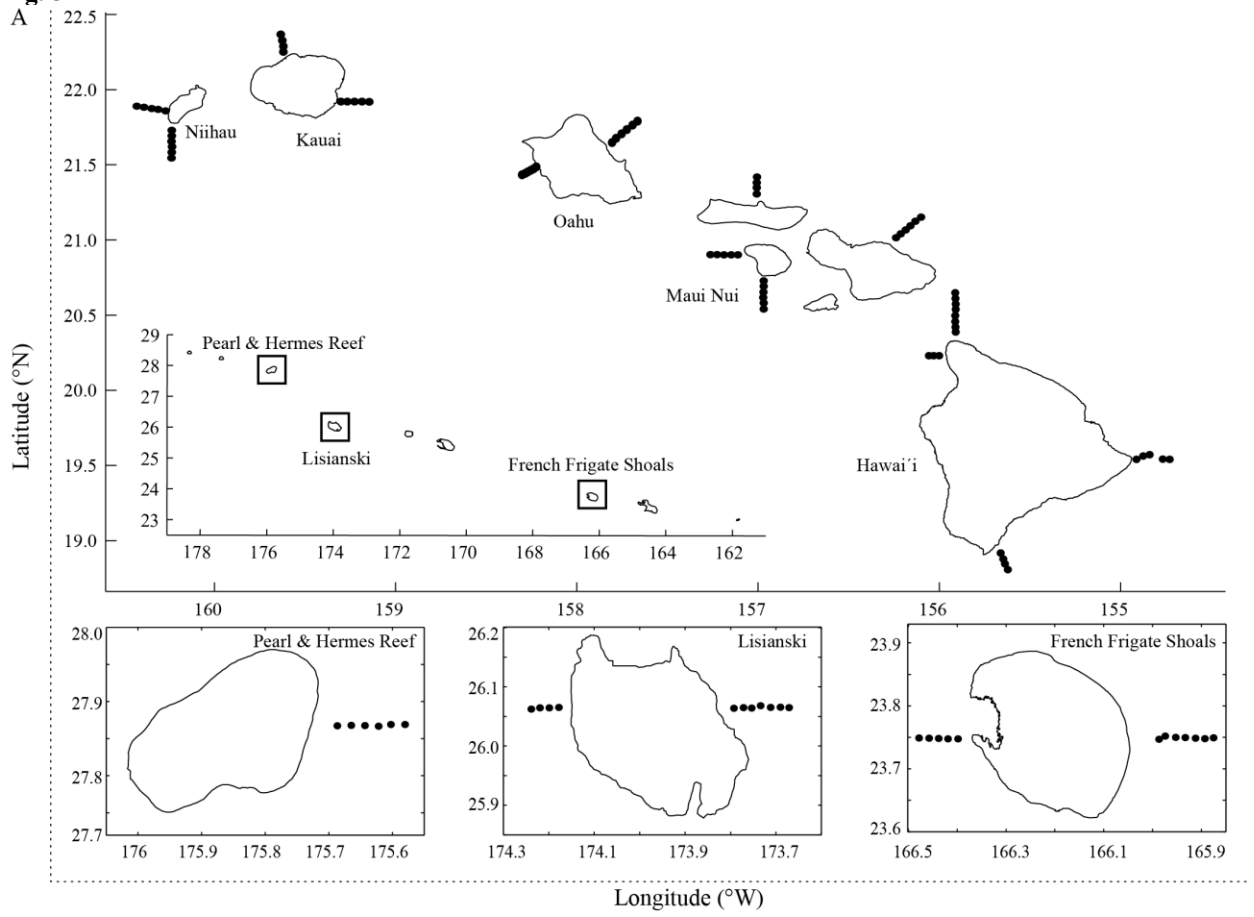


Fig. 5



References

- Adler, R. F. and others 2003. The Version-2 Global Precipitation Climatology Project (GPCP) Monthly Precipitation Analysis (1979–Present). *Journal of Hydrometeorology* **4**: 1147-1167.
- Anderson, D. M., P. M. Glibert, and J. M. Burkholder. 2002. Harmful algal blooms and eutrophication: nutrient sources, composition, and consequences. *Estuaries* **25**: 704-726.
- Anthony, K. R. N., and K. E. Fabricius. 2000. Shifting roles of heterotrophy and autotrophy in coral energetics under varying turbidity. *J Exp Mar Biol Ecol* **252**: 221-253.
- Anthony, K. R. N., P. V. Ridd, A. R. Orpin, P. Larcombe, and J. Lough. 2004. Temporal Variation of Light Availability in Coastal Benthic Habitats: Effects of Clouds, Turbidity, and Tides. *Limnol Oceanogr* **49**: 2201-2211.
- Atkinson, M. 2011. Biogeochemistry of Nutrients, p. 199-206. *In* Z. Dubinsky and N. Stambler [eds.], *Coral Reefs: An Ecosystem in Transition*. Springer Netherlands.
- Aucan, J., R. Hoeke, and M. A. Merrifield. 2012. Wave-driven sea level anomalies at the Midway tide gauge as an index of North Pacific storminess over the past 60 years. *Geophys Res Lett* **39**: L17603.
- Baird, R. W., D. L. Webster, S. D. Mahaffy, D. J. Mcsweeney, G. S. Schorr, and A. D. Ligon. 2008. Site fidelity and association patterns in a deep-water dolphin: Rough-toothed dolphins (*Steno bredanensis*) in the Hawaiian Archipelago. *Marine Mammal Science* **24**: 535-553.
- Bak, R. P. M., M. Joenje, I. D. Jong, D. Y. M. Lambrechts, and G. Nieuwland. 1998. Bacterial suspension feeding by coral reef benthic organisms. *Marine Ecology Progress Series* **175**: 285-288.
- Becker, J. J. and others 2009. Global Bathymetry and Elevation Data at 30 Arc Seconds Resolution: SRTM30_PLUS. *Marine Geodesy* **32**: 355-371.
- Benoit-Bird, K. J., and W. W. L. Au. 2003a. Echo strength and density structure of Hawaiian mesopelagic boundary community patches. *The Journal of the Acoustical Society of America* **114**: 1888-1897.
- Benoit-Bird, K. J., and W. W. L. Au. 2003b. Prey dynamics affect foraging by a pelagic predator (*Stenella longirostris*) over a range of spatial and temporal scales. *Behav Ecol Sociobiol* **53**: 364-373.
- . 2006. Extreme diel horizontal migrations by a tropical nearshore resident micronekton community. *Marine Ecology Progress Series* **319**: 1-14.
- Benoit-Bird, K. J., W. W. L. Au, R. E. Brainard, and M. O. Lammers. 2001. Diel horizontal migration of the Hawaiian mesopelagic boundary community observed acoustically. *Marine Ecology Progress Series* **217**: 1-14.
- Blanchard, J. L. and others 2012. Potential consequences of climate change for primary production and fish production in large marine ecosystems. *Philosophical Transactions of the Royal Society B: Biological Sciences* **367**: 2979-2989.
- Boss, E., and J. R. V. Zaneveld. 2003. The effect of bottom substrate on inherent optical properties: Evidence of biogeochemical processes. *Limnol Oceanogr* **48**: 346-354.
- Brander, K. M. 2007. Global fish production and climate change. *Proceedings of the National Academy of Sciences* **104**: 19709-19714.
- Brill, R. W., B. A. Block, C. H. Boggs, K. A. Bigelow, E. V. Freund, and D. J. Marcinek. 1999. Horizontal movements and depth distribution of large adult yellowfin tuna (*Thunnus*

- albacares) near the Hawaiian Islands, recorded using ultrasonic telemetry: implications for the physiological ecology of pelagic fishes. *Mar Biol* **133**: 395-408.
- Bucciarelli, E., S. Blain, and P. Tréguer. 2001. Iron and manganese in the wake of the Kerguelen Islands (Southern Ocean). *Marine Chemistry* **73**: 21-36.
- Burkepile, D. E. and others 2013. Nutrient supply from fishes facilitates macroalgae and suppresses corals in a Caribbean coral reef ecosystem. *Scientific reports* **3**.
- Callaghan, D. P., P. Nielsen, N. Cartwright, M. R. Gourlay, and T. E. Baldock. 2006. Atoll lagoon flushing forced by waves. *Coast Eng* **53**: 691-704.
- Caperon, J., S. A. Cattell, and G. Krasnick. 1971. Phytoplankton Kinetics in a Subtropical Estuary: Eutrophication. *Limnol Oceanogr* **16**: 599-607.
- Carder, K. L., Chen, R.F., Hawes, S.K. 2003. Instantaneous Photosynthetically Available Radiation and Absorbed Radiation by Phytoplankton: Algorithm Theoretical Basis Document *In* M. O. S. Team [ed.]. National Aeronautics and Space Administration.
- Carter, G. S., M. C. Gregg, and M. A. Merrifield. 2006. Flow and Mixing around a Small Seamount on Kaena Ridge, Hawaii. *Journal of Physical Oceanography* **36**: 1036-1052.
- Chassot, E. and others 2010. Global marine primary production constrains fisheries catches. *Ecol Lett* **13**: 495-505.
- Connolly, S. R., M. A. Lopez-Yglesias, and K. R. N. Anthony. 2012. Food availability promotes rapid recovery from thermal stress in a scleractinian coral. *Coral Reefs* **31**: 951-960.
- Coutis, P. F., and J. H. Middleton. 1999. Flow-topography interaction in the vicinity of an isolated, deep ocean island. *Deep Sea Research Part I: Oceanographic Research Papers* **46**: 1633-1652.
- Dandonneau, Y., and L. Charpy. 1985. An empirical approach to the island mass effect in the south tropical Pacific based on sea surface chlorophyll concentrations. *Deep Sea Research Part A. Oceanographic Research Papers* **32**: 707-721.
- Doney, S. C. 2010. The Growing Human Footprint on Coastal and Open-Ocean Biogeochemistry. *Science* **328**: 1512-1516.
- Doney, S. C. and others 2012. Climate Change Impacts on Marine Ecosystems. *Annu Rev Mar Sci* **4**: 11-37.
- Doty, M. S., and M. Oguri. 1956. The Island Mass Effect. *Journal du Conseil* **22**: 33-37.
- Duarte, C., and J. Cebrian. 1996. The fate of marine autotrophic production. *Limnol Oceanogr* **41**: 1758-1766.
- Fabricius, K., G. De'ath, L. Mccook, E. Turak, and D. M. Williams. 2005. Changes in algal, coral and fish assemblages along water quality gradients on the inshore Great Barrier Reef. *Mar Pollut Bull* **51**: 384-398.
- Fabricius, K. E. 2005. Effects of terrestrial runoff on the ecology of corals and coral reefs: review and synthesis. *Mar Pollut Bull* **50**: 125-146.
- Gierach, M. M., M. Messié, T. Lee, K. B. Karnauskas, and M.-H. Radenac. 2013. Biophysical Responses near Equatorial Islands in the Western Pacific Ocean during El Niño/La Niña Transitions. *Geophys Res Lett*: 2013GL057828.
- Gilmartin, M., and N. Revelante. 1974. The 'island mass' effect on the phytoplankton and primary production of the Hawaiian Islands. *J Exp Mar Biol Ecol* **16**: 181-204.
- Gove, J. M., M. A. Merrifield, and R. E. Brainard. 2006. Temporal variability of current-driven upwelling at Jarvis Island. *Journal of Geophysical Research: Oceans* **111**: C12011.
- Gove, J. M. and others 2013. Quantifying Climatological Ranges and Anomalies for Pacific Coral Reef Ecosystems. *Plos One* **8**: e61974.

- Grigg, R. W. 1983. Community Structure, Succession and Development of Coral Reefs in Hawaii. *Mar Ecol-Prog Ser* **11**: 1-14.
- Grottoli, A. G., L. J. Rodrigues, and J. E. Palardy. 2006. Heterotrophic plasticity and resilience in bleached corals. *Nature* **440**: 1186-1189.
- Hamner, W. M., and I. R. Hauri. 1981. Effects of island mass: Water flow and plankton pattern around a reef in the Great Barrier Reef Lagoon, Australia. *Limnol Oceanogr* **26**: 1084-1102.
- Hernández-León, S. 1991. Accumulation of mesozooplankton in a wake area as a causative mechanism of the "island-mass effect". *Mar Biol* **109**: 141-147.
- Hoegh-Guldberg, O. 1999. Climate change, coral bleaching and the future of the world's coral reefs. *Marine and Freshwater Research* **50**: 839-866.
- Holland, K. N., R. W. Brill, and R. K. C. Chang. 1990. Horizontal and vertical movements of yellowfin and bigeye tuna associated with fish aggregating devices. *Fishery Bulletin* **88**: 493-507.
- Iverson, R. L. 1990. Control of Marine Fish Production. *Limnol Oceanogr* **35**: 1593-1604.
- Jennings, S., F. Mélin, J. L. Blanchard, R. M. Forster, N. K. Dulvy, and R. W. Wilson. 2008. Global-scale predictions of community and ecosystem properties from simple ecological theory. *Proceedings of the Royal Society B: Biological Sciences* **275**: 1375-1383.
- Karnauskas, K. B., and A. L. Cohen. 2012. Equatorial refuge amid tropical warming. *Nature Clim. Change* **2**: 530-534.
- Kilpatrick, K. A., G. P. Podesta, and R. Evans. 2001. Overview of the NOAA/NASA advanced very high resolution radiometer Pathfinder algorithm for sea surface temperature and associated matchup database. *J Geophys Res-Oceans* **106**: 9179-9197.
- Leichter, J. J., and S. L. Miller. 1999. Predicting high-frequency upwelling: Spatial and temporal patterns of temperature anomalies on a Florida coral reef. *Cont Shelf Res* **19**: 911-928.
- Leichter, J. J., G. Shellenbarger, S. J. Genovese, and S. R. Wing. 1998. Breaking internal waves on a Florida (USA) coral reef: a plankton pump at work? *Marine Ecology Progress Series* **166**: 83-97.
- Leichter, J. J., H. L. Stewart, and S. L. Miller. 2003. Episodic nutrient transport to Florida coral reefs. *Limnol Oceanogr*: 1394-1407.
- Leichter, J. J., M. D. Stokes, J. L. Hench, J. Witting, and L. Washburn. 2012. The island-scale internal wave climate of Moorea, French Polynesia. *Journal of Geophysical Research: Oceans* **117**: C06008.
- Maina, J., T. R. Mcclanahan, V. Venus, M. Ateweberhan, and J. Madin. 2011. Global Gradients of Coral Exposure to Environmental Stresses and Implications for Local Management. *Plos One* **6**.
- Mcmanus, M. A., K. J. Benoit-Bird, and C. Brock Woodson. 2008. Behavior exceeds physical forcing in the diel horizontal migration of the midwater sound-scattering layer in Hawaiian waters. *Marine Ecology Progress Series* **365**: 91-101.
- Merrifield, M. A., and P. E. Holloway. 2002. Model estimates of M2 internal tide energetics at the Hawaiian Ridge. *Journal of Geophysical Research: Oceans* **107**: 5-1-5-12.
- Mumby, P. J. and others 2004. Remote sensing of coral reefs and their physical environment. *Mar Pollut Bull* **48**: 219-228.
- Musyl, M. K., R. W. Brill, C. H. Boggs, D. S. Curran, T. K. Kazama, and M. P. Seki. 2003. Vertical movements of bigeye tuna (*Thunnus obesus*) associated with islands, buoys, and

- seamounts near the main Hawaiian Islands from archival tagging data. *Fisheries Oceanography* **12**: 152-169.
- Palacios, D. M. 2002. Factors influencing the island-mass effect of the Galapagos Archipelago. *Geophys Res Lett* **29**: 2134.
- Pandolfi, J. M., S. R. Connolly, D. J. Marshall, and A. L. Cohen. 2011. Projecting Coral Reef Futures Under Global Warming and Ocean Acidification. *Science* **333**: 418-422.
- Papastamatiou, Y. P., C. G. Meyer, F. Carvalho, J. J. Dale, M. R. Hutchinson, and K. N. Holland. 2013. Telemetry and random-walk models reveal complex patterns of partial migration in a large marine predator. *Ecology* **94**: 2595-2606.
- Pastorok, R. A., and G. R. Bilyard. 1985. Effects of sewage pollution on coral-reef communities. *Marine Ecology Progress Series* **21**: 175-189.
- Pauly, D., and V. Christensen. 1995. Primary production required to sustain global fisheries. *Nature* **376**: 279-279.
- Pernthaler, J. 2005. Predation on prokaryotes in the water column and its ecological implications. *Nat Rev Micro* **3**: 537-546.
- Poloczanska, E. S. and others 2013. Global imprint of climate change on marine life. *Nature Clim. Change* **3**: 919-925.
- Reid, S. B., J. Hirota, R. E. Young, and L. E. Hallacher. 1991. Mesopelagic-boundary community in Hawaii: Micronekton at the interface between neritic and oceanic ecosystems. *Mar Biol* **109**: 427-440.
- Roder, C., L. Fillinger, C. Jantzen, G. M. Schmidt, S. Khokiattiwong, and C. Richter. 2010. Trophic response of corals to large amplitude internal waves. *Marine Ecology Progress Series* **412**: 113-128.
- Rooney, J. and others 2008. Geology and Geomorphology of Coral Reefs in the Northwestern Hawaiian Islands, p. 519-571. *In* B. Riegl and R. Dodge [eds.], *Coral Reefs of the USA. Coral Reefs of the World*. Springer Netherlands.
- Sander, F. 1981. A preliminary assessment of the main causative mechanisms of the "island mass" effect of Barbados. *Mar Biol* **64**: 199-205.
- Sander, F., and D. M. Steven. 1973. Organic productivity of inshore and offshore waters of Barbados: A study of the island mass effect. *B Mar Sci* **23**: 771-792.
- Schils, T., P. S. Vroom, and A. D. Tribollet. 2013. Geographical partitioning of marine macrophyte assemblages in the tropical Pacific: a result of local and regional diversity processes. *J Biogeogr* **40**: 1266-1277.
- Sebens, K. P., K. S. Vandersall, L. A. Savina, and K. R. Graham. 1996. Zooplankton capture by two scleractinian corals, *Madracis mirabilis* and *Montastrea cavernosa*, in a field enclosure. *Mar Biol* **127**: 303-317.
- Sevadjian, J. C., M. A. Mcmanus, K. J. Benoit-Bird, and K. E. Selph. 2012. Shoreward advection of phytoplankton and vertical re-distribution of zooplankton by episodic near-bottom water pulses on an insular shelf: Oahu, Hawaii. *Cont Shelf Res* **50-51**: 1-15.
- Signorini, S. R., C. R. McClain, and Y. Dandonneau. 1999. Mixing and phytoplankton bloom in the wake of the Marquesas Islands. *Geophys. Res. Lett.* **26**: 3121-3124.
- Smith, S. V., W. J. Kimmerer, E. A. Laws, R. E. Brock, and T. W. Walsh. 1981. Kaneohe Bay sewage diversion experiment: perspectives on ecosystem responses to nutritional perturbation.

- Smith, V. H., G. D. Tilman, and J. C. Nekola. 1999. Eutrophication: impacts of excess nutrient inputs on freshwater, marine, and terrestrial ecosystems. *Environmental Pollution* **100**: 179-196.
- Smith, W. H. F., and D. T. Sandwell. 1997. Global Sea Floor Topography from Satellite Altimetry and Ship Depth Soundings. *Science* **277**: 1956-1962.
- Storlazzi, C. D., M. E. Field, O. M. Cheriton, M. K. Presto, and J. B. Logan. 2013. Rapid fluctuations in flow and water-column properties in Asan Bay, Guam: implications for selective resilience of coral reefs in warming seas. *Coral Reefs*: 1-13.
- Strickland, J. D. H., and T. R. Parsons. 1972. *A Practical Handbook of Seawater Analysis*. Fisheries Research Board of Canada.
- Suzuki, Y., and B. E. Casareto. 2011. The Role of Dissolved Organic Nitrogen (DON) in Coral Biology and Reef Ecology, p. 207-214. *In* Z. Dubinsky and N. Stambler [eds.], *Coral Reefs: An Ecosystem in Transition*. Springer Netherlands.
- Swearer, S. E., J. E. Caselle, D. W. Lea, and R. R. Warner. 1999. Larval retention and recruitment in an island population of a coral-reef fish. *Nature* **402**: 799-802.
- Vitousek, P. M. and others 1997a. Human Alteration of the Global Nitrogen Cycle: Sources and Consequences. *Ecol Appl* **7**: 737-750.
- Vitousek, P. M., H. A. Mooney, J. Lubchenco, and J. M. Melillo. 1997b. Human Domination of Earth's Ecosystems. *Science* **277**: 494-499.
- Williams, G. J., J. M. Gove, B. J. Zgliczynski, and S. A. Sandin. 2013. Local human impacts and regional scale gradients in environmental forcings drive coral reef benthic community organisation across the Pacific. *Global Ecology and Biogeography*. In review.
- Williams, I. D. and others 2011. Differences in Reef Fish Assemblages between Populated and Remote Reefs Spanning Multiple Archipelagos Across the Central and Western Pacific. *Journal of Marine Biology* **2011**.
- Williams, S. L., and R. C. Carpenter. 1988. Nitrogen-limited primary productivity of coral reef algal turfs: potential contribution of ammonium excreted by *Diadema antillarum*. *Marine Ecology Progress Series* **47**: 145-152.
- Wolanski, E., and E. Deleersnijder. 1998. Island-generated internal waves at Scott Reef, Western Australia. *Cont Shelf Res* **18**: 1649-1666.
- Wolanski, E., and B. Delesalle. 1995. Upwelling by internal waves, Tahiti, French Polynesia. *Cont Shelf Res* **15**: 357-368.
- Wolanski, E., and W. Hamner. 1988. Topographically Controlled Fronts in the Ocean and Their Biological Influence. *Science* **241**: 177-181.
- Wooldridge, S. A. 2009. Water quality and coral bleaching thresholds: Formalising the linkage for the inshore reefs of the Great Barrier Reef, Australia. *Mar Pollut Bull* **58**: 745-751.

CHAPTER IV

**INTRA-ISLAND GRADIENTS IN PHYSICAL FORCINGS DRIVE SPATIAL
PATTERNING IN CORAL REEF BENTHIC COMMUNITIES**

Jamison M. Gove^{1,2}, Gareth J. Williams³, Margaret A. McManus⁴, Jeanette S. Clark⁴, Julia S. Ehses^{1,2}, Lisa M. Wedding⁵

¹Coral Reef Ecosystem Division, NOAA Pacific Islands Fisheries Science Center, Honolulu, Hawai'i, United States of America

²Joint Institute for Marine and Atmospheric Research, University of Hawai'i at Mānoa, Honolulu, Hawai'i, United States of America

³Center for Marine Biodiversity and Conservation, Scripps Institution of Oceanography, La Jolla, California, United States of America

⁴School of Ocean and Earth Science and Technology, University of Hawai'i at Mānoa, Honolulu, Hawai'i, United States of America

⁵Center for Ocean Solutions, Stanford University, Monterey, California, United States of America

Abstract

This study focused on a remote oceanic atoll in the central equatorial Pacific with over a half-century of minimal human influence to assess the independent effects of physical forcings in structuring coral reef benthic communities in the absence of local human impacts. Moored in situ oceanographic measurements, combined with a nearshore numerical model, revealed complex intra-island gradients in physical forcings influenced by a combination of regional currents, offshore bathymetry, and spatial differences in the prevailing wave climate. Benthic community composition, assessed via towed-diver imagery collected in a complete circumnavigation of the atoll, exhibited considerable spatial heterogeneity and evidence of distinct shifts in benthic community regimes. Predictive modeling (boosted regression trees) highlighted bed shear stress (BSS) and reef geomorphology as key physical drivers of community structure, with distinct biophysical relationships among key benthic competitors. For example, the cover of crustose coralline algae (CCA) was negatively related to mean BSS, while turf algae (a key competitor of CCA), was positively related. Model performance varied (52 – 79% variation explained) and improved 3 – 5 fold when hard coral cover was modeled in distinct morphological groups (encrusting, plating, branching). Our results highlight the flexibility of benthic communities to reorganize in response to extrinsic physical forcings on coral reefs.

Introduction

From ocean basins to individual organisms, physical oceanographic forcings influence benthic coral reef community dynamics. For example, the global latitudinal range in temperature is a principle driver in the geographic extent of reef-building corals (Kleypas et al. 1999). Across islands, eddies and wake effects can provide an allocthonous source of nutrients, effecting food web dynamics and enhancing reef ecosystem productivity (Wolanski and Hamner 1988). At the single coral colony level, water motion can regulate the thickness of benthic boundary layers, mediating mass transfer and nutrient uptake (Atkinson and Bilger 1992; Thomas and Atkinson 1997).

Within individual islands and atolls, current fluctuations and wave energy are key forcings driving coral reef benthic community organization. For example, current-topographic interactions can drive vertical transport of oceanic water masses (Hendry and Wunsch 1973), delivering cold, nutrient-rich waters to shallow-water benthic coral reef communities (Andrews and Gentien 1982). Similarly, internal wave events caused by tidal currents interacting with steep topography can lead to localized, high-frequency variations in water flow, temperature, nutrients, and suspended particles (Leichter et al. 1998). Internal waves influence benthic production (Leichter et al. 2003), coral and algal growth rates (Roder et al. 2010; Smith et al. 2004) and drive intra-island gradients in benthic communities (Roder et al. 2010). Gradients in wave forcing also drive benthic community spatial patterns and species zonation (Bradbury and Young 1981; Dollar 1982; Done 1982). High wave energy can reduce overall coral cover and favor wave-tolerant morphologies, such as encrusting or thickly branched corymbose corals (Dollar 1982; Madin et al. 2006; Storlazzi et al. 2005). Repeated wave forcing may also shift the benthic community to low-lying, fast-growing algal species, such as turf and crustose coralline algae

(Williams et al. 2013). Therefore, long-term gradients in physical forcings should lead to clear spatial patterning in the benthic community as it organizes to adapt to local conditions (Hughes et al. 2012), even within an island system (Williams et al. 2013).

Human activities can also heavily influence coral reef benthic community structure. Urbanization, coastal development and land use can cause increased sedimentation and nutrient enrichment to coastal marine ecosystems, resulting in reef degradation and coral mortality (Fabricius et al. 2005; Wooldridge 2009). Similarly, overfishing, particularly the depletion of herbivorous fishes, can alter competitive interactions within the benthic community (McCook et al. 2001) and lead to alternate benthic regimes (Hughes 1994; Nyström et al. 2000) and a loss of ecosystem structure and function (Done 1992; Jackson et al. 2001). Human disturbance can therefore fundamentally alter biophysical interactions in coral reef ecosystems, making it challenging to distinguish between natural and human-induced shifts in community organization.

In this study, we used Palmyra Atoll – a remote, steep-sided, oceanic atoll that has been exposed to minimal human influence over the last half century – to examine intrinsic biophysical relationships in coral reef ecosystems (Fig. 1). Specifically, our aim was to assess the effects of key physical forcings on coral reef benthic community organization in the absence of confounding local human impacts. To address this overall goal, we assessed intra-island gradients in oceanographic conditions (currents, temperature, and waves) collected from six equally spaced locations around the perimeter of Palmyra over a year-long period. In situ wave data were used to ground-truth a global wave model to set boundary conditions for a coupled hydrodynamic-wave model, enabling a high spatial resolution assessment of wave-induced stress on the benthos. We examined spatial distributions in coral reef benthic communities from quantitative analysis of thousands of digital images collected via towed divers in a complete

circumnavigation of Palmyra (~40 km of coastline). Specifically, we quantified percent cover of five benthic functional groups (hard coral, crustose coralline algae (CCA), macroalgae, turf algae, soft coral) as well as specific coral morphologies (encrusting, plating, branching). We then used boosted regression trees (BRT) to examine the relationships between the benthic response variables (e.g. coral cover) and the environmental predictor variables, specifically wave forcing (i.e. bed shear stress) and reef geomorphological characteristics (i.e. reef slope, slope of slope, bathymetric position index).

Materials and Methods

Study site – Palmyra Atoll is a remote, oceanic atoll in the northern Line Islands in the equatorial Pacific, approximately 1600 km south of Hawai‘i (Fig. 1). Palmyra’s coral reef ecosystem is dominated by calcifying (reef-building) benthic organisms and a fish community characterized by high biomass and large numbers of predators (Demartini et al. 2008; Sandin et al. 2008; Williams et al. 2013). Over the past half century, Palmyra has experienced limited human influence, with official protection as a U.S. National Wildlife Refuge in 2001 and further protection under the recently established Pacific Remote Islands Marine National Monument in 2009.

Oceanographic data – In situ oceanographic moorings were deployed at six forereef locations roughly equally spaced around Palmyra (Fig. 1). All moorings were affixed to the benthos at ~20 m. High-frequency temperature data were collected at all six moorings using a Sea Bird Electronics SBE 37 (accuracy of 0.002°C) at 150 s sampling interval. Profiling current and spectral wave data were collected at a subset of these locations (i.e. Northwest, Northeast, Southeast, and Southwest; Fig. 1) with a 1 MHz Nortek Aquadopp acoustic Doppler profiler

(ADP). Currents were sampled at 1 m depth bins averaged over 35 s for every 60 s. Wave data were burst sampled at 2 Hz for 20 min every 3 h and processed using Nortek's QuickWave v.2.10. Oceanographic sensors were programmed to record information beginning in April 2010. Individual data set lengths varied due to battery and/or instrument failure (Table 1).

Island-specific climatological and time series data of sea surface temperature (SST) and wave energy were obtained from Gove et al. (2013). SST data were derived from 4 km Pathfinder v5.0 (<http://pathfinder.nodc.noaa.gov>) and wave energy was calculated from NOAA's Wave Watch III (WWIII; <http://polar.ncep.noaa.gov/waves>); a global, full spectral wave model at one-degree spatial resolution. Ocean current data were obtained from NOAA's OSCAR (Ocean Surface Current Analysis – Real time; www.oscar.noaa.gov); a one-degree monthly data set. Monthly climatological calculations were from 1993 – 2010. The Multivariate ENSO Index (MEI) was obtained from NOAA's Earth System Research Lab (www.esrl.noaa.gov).

Waves – We quantified wave information at temporal scales corresponding to ecological data collection using time series data from WWIII. Specifically, we incorporated the one-degree, 3-hr output of mean significant wave height (H_s), peak period (T_p), and peak direction (θ_p).

WWIII model performance at Palmyra was assessed by comparing the model with in situ wave data sets at each wave sensor location (Fig. 1). Wave power or wave energy flux (henceforth referred to as wave energy), in kilowatts per meter (kW m^{-1}), was calculated for both data sets based on the following equation:

$$E_f = \frac{\rho g^2}{64\pi} H_s^2 T_p * 1000$$

where ρ is the density of seawater (1024 kg m^{-3}) and g is the acceleration of gravity (9.8 m s^{-2}).

Wave energy combines H_s and T_p and provided a more representative metric of the most powerful wave events than either H_s or T_p . The 15 largest wave events (event = maximum daily

wave energy) from each sensor were identified, and differences between WWIII and in situ wave parameters were calculated for each event. The mean difference in H_s , T_p and θ_p was then used as a correction factor for peak wave events in the WWIII data record. Comparisons between data sets were constrained to incident (i.e. perpendicular) swell angles at each sensor, minimizing shadowing and other wave-bathymetry interactions (e.g. refraction) that would bias the comparisons. Wave events captured at the Northwest mooring (Fig. 1) were limited due to instrument flooding and data collection occurring in boreal summer – a lull in northern hemisphere wave activity. However, we captured two wave events originating from the northwest and found no difference in H_s , T_p , and θ_p ; therefore, no WWIII correction was applied for northwest swell events.

To provide a high-resolution, nearshore spatial assessment of wave forcing at Palmyra, we used a coupled hydrodynamic model developed by Delft Hydraulics (Delft3D; <http://oss.deltares.nl/web/delft3d>). Delft3D resolves complex processes such as wave propagation, refraction, wind generation, dissipation, and non-linear wave-wave interactions. A full description of the model is given by Lesser et al. (2004), with detailed information on the waves portion of the model given by Booij et al. (1999).

A total of three model runs were performed, one for each wave regime (Fig. 1): northwest swell ($H_s = 3.4$ m, $T_p = 16.9$ s, $\theta_p = 330^\circ$), northeast trade wind swell ($H_s = 4$ m, $T_p = 10$ s, $\theta_p = 41^\circ$), and south swell ($H_s = 2.8$ m, $T_p = 14$ s, $\theta_p = 172^\circ$). Modeled wave conditions corresponded to a wave regime-specific annual maximum H_s , T_p , and θ_p , calculated by averaging the largest annual events for each wave regime from January 2005 – April 2010 ($n = 5$). This represented one calendar year prior to the first ecological survey up to the most recent ecological survey used in this analysis. Each model was run on a 7x20 km rectangular grid with a 50 m resolution and a

1 min time step over a 12 hr period, with a coupling interval of 1 hr between wave and current models. Water level (0.3 m) and winds (5 m s^{-1} from the northeast) were held constant over the model runs, representing average tidal and wind conditions for Palmyra.

Bed shear stress – hydrodynamic stress induced by waves and currents near the benthic-water interface – was used here to represent wave forcing at Palmyra. Bed shear stress was chosen over more traditional wave metrics (e.g. wave height) because it specifically quantifies forcing at the depth of benthic organisms and is a major determinant of benthic coral community composition on wave-dominated reefs (Storlazzi et al. 2005). In the model, wave- and current-induced bed shear stress were combined following parameterizations from Soulsby et al. (1993) that account for the enhancement of bed shear stress due to non-linear wave-current interactions. Full representations of wave- and current-induced bed shear stress are given by Lesser et al. (2004). Following both numerical models and observations in similar coral reef environments, the wave friction factor was set to 0.3 (Péquignot et al., 2011; Storlazzi et al., 2002; Van Dongeren et al., 2013), and the current friction factor was set to 0.2 (Hench et al. 2008; Lowe et al. 2009; Van Dongeren et al. 2013). The numerical model was run under all three wave regimes (i.e. northwest swell, northeast trade wind swell, and south swell) Palmyra is exposed to and combined to calculate an annual average maximum, mean, and range in H_s , T_p , and bed shear stress.

Subsurface temperature variability – Time series of temperature data at each of the six mooring locations revealed rapid, successive pulses of colder waters ($0.3 - 1.8^\circ$) multiple times per day. Following Sevadjan et al. (2012), we quantified the total number of cold pulses based on the following equations:

$$\frac{T_{i+n} - T_i}{t_{i+n} - t_i} \leq -0.3^\circ\text{C} (240 \text{ min})^{-1}$$

$$T_{i+n} - T_i \leq -0.3^{\circ}\text{C}$$

where T is temperature, t is time, and for the i th temperature measurement, $n = 1, 2, 3, \dots, m$. To be considered a cold pulse, the following criteria had to be satisfied: (1) the rate of change of temperature (T) with respect to time (t) must maintain a gradient of $\leq -0.3^{\circ}\text{C}/240$ min, and (2) the total decrease in temperature (ΔT) must be $\leq -0.3^{\circ}\text{C}$. The duration of a cold pulse was the time from the initial decrease in temperature to the minimum temperature. A cold pulse ended when temperature returned to $0.5 * \Delta T$. Cold pulse events extending beyond tidal frequencies (> 12 h) were not included in these analyses.

Geomorphological data – Multibeam bathymetric data were collected during NOAA’s Reef Assessment and Monitoring Program (RAMP) surveys of Palmyra aboard the NOAA Ship *Hi’ialakai* and the survey launch R/V *AHI* (Acoustic Habitat Investigator). The *Hi’ialakai* is equipped with two Kongsberg/Simrad multibeam sonars: a 30-kHz EM300 with mapping capability from ~100 – 3000+ m and a 300-kHz EM3002D with mapping capability from ~5 – 150 m. The R/V *AHI* has a 240-kHz Reson 8101ER with mapping capability from ~5 – 300 m. Both vessels have Applanix POS/MV motion sensors, which provide navigation and highly accurate readings of the vessel motion in all axes. Data were post-processed data and provided in a gridded format by the Pacific Islands Benthic Habitat Mapping Center (<http://www.soest.hawaii.edu/pibhmc>). Multibeam data collection was incomplete from 0 – 30 m depth due to navigational hazards associated with shallow reef environments. To create a seamless bathymetric product, IKONOS images can be used to create “estimated depths” to fill bathymetric gaps in very shallow water areas (Stumpf et al. 2003). Surface whitewash in the IKONOS image resulted in the identification of false depth estimates at select locations around

Palmyra. These areas were manually removed and filled using a nearest neighbor interpolation method in ArcGIS Spatial Analyst (v 10.1, <http://www.esri.com>), resulting in a seamless 5 m bathymetry data set.

To quantify the spatial complexity of the underlying habitat at Palmyra, three geomorphic metrics were derived from the 5 m gridded bathymetry data: slope, the rate of change of slope (i.e. slope of slope), and bathymetric position index (BPI). Slope and slope of slope (calculated in degrees) were derived from the bathymetric grids using the ArcGIS Spatial Analyst extension slope function, where the raster cell values represented the maximum rate of maximum slope change between neighboring cells. BPI represents a location's elevation relative to overall surrounding seascape (Lundblad et al. 2006). A negative value representing a location lower than neighboring locations (e.g., sand channel, groove), a positive value representing a location higher than neighboring locations (e.g., pinnacle top), and flat areas produce near-zero values. BPI can be used to locate sand channels, spur and groove features and submarine canyons (Lundblad et al. 2006) and has been applied to characterize geomorphic features to support spatial modeling efforts (Young et al. 2010). BPI was calculated with a search radius of 10 cells (i.e. 50 m) using the Bathymetric Terrain Modeler application in ArcGIS 10.1 (Wright 2012).

Ecological data – Benthic community composition data were collected via towed-diver surveys of Palmyra in 2006, 2008, and 2010. Towed-diver surveys incorporated divers on SCUBA that maneuver instrumented boards 1 m above the benthos while being towed behind a small boat at $\sim 3 \text{ km hr}^{-1}$. The board is equipped with a high-resolution digital camera (Canon EOS-10D), strobes to illuminate the bottom substrate, a pair of red lasers at a known distance apart to assess area per frame, and a temperature-depth recorder. Position information was recorded by an onboard Global Positioning System (GPS), to which a layback model was applied

to accurately georeference each individual benthic photograph. Benthic photographs were obtained at a 15 s interval. A detailed description of the towed-diver technique is given by Kenyon et al. (2006).

Benthic photographs from the forereef habitat (depth constrained between 15 – 20 m isobaths) were analyzed for percent cover of five benthic categories (hard coral, crustose coralline algae (CCA), macroalgae, turf algae, and soft coral) using Coral Point Count with Excel Extensions (Kohler and Gill 2006). Within the hard coral category, five morphological categories (encrusting, branching, plating, massive, and free-living) were also quantified following (Veron and Terence 2000).

Wave and geomorphological information were identified for each individual photograph using the Sample routine in the ArcGIS v10.1 Spatial Analyst toolbox. In total, 3237 photographs with an average distance of 11.7 m (SD \pm 30) between photographs were incorporated into analyses.

Statistical analyses – To identify the spatial scale at which to investigate biophysical relationships without spatial autocorrelation, two techniques were employed: empirical semivariance (Meisel and Turner 1998) and lacunarity (Gefen et al. 1983; Mandelbrot 1983; Plotnick et al. 1993). Benthic data were first averaged over 50 m linear segments in a continuous fashion around the circumference of Palmyra’s forereef. We then calculated the empirical semivariance, $\gamma(h)$ for separation h as:

$$\gamma(h) = \frac{1}{2N(h)} \sum_{i,j \in S(h)} (z_i - z_j)^2$$

where $N(h)$ is equal to the number of pairs of observations having separation h , $S(h)$ is the set of pairs of observations denoted by i and j that have separation h , and z_i is the benthic cover value for the i^{th} observation. The separations h were defined as:

$$h_{i,j} = j - i \quad j - i \leq \frac{n}{2}$$

$$h_{i,j} = n - (j - i) \quad j - i > \frac{n}{2}$$

where n is the number of discrete 50 m segments. Empirical semivariance calculations were completed using the *vgm* function in the *gstat* package (Pebesma 2004) linked to a custom coded function in R (v2.15.1, R Development Core Team, www.r-project.org). By plotting semivariance against distance, we were able to estimate at what point the relationship reached an asymptote, thus indicating the minimum distance required between sampling units to avoid spatial autocorrelation and achieve true independence of data points. We further used lacunarity indices to avoid averaging over distances that were either too large (i.e. averaging across true signal in the data) or too small (i.e. incorporating noise into the signal). Lacunarity assess how similar parts from different regions of a geometric object are to each other at a given scale (Gefen et al. 1983), thus providing an assessment of the scale of autocorrelation. Using a custom function in R, lacunarity was calculated as a function of window size, with the first and second derivatives plotted to aid interpretation. All points c within any window size s were taken to obtain a *mean* for that location. For a window situated at position i , this *mean* can be defined as:

$$\mu_i(s) = \frac{1}{\sum_{j=i}^{j=i+s-1} \delta_j} \sum_{j=i}^{j=i+s-1} c_j$$

where $\delta_j=1$ if data are present and 0 otherwise. The window was then moved one unit further along and the next value obtained. For a given window size, we thus obtained a sequence of *mean* values $\mu_1(s), \mu_2(s), \mu_3(s) \dots \mu_n(s) = \boldsymbol{\mu}(s)$, where n is the number of sampling units. The lacunarity $l(s)$ for size s was defined as:

$$l(s) = 1 + \frac{\text{var}(\boldsymbol{\mu}(s))}{\text{mean}(\boldsymbol{\mu}(s)^2)}$$

In summary, across all five benthic functional groups, both the empirical semivariance curves and the lacunarity indices indicated a non-independence of data at the 50 m segment scale. The semivariance curves showed a complete loss of spatial autocorrelation beyond distances of 500 m for all benthic categories, with the exception of macroalgae, and the lacunarity indices indicated that 500 m was an optimal spatial scale at which to model the benthic data. We therefore scaled all the biological response variables and predictor variables (wave and geomorphological metrics) to a segment size of 500 m and only included segments ≥ 500 m apart during re-sampling of the data when creating independent data sets for our predictive modeling.

Boosted regression trees (BRTs) (Elith et al. 2008) were used to examine the relationship between the benthic response variables and the oceanographic and geomorphological predictors. BRTs use a boosting algorithm to assemble a series of regression trees in an additive, stage-wise fashion and include elements of stochasticity to improve model accuracy and reduce over-fitting; the technique is becoming popular in ecology (e.g. Franklin et al. 2013; Leathwick et al. 2008; Williams et al. 2010). BRTs were constructed using the routines *gbm* (Ridgeway 2012) and *gbm.step* (Elith et al. 2008) in R. Benthic percent cover values were arcsine transformed to achieve normality and modeled using a Gaussian distribution. We used 10-fold cross validation for model development and validation and cross validation deviance (CVD) to assess model performance; lower values indicate greater model predictive performance. Also, the overall percent deviance explained by each model was quantified to provide a more widely understood

metric of model performance. Model optimization was achieved by varying three key parameters: tree complexity (tc , number of nodes in the tree), learning rate (lr , contribution of each tree as it is added to the model), and the bag-fraction (bf , proportion of data to be selected at each step of the model). The optimal combination of these three parameters was identified using a customized loop routine (Richards et al. 2012) that ran all possible combinations of the following parameter settings: tc (1 – 5), lr (0.001, 0.0001, 0.00001), bf (0.5, 0.7, 0.8). The parameter combination giving the lowest CVD while maintaining a minimum of 1000 fitted trees was used to fit the final model. The relative importance of each predictor variable to the final model was quantified based on the number of times it was selected for splitting, weighted by the squared improvement to the model as a result of each split and averaged over all trees (Elith et al. 2008; Friedman and Meulman 2003). Partial dependency plots were created using the function *gbm.plot* (Elith et al. 2008) to interpret the relationship between each predictor and the final fitted function of the model in a conditional manner. To quantify interaction effects between predictors within each model (departure from a purely additive effect), we used the function *gbm.interactions* (Elith et al. 2008).

Results

Island-scale climatological conditions – Climatological oceanographic conditions at Palmyra were characterized by a clear, but relatively weak annual cycle. The long-term mean in SST at Palmyra was 28°C with a narrow annual range of 1.46°C (27.3 – 28.76°C) (Fig. 2A). Currents were predominantly eastward due to the influence of the North Equatorial Countercurrent (NECC; Fig. 1), with maximum climatological flow of 0.3 m s⁻¹ peaking in late August (Fig. 2B). Climatological wave energy exhibited a comparatively greater annual cycle,

with a maximum of $\sim 100 \text{ kW m}^{-1}$ in boreal winter due to highly energetic storms generated in the north Pacific (Fig. 2C). On shorter time scales, oceanographic conditions exhibited more pronounced variability, principally in accordance with El Niño Southern Oscillation (ENSO) forcing. Over the period spanning the ecological surveys and mooring deployments (2006 – 2011), the equatorial Pacific oscillated between El Niño and La Niña phases of ENSO multiple times (Fig. 2D). SST, currents, and waves each exhibited an overall positive correlation with ENSO; El Niño (La Niña) forcing resulted in warmer (cooler) than average SST (Fig. 2A), stronger (weaker) than average surface currents (Fig. 2B), and higher (lower) than average wave power (Fig. 2C).

Nearshore currents – Variance ellipses for nearshore currents centered at 0.9 m above the reef substrate (18 – 20.4 m depth for all moorings; Table 1) indicated that near-bottom current orientation was heavily influenced by proximate bathymetry (Fig. 3A). At the Northeast mooring, located proximate to shallow and emergent reef with generally parallel isobaths offshore, current was predominantly along these isobaths (i.e. \pm along-shelf), aligning with underlying bathymetry. Conversely, the Southeast mooring was situated along the Eastern Terrace; a broad, open area of reef with generally consistent depth ($\sim 10 - 15 \text{ m}$) (Fig. 1). With few obstructions, currents were more likely to cross bathymetric contours in this area. At the Southwest mooring, located on a small outcropping in bathymetry that extended $\sim 500 \text{ m}$ southwest from the east-west orientation of the atoll, currents were primarily along-shelf but also had a strong component that flowed perpendicular to isobaths (i.e. \pm cross-shelf). Currents at the Northwest mooring, in contrast to all others, were predominantly cross-shelf, perhaps due to deep offshore channels funneling water up-slope at this location (Figs. 1 and 3A). Data collection was temporally limited (08 Apr 2010 – 29 July 2010) at this location relative to the other sites

(Table 1), but variance ellipses for all locations were relatively unchanged over this shortened time period (data not shown), supporting the notion that offshore channels are important to near-bottom currents at this location.

Current frequencies at all moorings varied primarily at tidal frequencies, with the diurnal (K_1 ; 23.934 hours per cycle) and semi-diurnal (M_2 ; 12.421 hours per cycle) as the principle tidal constituents (Figs. 3B-E). The M_2 tide was the strongest influence on current oscillations at the Northwest, Northeast, and Southeast moorings, whereas the M_2 and K_1 were equally influential at the Southwest mooring.

Temperature variability – Time series of high-frequency temperature measurements revealed a complex and dynamic thermal environment on Palmyra's forereef (Fig. 4). Over the yearlong record, low-frequency seasonal forcing was weakly evident in all temperature records, with overall warming in July and cooling in February (Fig. 4A). On intra-seasonal time scales, large-amplitude temperature decreases of 1.0 – 4.0°C were recorded, often persisting for days to weeks. The two most prominent temperature drops were observed in October and November, driving strong temperature changes at all moorings lasting for ~4 weeks (Fig. 4A). Superimposed on the seasonal and intra-seasonal variability were high-frequency cold pulses of 0.3 – 1.8°C occurring multiple times daily and lasting for minutes to hours (Figs. 4A and 4B). Cold pulse characteristics were variable; many were solitary, knife-like temperature drops with a subsequent and equally rapid recovery to ambient temperatures. However, cold pulses also arrived as a series of discrete, successional temperature drops of varying magnitude occurring in packets of 3 – 10; a sharp decrease followed by gradual recovery; a gradual decrease superimposed with saw-toothed oscillations; and a step-like decrease characterized by a sharp temperature drop that persisted for several hours before sharply returning to pre-event temperatures (Fig. 4B).

Cold pulses were recorded at all moorings over the 12.5-month time period; however, their number, magnitude, and duration differed among locations (Table 2). The greatest number of cold pulses (339) occurred at the East mooring (Fig. 1). In contrast, 102 and 109 cold pulses were recorded at the Northwest and Southwest moorings, respectively; a 68 – 70% difference from the East mooring. With respect to duration, nearly half (48%) of all cold pulses at the Southeast mooring lasted for 120 – 720 min, while approximately the same proportion (43 – 52%) at all other locations occurred over shorter time scales (30 – 120 min; Table 2).

Changes in near-bottom currents were often observed in conjunction with cold pulses (Fig. 5). Prior to a cold pulse, cross-shelf currents increased $0.5 - 0.2 \text{ m s}^{-1}$ in the shoreward direction (Fig. 5C) and vertical currents increased $0.05 - 0.1 \text{ m s}^{-1}$ in the positive (upward) direction (Fig. 5D). As the cold pulse reached a temperature minimum, currents typically reversed, flowing offshore and downward. Along-shelf currents were less concordant with shorter-frequency cold pulses (Fig. 5B) but often fluctuated in concert with cold pulses occurring at tidal frequencies.

Wave forcing – Wave forcing at Palmyra was quantified by combining the numerical model results from each wave regime (i.e. northwest swell, northeast trade wind swell, and south swell; Fig. 1) over the time period encompassing the ecological surveys (2005 – 2010).

Consistent features emerged from the wave model. First, the central lagoon-reef complex partially blocks incoming waves along the southern portion of the atoll, creating a lee from the largest wave source (Fig. 6). Second, wave forcing was markedly enhanced over the emergent reef encircling the lagoon-reef complex, particularly with respect to maximum bed shear stress (BSS_{max} ; Fig. 6C). Strong dissipation occurs over the emergent reef due to increased bed shear stress associated with breaking waves. Third, wave forcing was enhanced over portions of the

Western and Eastern Terrace, likely due to increased exposure to multiple wave regimes and wave-bathymetry interactions resulting in increased shoaling.

Intra-island gradients in wave forcing were also observed in the depth-constrained (15 – 20 m) and spatially averaged (50 m linear segments) model results, calculated continuously around the circumference of the forereef where benthic data were collected (Figs. 7A and 7B). In general, mean bed shear stress (BSS_{mean}) was greatest along the SW, W, and NW sections of the atoll, with BSS_{max} peaking (142 N m^{-2}) between the SW and W (Fig. 7B). This area was also characterized by the largest range in bed shear stress ($BSS_{range} = 119 \text{ N m}^{-2}$), indicating highly variable annual wave forcing. From the NW towards the N and NE, bed shear stress declined by ~50% before increasing proximate to the eastern tip. Wave forcing near the SE and S sections was relatively low ($BSS_{max} = 10 - 20 \text{ N m}^{-2}$, $BSS_{mean} = 1 - 10 \text{ N m}^{-2}$, $BSS_{range} = 10 - 20 \text{ N m}^{-2}$).

Geomorphology – While Palmyra’s forereef is generally characterized by a slope range of $10 - 15^\circ$ (Fig. 7C), steeper slopes ($25 - 30^\circ$) were consistently observed along the southern forereef, with some areas up to 45° . Further, areas in the south also had the greatest range of structural habitat complexity, represented by the rate of change in slope ($50 - 60^\circ$) (Fig. 7C). Structural habitat complexity also showed enhanced variability at finer spatial scales, with proximate segments (i.e. separated by 50 m) regularly characterized by a rate of slope change of $10 - 20^\circ$, with some segments differing by 45° . Intra-island differences in bathymetric position index indicated variability in relative reef elevation, often exhibiting a close, negative relationship with slope of slope (Fig. 7D).

Benthic community spatial patterns – Palmyra’s benthic communities were dominated by calcifying (reef-building) organisms, namely hard coral (atoll-wide mean cover = 27.3%) and crustose coralline algae (CCA) (21.8%). The remaining space was dominated by turf algae

(16.5%), soft coral (14.5%), and macroalgae (both calcifying and fleshy) (10.8%). On intra-island scales, benthic community organization was spatially heterogeneous with uniquely varying patterns (Figs. 7E – 7I). Hard coral cover was variable at both large and small spatial scales (Fig. 7E). Relatively high coral cover ($> 50\%$) was observed in the W, NE, SE, and sections of the forereef; however, 10 – 20% changes in coral cover also occurred within relatively small distances (< 250 m) across much of the forereef. Conversely, macroalgae cover patterns were far less spatially complex (Fig. 7G). Nearly all macroalgae were observed in two distinct areas: a small section to the N and a much larger section to the S, where cover was regularly $> 30\%$ and as high as 100%. The majority (73%) of all other areas surveyed had $< 15\%$ macroalgae cover, with approximately half (52%) characterized by $\leq 5\%$. CCA, turf algae, and soft coral were also spatially heterogeneous, varying from a minimum ($< 5\%$) to a majority ($> 50\%$) of the benthic substrate (Figs. 7F, 7H – 7I).

The three most dominant coral morphologies also exhibited complex intra-island spatial patterning (Fig. 7J). Encrusting coral was by far the most dominant morphology, accounting for 25 – 50% of overall hard coral cover. At select locations, however, all three morphologies or a complete dominance of either plating or branching morphologies occurred. Near the western tip of the atoll, for example, encrusting and plating morphologies were equally present, each accounting for 25 – 40% of hard coral cover. Towards the NE, a small stretch of reef had 30 – 45% branching corals, while areas to the south had 65 – 75% plating corals (Fig. 7J).

Biophysical relationships – Overall, hard coral cover was positively related to BSS_{range} and negatively related to slope, while cover was weakly positively related at lower BPI values and negatively related at higher BPI values (Table 3 and Fig. 8A). Because total variation explained for hard coral cover was low (10.8%), these relationships should be interpreted with

caution. However, predictive performance improved 3 – 5 fold when hard coral morphological categories were used as the response variables (Table 3).

Encrusting coral: Models explained 55.7% of total variation in encrusting coral cover, principally driven by a strong positive relationship with $BSS_{range} > 10 \text{ N m}^{-2}$ (Table 3 and Fig. 8F). The relationship with BPI was mixed (positively related below -3 and a negatively related above -1), while the relationship with slope was negative above 15° .

Plating coral: Models explained 34.1% of total variation in plating coral cover. BSS_{range} was the strongest predictor, showing a positive relationship where $BSS_{range} < 10 \text{ N m}^{-2}$, a negative relationship between $10 - 22 \text{ N m}^{-2}$, and a positive relationship $> 22 \text{ N m}^{-2}$ (Table 3 and Fig. 8G). Slope of slope was negatively correlated with plating coral cover between $12 - 32^\circ$ and positively correlated between $38 - 40^\circ$. The relationship was positive where $BSS_{max} > 45 \text{ N m}^{-2}$.

Branching coral: Models explained 33.6% of total variation in branching coral cover. BSS_{range} was the strongest predictor, showing a negative relationship where $BSS_{range} > 22 \text{ N m}^{-2}$ (Table 3 and Fig. 8H). Slope and slope of slope were the second and third strongest predictors, showing a generally negative and positive relationship, respectively.

Crustose coralline algae (CCA): Models explained 69.6% of total variation in CCA cover, with a strong negative relationship where $BSS_{mean} > 18 \text{ N m}^{-2}$ (Table 3 and Fig. 8B). Slope of slope was neutrally related to CCA cover up to $\sim 27^\circ$, positively related from $27 - 30^\circ$, and negatively related from $30 - 40^\circ$. CCA was also positively related to slope overall.

Macroalgae: Models explained 79.6% of total variation in macroalgae cover (Table 3). Macroalgae was positively correlated with slope, showing a marked increase in cover above 10° (Table 3 and Fig. 8C). Macroalgae was negatively correlated with both BSS_{max} and BSS_{range} , declining in cover at relatively low values ($5 - 10 \text{ N m}^{-2}$).

Turf algae: Models explained 52.9% of total variation in turf algae cover (Table 3). A positive relationship with BSS_{mean} was the strongest predictor, with a sharp increase in turf cover above 18 N m^{-2} (Table 3 and Fig. 8D). Turf was negatively correlated with BSS_{range} , declining above 8 N m^{-2} . BPI had no influence on turf for strongly negative BPI values but showed a positive relationship where $BPI > -2$ and a negative relationship between $-0.5 - 1$.

Soft coral: Models explained 52.2% of total variation in soft coral cover (Table 3). BSS_{range} was the strongest predictor, with an increase in soft coral cover between $20 - 35 \text{ N m}^{-2}$ (Table 3 and Fig. 8E). Slope was generally positively related to soft coral between $8 - 13^\circ$ before becoming negatively related at slopes $> 17^\circ$. BPI was overall positively related above -3.5 .

Discussion

Intra-island gradients in physical forcings – Palmyra is an isolated, steep-sided atoll in the central equatorial Pacific characterized by a dynamic physical oceanographic environment. On climatological time scales, oceanographic conditions exhibit a relatively narrow range in annual forcing compared to other coral reef ecosystems across the Pacific (Gove et al. 2013). Atoll-wide oceanographic conditions, however, display salient year-to-year differences, principally in accordance with the El Niño Southern Oscillation (ENSO). At intra-island scales, in situ near-reef measurements of current and temperature, plus modeled wave forcing, demonstrated that physical forcings have complex spatiotemporal characteristics.

Near-reef current measurements from locations around the atoll exhibited variation in magnitude, orientation, and frequency of oscillations (Fig 3A). As Palmyra is elliptical in shape and primarily situated in the flow path of the eastward-flowing NECC, we anticipated nearshore currents to predominantly flow along isobaths (i.e. along-shelf). However, current measurements

were uniquely oriented at each mooring location, seemingly in accordance with proximate offshore bathymetry. Currents at all moorings principally oscillated at diurnal and semi-diurnal tidal frequencies, but the relative contribution of each tidal constituent differed among mooring locations (Fig. 3B).

In situ temperatures changed by 0.3 – 4.0°C on time scales of minutes to weeks (Fig. 4). Though not a focus of this research, we hypothesize the temperature fluctuations that persisting for multiple weeks (e.g. November, Fig. 4A) were associated with tropical instability waves (TIWs), mid-ocean mesoscale eddies spawned by interactions between the NECC and the South Equatorial Current (SEC) (Tomczak and Godfrey 1994). TIWs drive changes in sea surface height, SST, and thermocline depth on similar time scales as those observed in our temperature data in the latitudinal vicinity of Palmyra (Lyman et al. 2007).

Superimposed on the comparatively lower frequency events were high frequency cold pulses, characterized by the arrival of cold, subsurface derived waters with decreases of 0.3 to 1.8°C lasting time periods of minutes – hours (Fig. 4B). Where contemporaneous current measurements existed, increases in positive vertical (upward) and cross-shelf (shoreward) flow were often observed in conjunction with cold pulse events (Fig. 5). The observed cold pulses appear to be attributable to internal waves, resultant from tidal currents interacting with steep topography, leading to high-frequency vertical perturbations in the background stratification. Similar temperature fluctuations have been observed elsewhere in the Line Islands (Jarvis Island) (Gove et al. 2006) as well as on coral reefs in Hawai‘i (Mcmanus et al. 2008; Sevadjian et al. 2012), the Florida Keys (Leichter et al. 2005; Leichter and Miller 1999), French Polynesia (Leichter et al. 2012; Wolanski and Delesalle 1995), the Andaman Sea (Roder et al. 2010; Roder et al. 2011) and the Great Barrier Reef (Wolanski and Deleersnijder 1998).

Despite the presence of cold pulses in all in situ temperature data sets, site-specific characteristics of cold pulses differed with respect to frequency, magnitude, and duration (Table 2). The present instrument deployment configuration was unable to resolve the ultimate causes of spatial gradients in cold pulses; however, it is likely that interactions between the NECC and Palmyra's abrupt bathymetry contributed to the observed asymmetry. Previous research has shown that current-topographic interactions influence background stratification at Palmyra, due to a blocking effect in currents causing flow stagnation and vertical displacement of subsurface isotherms (Hamann et al. 2004). Isotherm displacements at Palmyra were observed to be particularly accentuated upstream and downstream of the primary flow pattern (Hamann et al. 2004). Hence, the 2 – 3 fold increases in cold pulse events at the western (upstream) and eastern (downstream) end of the atoll may have resulted from a somewhat persistent spatial difference in stratification.

Combining numerically modeled wave conditions enabled a synoptic, high-resolution spatial assessment of annual wave forcing around Palmyra (Fig. 6). Areas exposed to the northwest wave regime and areas exposed to multiple wave regimes, such as sections of the Western and Eastern Terrace regions, experienced the largest annual wave forcing. Areas in the lee of the lagoon (e.g. southern forereef) were least exposed, as the emergent reef and vegetated islands comprising the lagoon block much of the strongest annual wave events, limiting exposure to only the most incident wave forcing. Depth-constrained horizontal comparisons further emphasized intra-island gradients in wave forcing, but also revealed marked differences with respect to the specific nature of wave forcing (Fig 7B). For example, areas exposed to similar annual mean bed shear stress (BSS) (e.g. between the W and NW, near the eastern edge, and between the SW and W) experienced highly differing maximum BSS, ranging from maximum

values that were over twice the annual mean (i.e. between the SW and W) to virtually no difference between maximum and mean wave forcing (i.e. near the eastern edge).

Intra-island spatial heterogeneity of benthic coral reef communities – Palmyra’s benthic community was dominated by calcifying (reef-building) organisms, namely hard coral and crustose coralline algae (CCA), corroborating previous studies (Sandin et al. 2008; Williams et al. 2013). On intra-island spatial scales, benthic community composition exhibited considerable spatial heterogeneity, with percent cover of each benthic functional group ranging from 0% to greater than 80% (Fig 7). Moreover, different benthic functional groups displayed different spatial patterning. Macroalgae, for example, was highly spatially clumped, monopolizing the benthos over a 5 – 7 km section of forereef to the south, whereas half of the remaining areas surveyed had 5% or less macroalgal cover. Hard coral cover, by contrast, was markedly variable, comprising > 50% of the benthic community at multiple locations around the atoll.

Proximate drivers of benthic community organization – Wave forcing (i.e. bed shear stress) and geomorphological characteristics (i.e. slope, slope of slope, and bathymetric position index [BPI]) were major drivers of benthic community organization around Palmyra, explaining 52.2 – 79.6% of the variability in benthic functional groups (i.e. CCA, macroalgae, turf algae, and soft coral; Table 3). Furthermore, we found distinct biophysical relationships existed among key benthic competitors (Fig. 8). For example, CCA and turf algae, both early colonizers and competitors for space on coral reefs (Grigg 1983; Hughes and Connell 1999), showed a distinct shift in dominance with increased mean bed shear stress. Specifically, a sharp decline in the abundance of CCA was coincident with an increase in the abundance of turf algae at 20 N m^{-2} . At Kingman Reef, located 70 km north of Palmyra, similar relationships exist between wave energy and both fleshy turf algae (positively correlated) and calcifying organisms (negatively

correlated) (Williams et al. 2013). It is unclear whether competitive exclusion results in a stable turf algae-dominated regime, or if the benthic community is continually re-set to an earlier successional state (Hughes & Connell 1999). Nevertheless, our results indicate that physical drivers are capable of shifting a coral reef benthic community from a dominance of calcifying organisms, such as CCA, to a dominance of fleshy algae, such as turf algae, even in the absence of local human impacts.

Macroalgae dominated the benthos over a small region characterized by steep slopes and low maximum and mean annual wave forcing. Due to increased vulnerability to physical dislodgement (Engelen et al. 2005), macroalgae cover is often negatively correlated with wave forcing (Kilar 1989; Page-Albins et al. 2012). Steep slopes may also favor macroalgae by regulating waves, as the location at which waves break, and therefore the maximum bed shear stress, is pushed shoreward in more steeply sloped regions compared to those with more gradual slopes (Raubenheimer and Guza 1996). Alternatively, at the location where we observed high macroalgae cover (i.e. peak cover between the SE and S locations in Fig. 7A), Williams et al. (2011) found relatively high levels of fine sediment. Palmyra's lagoon was heavily impacted by the U.S. military during WWII, resulting in a severely degraded system with low mixing and high sediment concentrations (Maragos et al. 2008). Increased sedimentation and nutrient concentrations can increase macroalgae abundance (Fabricius et al. 2005; Mccook 1996) and shift coral community organization at Palmyra (Williams et al. 2011). We postulate that nutrient-laden sediments may flow out of the lagoon in this area, and in concert with low annual wave forcing, help tip the benthic competitive balance in favor of macroalgae over corals.

Coral communities are flexible, with the abundance of individual taxa distinctly varying in response to environmental gradients (Hughes et al. 2012). Here, the 3 – 5 fold improvement in

model results when hard coral morphologies were used indicated unique responses within the coral community to intra-island gradients in physical forcings. Encrusting corals, being low-lying and able to persist in areas of increased hydrodynamic disturbance (Franklin et al. 2013; Jokiel et al. 2004), were found across a broad range of reef slopes and reef elevations that were exposed to moderate annual ranges of bed shear stress. Plating corals, which have relatively higher colony shape factors (Madin, 2005) and are more vulnerable to dislodgement at increased wave forcing than encrusting growth forms, were found in locations of low to moderate range in wave exposure, but only in areas where reef slopes were low and relatively constant. Branching corals, which are highly susceptible to dislodgment and breakage (Madin 2005), often show reduced cover at higher wave exposures (Williams et al., 2013); these corals were found mostly in areas of low, moderately changing slope with minimal range in bed shear stress, rapidly declining in cover in areas with increased wave forcing that were more suitable for other growth forms. These results demonstrate that coral assemblages can reorganize in response to gradients in physical properties even within an individual island, as opposed to a wholesale change in coral cover resulting from extrinsic environmental forcing.

Wave exposure is an important driver of coral reef benthic community structure (Done 1999; Hughes and Connell 1999; Page-Albins et al. 2012) and coral species composition (Dollar 1982; Jokiel et al. 2004; Storlazzi et al. 2005). Here, bed shear stress is an effective predictor of coral reef benthic community composition, but the specific nature of wave forcing (i.e. maximum, mean, range) influenced benthic organisms differently. For example, BSS_{range} and BSS_{mean} were rarely concurrent predictors, such that for benthic functional groups where BSS_{range} was the strongest predictor (i.e. hard coral, soft coral, and encrusting, plating, and branching coral morphologies), BSS_{mean} had minimal influence. Similarly, BSS_{mean} predicted

nearly 50% of the variation in percent cover of CCA around Palmyra, whereas BSS_{range} contributed < 3%. These results suggest that within islands, benthic communities are influenced not only by spatial gradients in wave forcing (Franklin et al. 2013; Williams et al. 2013), but also by spatial differences in the temporal characteristics of annual wave forcing (i.e. annually variable versus annually consistent).

Additional physical forcings beyond those included in our BRT models can influence coral reef benthic communities. Specifically, internal waves deliver increased nutrients and suspended particles to shallower depths (Leichter et al. 1998; Leichter et al. 2003), influencing benthic sessile organisms (i.e. coral and algae) that benefit from allocthonous food delivery (Leichter and Genovese 2006; Smith et al. 2004). Furthermore, intra-specific differences in coral zooxanthellae density, pigment concentrations, and heterotrophy can vary on intra-island scales in response to gradients in internal wave activity (Roder et al. 2010; Roder et al. 2011). Spatial gradients in cold pulses around Palmyra are therefore potentially important drivers of coral reef benthic community organization. Future research quantifying cold pulses at a spatial resolution similar to that of wave forcing presented here (i.e. 50 m) would presumably strengthen the predictive performance of our BRT models.

Due to its remote oceanic environment and absence of direct human impact, Palmyra Atoll provides a unique opportunity to study biophysical interactions in coral reef benthic communities. We conclude that coral reef benthic community organization can exhibit considerable spatial heterogeneity driven by intra-island gradients in physical forcings. Furthermore, we find that physical forcings may tip the balance of competitive interactions between benthic functional groups, helping to decide who “wins” by favoring individual organisms and morphologies. While human activities clearly play an important role in

structuring coral reef benthic communities, it is important to also consider naturally coupled biophysical relationships, as shifts in benthic community regimes from calcifying (i.e. corals and CCA) to non-calcifying (i.e. turf algae and macroalgae) can occur even in the absence of local human impacts. Our study highlights the capacity for coral reef benthic communities, particularly corals, to reorganize at an intra-island scale in response to environmental change, helping to predict future trajectories of coral reef ecosystems in a rapidly changing climate.

Acknowledgments

This work was part of an interdisciplinary effort by the NOAA Pacific Islands Fisheries Science Center's Coral Reef Ecosystem Division (CRED) to assess, understand, and monitor coral reef ecosystems of the U.S. Pacific. The authors would like to thank Rusty Brainard, Principle Investigator of CRED, for his support of this research. We would also like to thank Oliver Vetter, Chip Young, Noah Pomeroy, Ronald Hoeke, and Daniel Merritt for their invaluable assistance in mooring deployments and data gathering, the CRED tow-board team, and the officers and crew of the NOAA ship *Hi'ialakai* for logistic support and field assistance. Jeff Sevadjian, Timothy Jones and Jessica Blakely provided important input related to data analysis, and Alan Friedlander, Jeff Drazen, Craig Smith, and Mark Merrifield provided helpful comments and guidance on this work. Funding for surveys (as part of the Pacific Reef Assessment and Monitoring Program, RAMP) was provided by NOAA's Coral Reef Conservation Program.

Tables and Figures

Table 1: Table of information pertaining to each of the physical data types used in the analysis, including location, parameters measured, depth, date range, data source, and other relevant information (e.g. sampling interval). Please see Fig.1 for locations of in situ oceanographic moorings.

Location	Parameters	Depth (m)	Date Range	Data Source	Relevant Information
<i>In situ Oceanographic Data</i>					<i>Sampling Interval</i>
West	T	19.2	16-Apr-10 – 03-May-11	SBE37	2.5 min
Northwest	T Currents Waves	21.5	16-Apr-10 – 03-May-11	SBE37	2.5 min
			08-Apr-10 – 29-July-10	Nortek 1Mz	1 min native/20 min average
			08-Apr-10 – 29-July-10	Aquadopp	20 min burst every 3 h
Northeast	T Currents Waves	19.8	16-Apr-10 – 03-May-11	SBE37	2.5 min
			09-Apr-10 – 15-Oct-10	Nortek 1Mz	1 min native/20 min average
			09-Apr-10 – 15-Oct-10	Aquadopp	20 min burst every 3 h
East	T	21	16-Apr-10 – 03-May-11	SBE37	2.5 min
Southeast	T Currents Waves	18.9	16-Apr-10 – 03-May-11	SBE37	2.5 min
			09-Apr-10 – 29-Dec-10	Nortek 1Mz	1 min raw/20 min average
			09-Apr-10 – 29-Dec-10	Aquadopp	20 min burst every 3 hrs
Southwest	T Currents Waves	19.8	16-Apr-10 – 03-May-11	SBE37	2.5 min
			08-Apr-10 – 20-Dec-10	Nortek 1Mz	1 min raw/20 min average
			08-Apr-10 – 20-Dec-10	Aquadopp	20 min burst every 3 h
<i>Gridded Data</i>					<i>Resolution</i>
Atoll wide	Bathymetry	0 – 3000	N/A	Ship-based multibeam and Ikonos imagery	5 m resolution
Forereef	Slope Slope of Slope BPI	15 – 20	N/A	ArcGIS 10.1	5 m resolution
<i>Modeled Data</i>					
Atoll wide	Wave Height Peak Period Peak Direction	N/A	1-Jan-05 – 12-Apr-10	Wave Watch III	1° resolution
Forereef	Bed Shear Stress: Maximum Mean Range	15 – 20	1-Jan-05 – 12-Apr-10	Delft3D	50 m resolution

Table 2: Summary of cold pulses by mooring location from April 2010 – May 2011. All data were sampled at 2.5 min intervals from ~20 m depth. Please see Fig. 1 for mooring locations and Table 1 for additional information pertaining to each mooring.

Total number cold pulse events: temperature change (°C)								
	0.3 - 0.5	fraction	0.5 - 1.0	fraction	> 1.0	fraction	max	Total
West	128	0.60	78	0.36	9	0.04	1.33	215
Northwest	67	0.66	31	0.30	4	0.04	1.48	102
Northeast	81	0.70	28	0.24	6	0.05	1.44	115
East	206	0.61	105	0.31	28	0.08	1.56	339
Southeast	77	0.58	40	0.30	15	0.11	1.73	132
Southwest	59	0.54	38	0.35	12	0.11	1.49	109
Total number of cold pulse events: time elapsed to minimum temperature (min)								
	0 - 30	fraction	30-120	fraction	120 - 720	fraction	max	Total
West	36	0.17	94	0.44	85	0.40	542.5	215
Northwest	19	0.19	44	0.43	39	0.38	455	102
Northeast	23	0.20	52	0.45	40	0.35	422.5	115
East	60	0.18	176	0.52	103	0.30	560	339
Southeast	24	0.18	45	0.34	63	0.48	672.5	132
Southwest	15	0.14	57	0.52	37	0.34	522.5	109

Table 3. Results from boosted regression tree (BRT) analysis, including optimal parameter settings, predictive performance, and relative influence of environmental variables on percent cover of the five major benthic functional groups: hard coral (coral), crustose coralline algae (CCA), macroalgae, turf algae, and soft coral and three most dominant coral morphologies: encrusting, plating, and branching.

Model Parameters	Functional Group					Coral Morphologies		
	Coral	CCA	Macroalgae	Turf Algae	Soft Coral	Encrusting	Plating	Branching
Tree complexity	4	4	4	2	3	3	4	2
Learning rate	0.001	0.001	0.0001	0.001	0.001	0.0001	0.001	0.001
Bag fraction	0.8	0.8	0.7	0.7	0.8	0.8	0.8	0.7
Number of trees	2550	1450	26750	3350	1350	15400	1200	10650
Mean Total Deviance	0.00910	0.00784	0.01532	0.00684	0.00974	0.00680	0.00264	0.00110
CV Deviance (CVD)	0.00812	0.00239	0.00312	0.00322	0.00466	0.00301	0.00174	0.00073
CVD SE	0.00100	0.00122	0.00087	0.00082	0.00071	0.00110	0.00131	0.00081
Deviance explained (%)	10.8	69.6	79.6	52.9	52.2	55.7	34.1	33.6
Predictors	Relative Influence (%)							
Bed Shear Stress: Max	9.66	9.30	18.02	2.72	7.88	7.77	17.37	10.00
Bed Shear Stress: Mean	6.29	46.14	16.11	34.94	6.61	4.30	3.32	7.55
Bed Shear Stress: Range	33.90	3.11	2.48	21.56	49.49	46.56	38.46	41.87
Slope	24.29	11.13	58.04	17.27	16.58	12.57	8.36	18.13
Slope of Slope	12.31	20.31	2.48	5.39	4.94	8.96	27.51	15.68
BPI	13.55	10.01	2.88	18.13	14.50	19.85	4.98	6.79

Figure Legends

Fig. 1. Map of the U.S.-owned atolls in the northern Line Islands of the central Pacific (inset globe), highlighting the dominant wave regimes, regional currents, and seafloor bathymetry (top). Expanded view of Palmyra Atoll, with bathymetric contours and the six mooring locations where oceanographic time series data were collected along the ~20 m isobath (bottom).

Fig. 2. Climatological (thick lines) and time series (thin lines) of sea surface temperature (A), zonal (east-west) current (B), and wave energy (C) for Palmyra Atoll. Multivariate ENSO Index indicating the phase and strength of ENSO over the time period of interest, where positive (red) bars indicate El Niño years and negative (blue) bars represent La Niña years (D). Vertical gray bars in all panels represent ecological surveys. Shaded gray region represents the time period encompassing in situ mooring deployments.

Fig. 3. Bathymetric map of Palmyra Atoll depicting current variance ellipses calculated for ~19 m water depth (A). Major and minor axes of the ellipses correspond to the variance in the along-shore and cross-shore velocities, with magnitude indicated by the scale bar in the lower left corner. Power spectral density for U and V currents rotated about their principle axis for the Northwest, Northeast, Southeast, and Southwest moorings, from right to left, respectively (B). Peaks are observed primarily at diurnal (1 cycle per day or 23.924 hours per cycle) and semi-diurnal (1.934 cycles per day or 12.421 hours per cycle) tidal frequencies.

Fig. 4. In situ time series data of temperature from six mooring locations deployed at ~20 m depth (A). Two-week expansion of temperature data highlighting the high-frequency cold pulses observed at all locations (B). Legend in lower panel corresponds to both panels. Please see Fig. 1 for individual mooring locations.

Fig. 5. A cold pulse observed at the Southeast mooring showing concomitant changes in temperature (A), along-shelf current (positive = eastward) (B), cross-shelf current (positive = shoreward) (C), and vertical current (positive = upward) (D). Data were obtained over a 4 hr period on 29 August 2010. No current data are available for 21:00 – 21:20, when wave data were collected.

Fig. 6. Numerical wave model results representing the maximum values of significant wave height (A), period (B), and bed shear stress (C). Results represent the maximum of each grid cell from the combined numerical model runs for each swell regime (i.e. northwest swell, northeast trade wind swell, and south swell) at Palmyra Atoll (Fig. 1).

Fig. 7. Bathymetric map of Palmyra Atoll (left) with an expanded section (right) showing depth-constrained (15 – 20 m) and spatially averaged (50 m) towed-diver surveys (block dots) (A). Panels below represent corresponding wave, geomorphology, and coral reef benthic community data for each 50 m segment and include the following: bed shear stress (maximum, mean, and range) (B), slope (slope and slope of slope) (C), bathymetric position index (BPI) (D), and percent cover of hard coral (E), crustose coralline algae (CCA) (F), macroalgae (G), turf algae (H), soft coral (I), and the three most dominant coral morphologies (encrusting, plating, branching) (J). Note the x-axis corresponds to the map of Palmyra Atoll (A), showing all data in a clockwise fashion from left to right, starting at the western tip of the atoll (W) and moving northwest (NW), north (N), northeast (NE), east (E), southeast (SE), south (S), southwest (SW), and ending back at the western tip.

Fig. 8. Partial dependency response plots for the three most influential predictors of percent cover for each of the five benthic functional groups: hard coral (A), crustose coralline algae (CCA) (B), macroalgae (C), turf algae (D), and soft coral (E) and three most dominant coral morphologies: encrusting (F), plating (G) and branching (H). Relative influence of each variable is given in parentheses after the x-axis label. The y-axes are on logit scale and are centered to have zero mean over the data distribution. Tick marks along the inside top of each subpanel indicate distribution of sites for that variable (e.g. hard coral) across the corresponding predictor (e.g. slope). BPI represents bathymetric position index, while BSS_{max} , BSS_{mean} , BSS_{range} represent the max, mean, and range in bed shear stress values, respectively.

Fig. 1.

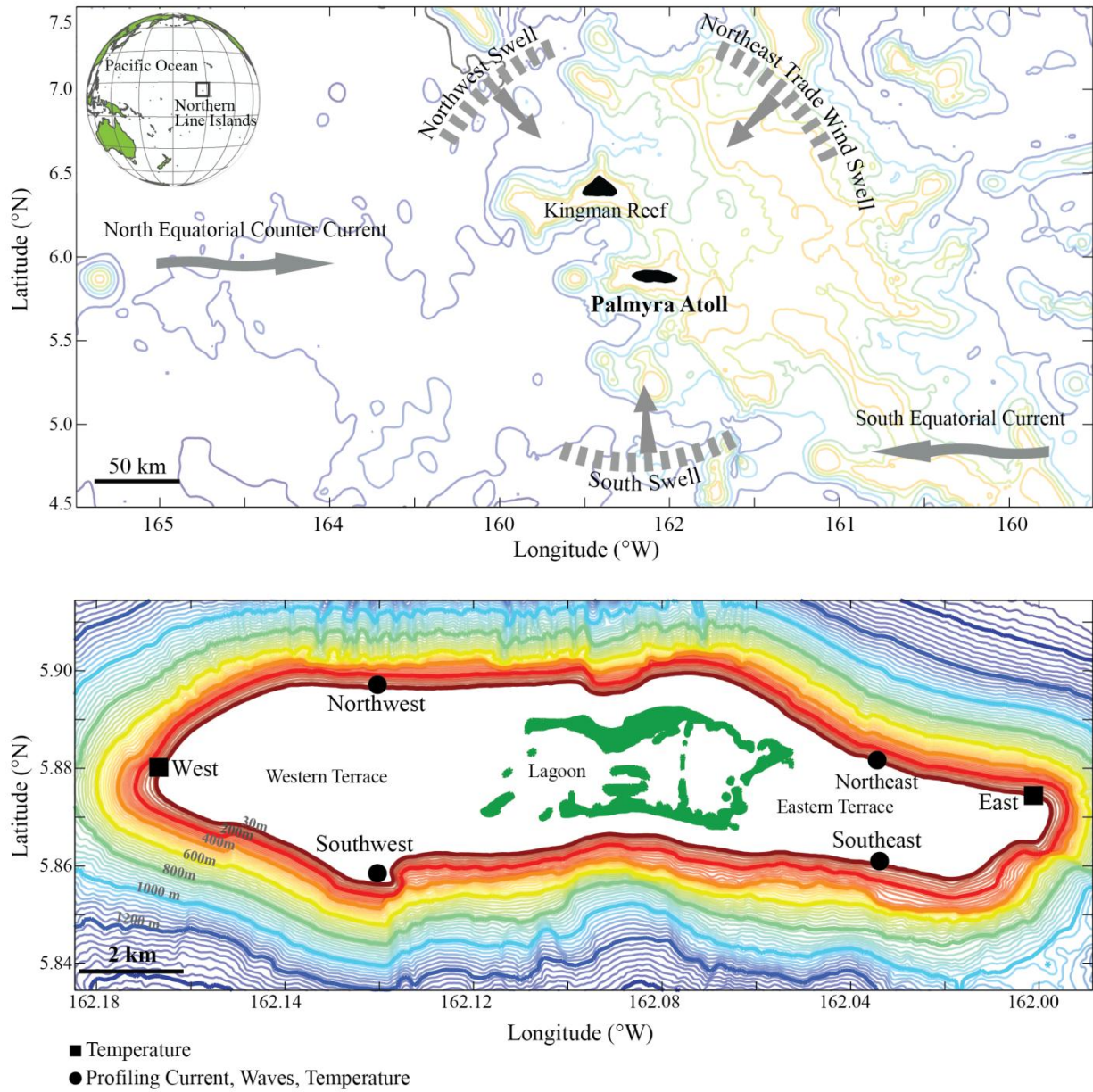


Fig. 2.

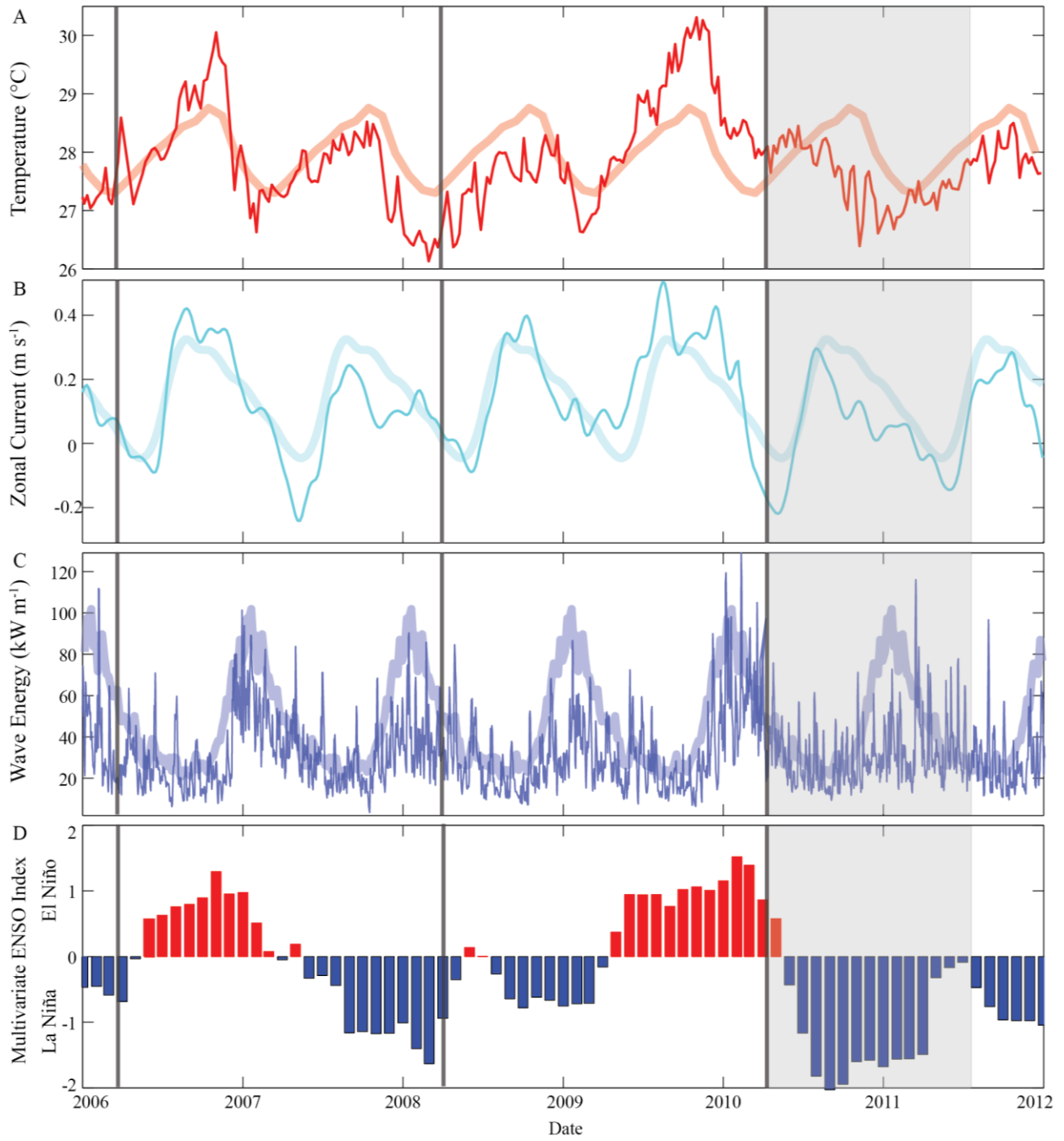


Fig. 3.

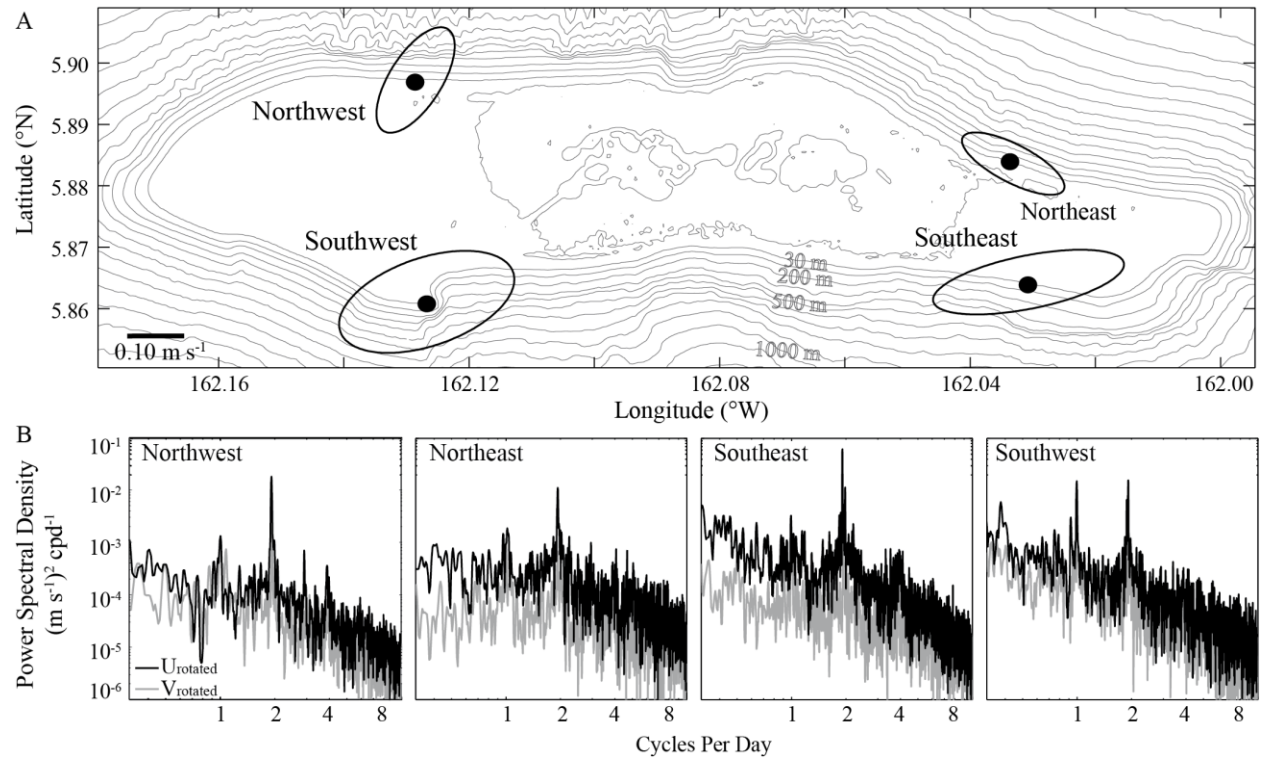


Fig. 4.

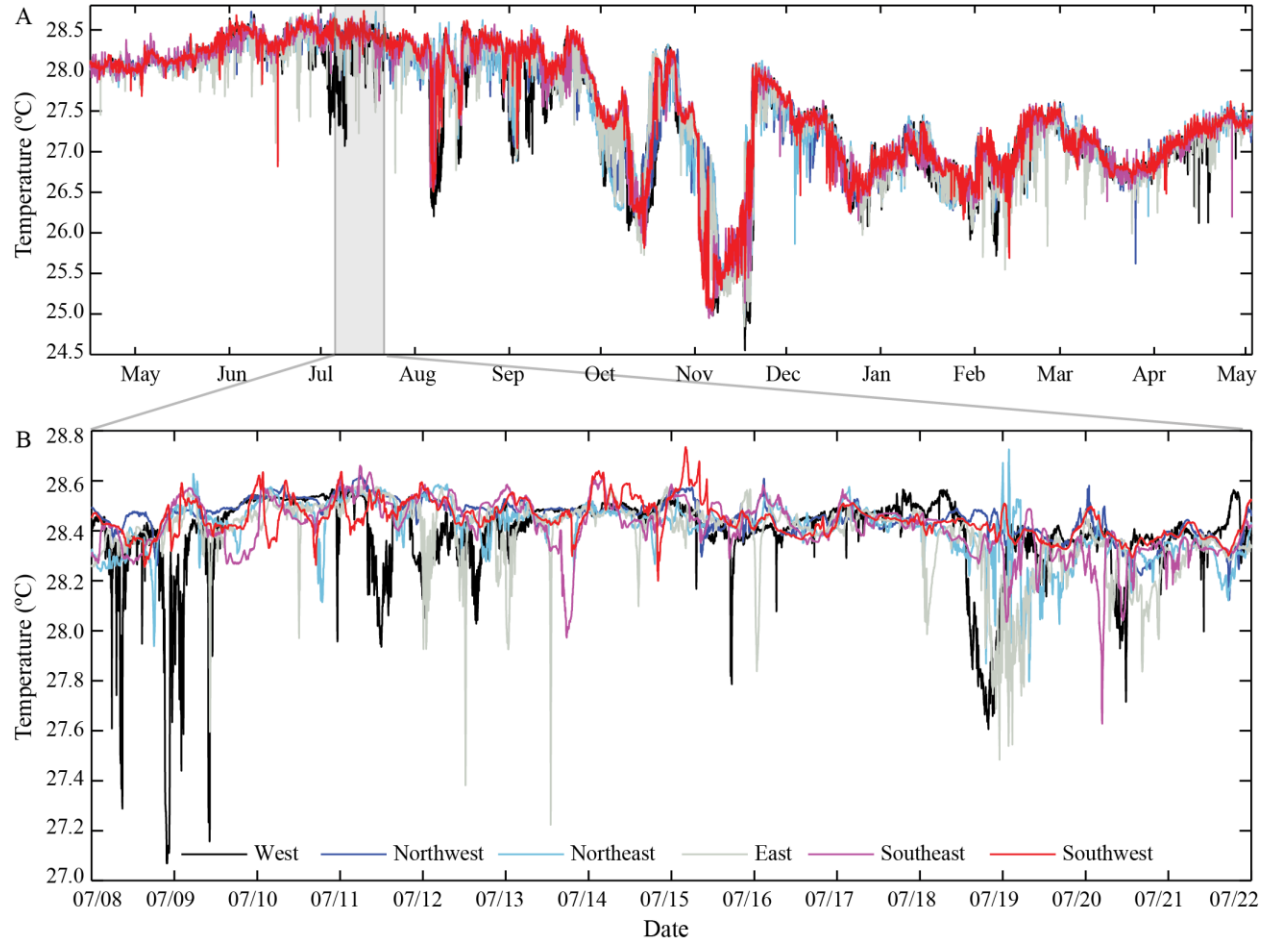


Fig. 5.

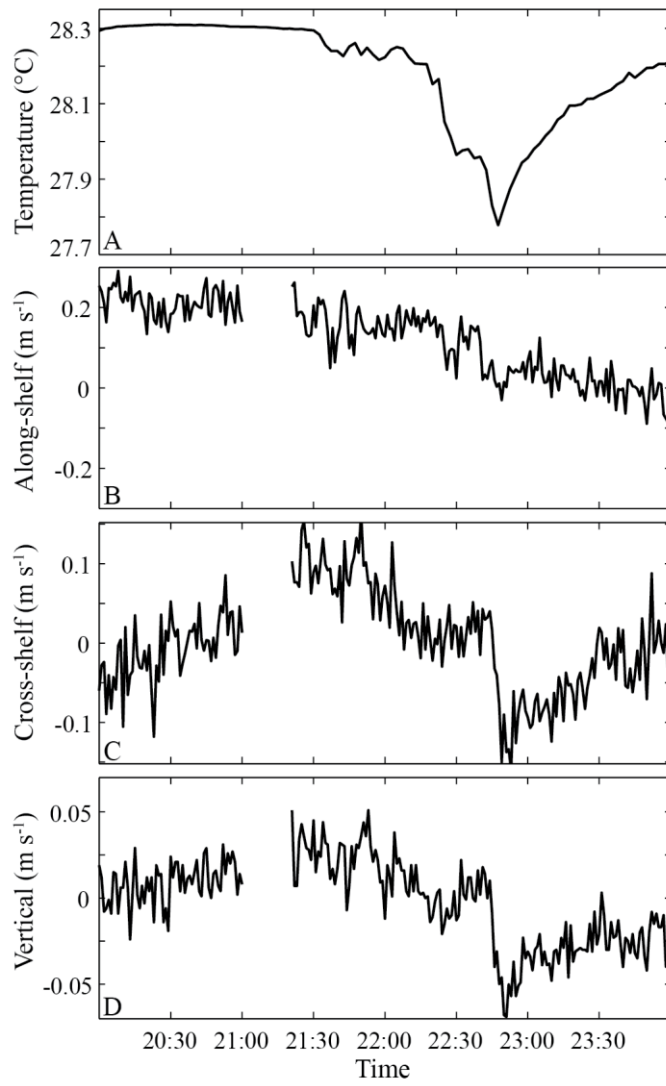


Fig. 6.

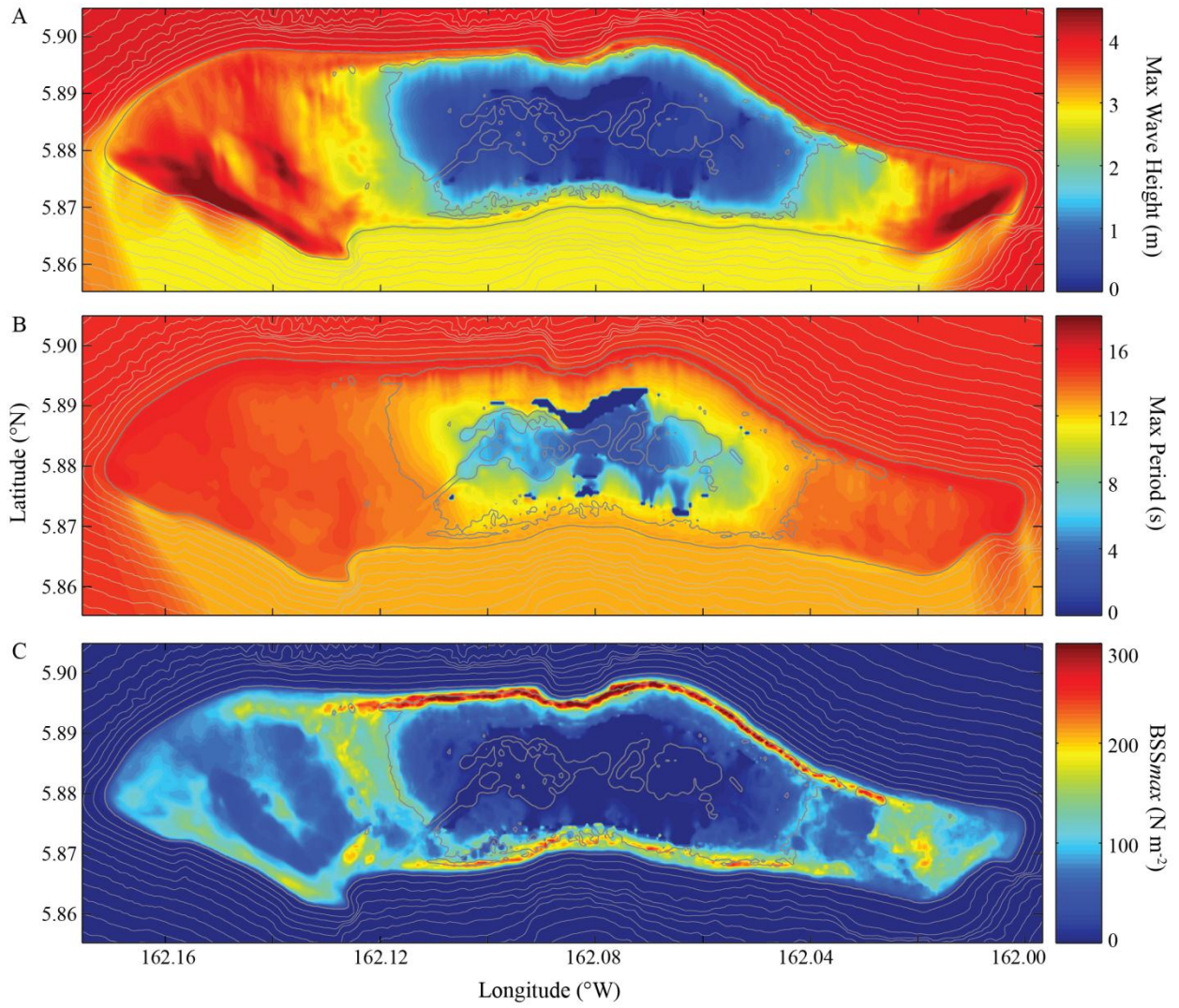


Fig. 7.

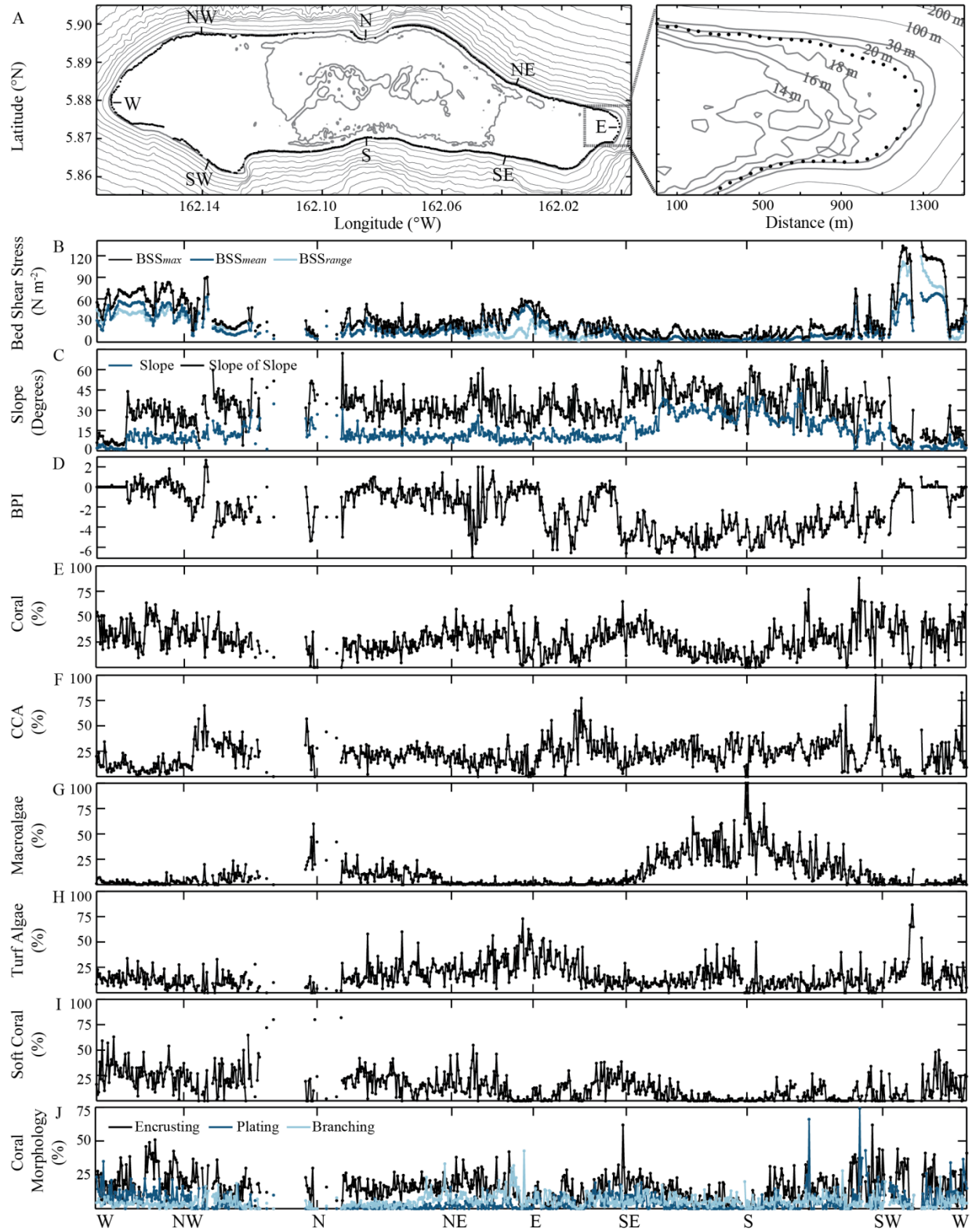
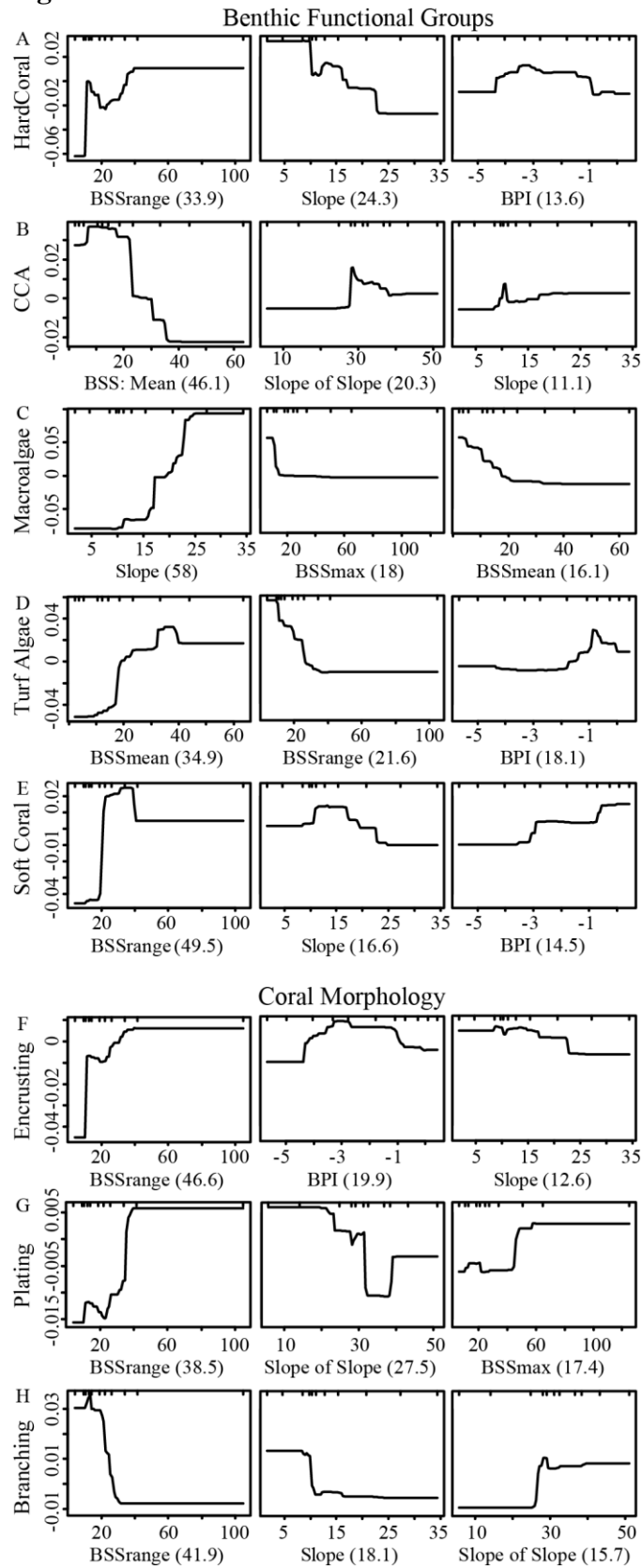


Fig. 8.



References

- Andrews, J. C., and P. Gentien. 1982. Upwelling as a Source of Nutrients for the Great Barrier Reef Ecosystems: A Solution to Darwin's Question? *Marine Ecology Progress Series* **8**: 257-269.
- Atkinson, M., and R. Bilger. 1992. Effects of water velocity on phosphate uptake in coral reef-flat communities. *Limnol Oceanogr* **37**: 273-279.
- Booij, N., R. C. Ris, and L. H. Holthuijsen. 1999. A third-generation wave model for coastal regions: 1. Model description and validation. *Journal of Geophysical Research: Oceans* **104**: 7649-7666.
- Bradbury, R. H., and P. C. Young. 1981. The Effects of a Major Forcing Function, Wave Energy, on a Coral-Reef Ecosystem. *Mar Ecol-Prog Ser* **5**: 229-241.
- Demartini, E. E., A. M. Friedlander, S. A. Sandin, and E. Sala. 2008. Differences in fish-assemblage structure between fished and unfished atolls in the northern Line Islands, central Pacific. *Mar Ecol-Prog Ser* **365**: 199-215.
- Dollar, S. J. 1982. Wave stress and coral community structure in Hawaii. *Coral Reefs* **1**: 71-81.
- Done, T. 1982. Patterns in the distribution of coral communities across the central Great Barrier Reef. *Coral Reefs* **1**: 95-107.
- Done, T. J. 1999. Coral community adaptability to environmental change at the scales of regions, reefs and reef zones. *American Zoologist* **39**: 66-79.
- Elith, J., J. R. Leathwick, and T. Hastie. 2008. A working guide to boosted regression trees. *J. Anim. Ecol.* **77**: 802-813.
- Engelen, A. H., P. Åberg, J. L. Olsen, W. T. Stam, and A. M. Breeman. 2005. Effects of wave exposure and depth on biomass, density and fertility of the furoid seaweed *Sargassum polyceratum* (Phaeophyta, Sargassaceae). *European Journal of Phycology* **40**: 149-158.
- Fabricius, K., G. De'ath, L. Mccook, E. Turak, and D. M. Williams. 2005. Changes in algal, coral and fish assemblages along water quality gradients on the inshore Great Barrier Reef. *Mar Pollut Bull* **51**: 384-398.
- Franklin, E. C., P. L. Jokiel, and M. J. Donahue. 2013. Predictive modeling of coral distribution and abundance in the Hawaiian Islands. *Marine Ecology Progress Series* **481**: 121-132.
- Friedman, J. H., and J. J. Meulman. 2003. Multiple additive regression trees with application in epidemiology. *Stat. Med.* **22**: 1365-1381.
- Gefen, Y., Y. Meir, and A. Aharony. 1983. Geometric implementation of hypercubic lattices with noninteger dimensionality by use of low lacunarity fractal lattices. *Physical Review Letters* **50**: 145-148.
- Gove, J. M., M. A. Merrifield, and R. E. Brainard. 2006. Temporal variability of current-driven upwelling at Jarvis Island. *Journal of Geophysical Research: Oceans* **111**: C12011.
- Gove, J. M. and others 2013. Quantifying Climatological Ranges and Anomalies for Pacific Coral Reef Ecosystems. *Plos One* **8**: e61974.
- Grigg, R. W. 1983. Community Structure, Succession and Development of Coral Reefs in Hawaii. *Mar Ecol-Prog Ser* **11**: 1-14.
- Hamann, I. M., G. W. Boehlert, and C. D. Wilson. 2004. Effects of steep topography on the flow and stratification near Palmyra Atoll. *Ocean Dynamics* **54**: 460-473.
- Hench, J. L., J. J. Leichter, and S. G. Monismith. 2008. Episodic circulation and exchange in a wave-driven coral reef and lagoon system. *Limnol Oceanogr* **53**: 2681-2694.

- Hendry, R., and C. Wunsch. 1973. High Reynolds number flow past an equatorial island. *J Fluid Mech* **58**: 97-114.
- Hughes, T. P. 1994. Catastrophies, phase-shifts, and large-scale degradation of a Caribbean coral reef. *Science* **265**: 1547-1551.
- Hughes, Terry p. and others 2012. Assembly Rules of Reef Corals Are Flexible along a Steep Climatic Gradient. *Curr. Biol.* **22**: 736-741.
- Hughes, T. P., and J. H. Connell. 1999. Multiple stressors on coral reefs: A long-term perspective. *Limnol Oceanogr* **44**: 932-940.
- Jokiel, P. L., E. K. Brown, A. Friedlander, S. K. U. Rodgers, and W. R. Smith. 2004. Hawai'i coral reef assessment and monitoring program: Spatial patterns and temporal dynamics in reef coral communities. *Pacific Science* **58**: 159-174.
- Kenyon, J. C., R. E. Brainard, R. K. Hoeke, F. A. Parrish, and C. B. Wilkinson. 2006. Towed-Diver Surveys, a Method for Mesoscale Spatial Assessment of Benthic Reef Habitat: A Case Study at Midway Atoll in the Hawaiian Archipelago. *Coast Manage* **34**: 339-349.
- Kilar, J. A., McLachlan, J. 1989. Effects of wave exposure on the community structure of a plant-dominated, fringing-reef platform: intermediate disturbance and disturbance mediated competition. *Mar Ecol-Prog Ser* **54**: 265-276.
- Kleypas, J. A., J. W. Mcmanus, and L. a. B. Menez. 1999. Environmental Limits to Coral Reef Development: Where Do We Draw the Line? *American Zoologist* **39**: 146-159.
- Kohler, K. E., and S. M. Gill. 2006. Coral Point Count with Excel extensions (CPCe): A Visual Basic program for the determination of coral and substrate coverage using random point count methodology. *Computers & Geosciences* **32**: 1259-1269.
- Leathwick, J. R., J. Elith, W. L. Chadderton, D. Rowe, and T. Hastie. 2008. Dispersal, disturbance and the contrasting biogeographies of New Zealand's diadromous and non-diadromous fish species. *J Biogeogr* **35**: 1481-1497.
- Leichter, J. J., G. B. Deane, and M. D. Stokes. 2005. Spatial and Temporal Variability of Internal Wave Forcing on a Coral Reef. *Journal of Physical Oceanography* **35**: 1945-1962.
- Leichter, J. J., and S. J. Genovese. 2006. Intermittent upwelling and subsidized growth of the scleractinian coral *Madracis mirabilis* on the deep fore-reef slope of Discovery Bay, Jamaica. *Marine Ecology Progress Series* **316**: 95-103.
- Leichter, J. J., and S. L. Miller. 1999. Predicting high-frequency upwelling: Spatial and temporal patterns of temperature anomalies on a Florida coral reef. *Cont Shelf Res* **19**: 911-928.
- Leichter, J. J., G. Shellenbarger, S. J. Genovese, and S. R. Wing. 1998. Breaking internal waves on a Florida (USA) coral reef: a plankton pump at work? *Marine Ecology Progress Series* **166**: 83-97.
- Leichter, J. J., H. L. Stewart, and S. L. Miller. 2003. Episodic nutrient transport to Florida coral reefs. *Limnol Oceanogr*: 1394-1407.
- Leichter, J. J., M. D. Stokes, J. L. Hench, J. Witting, and L. Washburn. 2012. The island-scale internal wave climate of Moorea, French Polynesia. *Journal of Geophysical Research: Oceans* **117**: C06008.
- Lesser, G. R., J. A. Roelvink, J. a. T. M. Van Kester, and G. S. Stelling. 2004. Development and validation of a three-dimensional morphological model. *Coastal Engineering* **51**: 883-915.
- Lowe, R., J. Falter, S. Monismith, and M. Atkinson. 2009. Wave-Driven Circulation of a Coastal Reef-Lagoon System. *Journal of Physical Oceanography* **39**: 873-893.

- Lundblad, E. R. and others 2006. A Benthic Terrain Classification Scheme for American Samoa. *Marine Geodesy* **29**: 89-111.
- Lyman, J. M., G. C. Johnson, and W. S. Kessler. 2007. Distinct 17- and 33-Day Tropical Instability Waves in Subsurface Observations*. *Journal of Physical Oceanography* **37**: 855-872.
- Madin, J. 2005. Mechanical limitations of reef corals during hydrodynamic disturbances. *Coral Reefs* **24**: 630-635.
- Madin, J., K. Black, and S. Connolly. 2006. Scaling water motion on coral reefs: from regional to organismal scales. *Coral Reefs* **25**: 635-644.
- Mandelbrot, B. B. 1983. *The fractal geometry of nature*. W.H. Freeman.
- Maragos, J. and others 2008. U.S. Coral Reefs in the Line and Phoenix Islands, Central Pacific Ocean: History, Geology, Oceanography and Biology. *In* R. E. Dodge and B. M. Riegl [eds.], *Coral Reefs of the United States of America*. Springer.
- McCook, L., J. Jompa, and G. Diaz-Pulido. 2001. Competition between corals and algae on coral reefs: a review of evidence and mechanisms. *Coral Reefs* **19**: 400-417.
- McCook, L. J. 1996. Effects of herbivores and water quality on *Sargassum* distribution on the central Great Barrier Reef: cross-shelf transplants. *Marine Ecology Progress Series* **139**: 179-192.
- McManus, M. A., K. J. Benoit-Bird, and C. Brock Woodson. 2008. Behavior exceeds physical forcing in the diel horizontal migration of the midwater sound-scattering layer in Hawaiian waters. *Marine Ecology Progress Series* **365**: 91-101.
- Meisel, J. E., and M. G. Turner. 1998. Scale detection in real and artificial landscapes using semivariance analysis. *Landscape Ecol.* **13**: 347-362.
- Nyström, M., C. Folke, and F. Moberg. 2000. Coral reef disturbance and resilience in a human-dominated environment. *Trends Ecol Evol* **15**: 413-417.
- Page-Albins, K. N., P. S. Vroom, R. Hoeke, M. A. Albins, and C. M. Smith. 2012. Patterns in Benthic Coral Reef Communities at Pearl and Hermes Atoll along a Wave-Exposure Gradient1. *Pacific Science* **66**: 481-496.
- Pebesma, E. J. 2004. Multivariable geostatistics in S: the gstat package. *Computers and Geosciences* **30**: 683-691.
- Plotnick, R. E., R. H. Gardner, and R. V. O'neil. 1993. Lacunarity indices as measures of landscape texture. *Landscape Ecol.* **8**: 201-211.
- Raubenheimer, B., and R. T. Guza. 1996. Observations and predictions of run-up. *Journal of Geophysical Research: Oceans* **101**: 25575-25587.
- Richards, B. L., I. D. Williams, O. J. Vetter, and G. J. Williams. 2012. Environmental factors affecting large-bodied coral reef fish assemblages in the Mariana Archipelago. *PLoS One* **7**: e31374.
- Ridgeway, G. 2012. Generalized boosted regression models. Documentation on the R package 'gbm', version 1.6–32, www.r-project.org/.
- Roder, C., L. Fillingner, C. Jantzen, G. M. Schmidt, S. Khokiattiwong, and C. Richter. 2010. Trophic response of corals to large amplitude internal waves. *Marine Ecology Progress Series* **412**: 113-128.
- Roder, C., C. Jantzen, G. M. Schmidt, G. Kattner, N. Phongsuwan, and C. Richter. 2011. Metabolic plasticity of the corals *Porites lutea* and *Diploastrea heliopora* exposed to large amplitude internal waves. *Coral Reefs* **30**: 57-69.

- Sandin, S. A. and others 2008. Baselines and Degradation of Coral Reefs in the Northern Line Islands. *Plos One* **3**:e1548
- Sevadjian, J. C., M. A. Mcmanus, K. J. Benoit-Bird, and K. E. Selph. 2012. Shoreward advection of phytoplankton and vertical re-distribution of zooplankton by episodic near-bottom water pulses on an insular shelf: Oahu, Hawaii. *Cont Shelf Res* **50–51**: 1-15.
- Smith, J. E., C. M. Smith, P. S. Vroom, K. L. Beach, and S. Miller. 2004. Nutrient and growth dynamics of *Halimeda* tuna on Conch Reef, Florida Keys: Possible influence of internal tides on nutrient status and physiology. *Limnol Oceanogr*: 1923-1936.
- Soulsby, R. L., L. Hamm, G. Klopman, D. Myrhaug, R. R. Simons, and G. P. Thomas. 1993. Wave-current interaction within and outside the bottom boundary layer. *Coast Eng* **21**: 41-69.
- Storlazzi, C. D., E. K. Brown, M. E. Field, K. Rodgers, and P. L. Jokiel. 2005. A model for wave control on coral breakage and species distribution in the Hawaiian Islands. *Coral Reefs* **24**: 43-55.
- Stumpf, R. P., K. Holderied, and M. Sinclair. 2003. Determination of water depth with high-resolution satellite imagery over variable bottom types. *Limnol Oceanogr* **48**: 547-556.
- Thomas, F. I. M., and M. J. Atkinson. 1997. Ammonium uptake by coral reefs: Effects of water velocity and surface roughness on mass transfer. *Limnol Oceanogr* **42**: 81-88.
- Tomczak, M., and J. S. Godfrey. 1994. *Regional oceanography: An Introduction*. Pergamon (Oxford, England and New York).
- Van Dongeren, A. and others 2013. Numerical modeling of low-frequency wave dynamics over a fringing coral reef. *Coastal Engineering* **73**: 178-190.
- Veron, J., and J. Terence. 2000. *Corals of The World Vol. 1-3*, Australian Institute of Marine Science. Townsville, Australia.
- Williams, G. J., G. S. Aeby, R. O. M. Cowie, and S. K. Davy. 2010. Predictive Modeling of Coral Disease Distribution within a Reef System. *Plos One* **5**: e9264.
- Williams, G. J., I. S. Knapp, J. E. Maragos, and S. K. Davy. 2011. Proximate environmental drivers of coral communities at Palmyra Atoll: Establishing baselines prior to removing a WWII military causeway. *Mar Pollut Bull* **62**: 1842-1851.
- Williams, G. J., J. E. Smith, E. J. Conklin, J. M. Gove, E. Sala, and S. A. Sandin. 2013. Benthic communities at two remote Pacific coral reefs: effects of reef habitat, depth, and wave energy gradients on spatial patterns. *PeerJ* **1**: e81.
- Wolanski, E., and E. Deleersnijder. 1998. Island-generated internal waves at Scott Reef, Western Australia. *Cont Shelf Res* **18**: 1649-1666.
- Wolanski, E., and B. Delesalle. 1995. Upwelling by internal waves, Tahiti, French Polynesia. *Cont Shelf Res* **15**: 357-368.
- Wolanski, E., and W. Hamner. 1988. Topographically Controlled Fronts in the Ocean and Their Biological Influence. *Science* **241**: 177-181.
- Wooldridge, S. A. 2009. Water quality and coral bleaching thresholds: Formalising the linkage for the inshore reefs of the Great Barrier Reef, Australia. *Mar Pollut Bull* **58**: 745-751.
- Wright, D. J., Pendleton, M., Boulware, J., Walbridge, S., Gerlt, B., Eslinger, D., Sampson, D., Hungtly, E. 2012. *Benthic Terrain Modeler*. Environmental Systems Research Institute.
- Young, M. A., P. J. Lampietro, R. G. Kvitek, and C. D. Garza. 2010. Multivariate bathymetry-derived generalized linear model accurately predicts rockfish distribution on Cordell Bank, California, USA. *Marine Ecology Progress Series* **415**: 247-261.

CHAPTER V

CONCLUSIONS

Coral reef benthic communities respond to spatial differences in environmental forcings and their structure reflects long-term gradients in environmental conditions (Hughes et al. 2012). While human activities clearly play an important role in structuring coral reef benthic communities (Hughes et al. 2003), it is important to also consider naturally coupled biological-physical relationships, as shifts in benthic community regimes from calcifying (i.e. corals and CCA) to non-calcifying (i.e. turf algae and macroalgae) can occur in the absence of local human impacts (Vroom and Braun 2010; Williams et al. 2013). Across 41 island- and atoll-reef ecosystems that spanned 45° of latitude and 65° longitude in the Pacific, environmental forcings displayed considerable island-scale variation, both between and within island archipelagos. Moreover, minimal correspondence between environmental forcings was observed across the study region, as the emergent spatial patterns and degree of variability were found to be forcing dependant. For example, wave energy was greatest at northern latitudes and generally decreased with latitude. In contrast, chlorophyll-*a* was greatest at reef ecosystems proximate to the equator and northern-most locations, showing little synchrony with latitude (Gove et al. 2013; Chapter II).

Previous research has reported spatial differences in species diversity, abundance, and community structure across the study region (Friedlander et al. 2003; Schils et al. 2013; Vroom and Braun 2010). Across remote, unpopulated locations, gradients in benthic community composition exist (Schils et al. 2013; Vroom et al. 2010), with a number of remote atolls characterized by a high proportion of macroalgae (Vroom and Braun 2010), even in the presence of an intact and healthy reef fish community (Friedlander and Demartini 2002). Our recent

research that incorporated the island-scale environmental metrics presented herein found complex relationships between local human habitation and regional-scale environmental gradients to drive spatial variation in island-scale benthic communities (Williams, Gove et al. submitted). Variations in hard coral cover, for example, were primarily driven by differences in chlorophyll-*a*, wave energy and the presence of human habitation. However, the relationship between coral cover and natural environmental forcings only held true for unpopulated locations, while no clear relationship existed across populated locations (Williams, Gove et al. submitted). Natural variations in environmental forcings are therefore important drivers of Pacific island- and atoll-reef communities; however, intrinsic stressors associated with human habitation may decouple important biological-physical relationships.

Phytoplankton primary production is an essential source of energy in the marine environment (Duarte and Cebrian 1996; Jennings et al. 2008). Near oceanic island and atoll coral reef ecosystems, the surrounding environment is often nutrient limited and lacking new production (Hamner and Hauri 1981; Sander 1981). Processes that enhance phytoplankton biomass are therefore particularly important to food-web dynamics and total ecosystem productivity (Hernández-León 1991; Sander and Steven 1973; Wolanski and Hamner 1988). Across the study region over a decadal time scale, a majority (91%) of island- and atoll-reef ecosystems exhibited nearshore enhancements in phytoplankton biomass compared to surrounding oceanic waters (Gove et al. in prep, Chapter III). However, characterized horizontal gradients in chlorophyll-*a* differed between study locations. Variations in reef area, bathymetric slope, geomorphic type (e.g. atoll *versus* island), and human population were identified as important drivers of inter-island differences in increased phytoplankton biomass, together explaining 77% of the variability observed.

Identifying locations with enhanced phytoplankton biomass may provide insight related to the interdependence of coral reef and pelagic marine ecosystems. For example, strong gradients in phytoplankton biomass were observed in the Hawaiian Archipelago, where enhanced phytoplankton biomass may elicit a bottom-up ecosystem response (Benoit-Bird and Au 2003). The mesopelagic boundary community – a distinct community of squids, fishes, and other micronekton (Reid et al. 1991) – exhibit strong diel horizontal migration patterns, transiting long distances (>5 km) towards shore at night before returning to deeper, oceanic waters in the day (Benoit-Bird and Au 2006; Benoit-Bird et al. 2001; Mcmanus et al. 2008). Moreover, pelagic predators exhibit spatiotemporal movements that suggest oceanic animals, such as dolphins (Baird et al. 2008; Benoit-Bird and Au 2003) and tuna (Holland et al. 1990; Musyl et al. 2003) cue in on shoreward migration of mesopelagic boundary organisms, exploiting the island-associated micronekton community as a food resource.

The relationship between environmental forcings and coral reefs may not be consistent across all spatial scales. For example, island-scale wave forcing and hard coral cover were found to be negatively related (Williams, Gove et al. submitted). This important island-scale biological-physical relationship was nearly absent at smaller spatial scales, as intra-island differences in hard coral cover were only weakly related to spatial gradients in wave forcing (Gove et al. submitted; Chapter IV). However, when hard coral was analyzed at morphological based categories (i.e. encrusting, plating, branching), wave forcing was found to be the most important environmental predictor of spatial differences in coral community organization (Gove et al. submitted; Chapter IV). These findings suggest that coral assemblages adjust to differences in wave forcing opposed to exhibiting a wholesale decline with increases in the prevailing wave climate. Intrinsic biological-physical interactions in coral reef communities may therefore be

scale-dependent, as the relationships between environmental forcings and benthic community patterns can change based on the spatial scale of focus.

Past research has identified internal waves as an important environmental forcing to coral reef communities (Leichter et al. 2003). Internal waves cause localized changes in water flow, temperature, nutrients, and suspended particles (Leichter et al. 1998) that influence benthic production (Leichter et al. 2003) and coral and algal growth rates (Roder et al. 2010; Smith et al. 2004). At Palmyra, the internal wave climate exhibited clear spatial patterning, with differences in the frequency, magnitude, and duration of internal wave events observed around the atoll (Gove et al. submitted; Chapter IV). However, the influence of internal waves on coral reef benthic community structure could be better quantified. Future research incorporating a nearshore hydrodynamic model would shed light on the contribution of internal waves to the spatial patterns observed in Palmyra's benthic community. Future research would also benefit from including reef ecosystems that experience large amplitude internal waves. For example, internal waves drive temperature changes of 6 – 8°C along the southern forereef of Pearl and Hermes Atoll (CRED, unpublished data), a 3 – 4 fold increase in the maximum temperature change observed at Palmyra. Low structural complexity and dense beds of *Microdictyon*, a frondose macroalgae, appear to monopolize the benthic community at Pearl and Hermes Atoll where these large amplitude internal waves occur (CRED unpublished data). I hypothesize that at Palmyra Atoll, internal waves serve as an important source of nutrients and suspended particles to the benthic community whereas at Pearl and Hermes Atoll, large amplitude internal waves deliver nutrient loads that offset the competitive balance between coral and algae, resulting in a naturally occurring alternate benthic regime dominated by macroalgae.

Human disturbance can drive benthic regime shifts that result in changes to reef ecosystem processes, functions and feedback mechanisms (Knowlton 2004; Norstrom et al. 2009), which can compromise the ecosystem services (e.g. fishing, tourism) that human populations rely on (Nyström et al. 2000). Quantifying natural and local human drivers of existing reef regimes will help elucidate the causes of benthic regime shifts and identify communities on the verge of tipping into an alternate benthic regime. For future work, I plan on working alongside social scientists to develop reef ecosystem models (e.g. Gove et al. submitted; Chapter IV) that include representative and similarly scaled metrics of natural and human disturbance. This is the focus of the upcoming “Ocean Tipping Points” project, a multi-disciplinary effort between CRED, Stanford University’s Center for Ocean Solutions (COS), and University of California Santa Barbara. Through “Ocean Tipping Points”, we have proposed to conduct a comprehensive scientific evaluation and identify drivers and ecosystem states on Hawaii’s coral reefs. Specifically, I will build upon the methodological approach and results presented in Chapter II (Gove et al. 2013) and Chapter IV (Gove et al. submitted) to develop modeled and satellite-based intra-island metrics of environmental forcings across the Hawaiian Archipelago. In addition, many of these data sets will be ‘tuned’ with in situ data, providing better representation of forcings on the benthic community. For example, by comparing CRED’s extensive network of high resolution, reef-level temperature data with satellite-derived SST, I will create a depth-corrected SST data set that can extend throughout the archipelago. With this information, we plan to develop a robust set of early warning indicators and define “safe-operating space” for reef management decisions in which alternate regimes are avoided and the resilience of coral reefs is maintained. The Humpback Whale National Marine Sanctuary is soon to include coral reef ecosystems and specifically intends to embed our results into their

management plan, serving as an important pilot for practical implementation of ecosystem-based management in coral reef ecosystems.

This research incorporated ecological and oceanographic data collected by Pacific-RAMP, a long-term effort lead by NOAA's Coral Reef Ecosystem Division to characterize coral reef ecosystems across the Pacific. The value of long-term monitoring efforts such as Pacific-RAMP cannot be overstated. Because monitoring efforts spanned a range of spatial scales and crossed gradients in human disturbance and oceanographic conditions, we can more accurately and effectively study intrinsic biological-physical relationships in coral reef ecosystems and how human disturbance influences those relationships. A number of researchers have used data collected via Pacific-RAMP, contributing critically important findings that provide invaluable insight into coral reef ecosystem process and function (e.g. Friedlander and Demartini 2002; Gove et al. in prep, Chapter III; Gove et al. submitted, Chapter IV; Gove et al. 2013, Chapter II; Schils et al. 2013; Vroom et al. 2010; Williams et al. 2011; Williams, Gove et al. submitted; Zgliczynski et al. 2013). Managers and policy makers tasked with designing coral reef ecosystem management plans require the ability to detect and assess variations in coral reef communities, and the key drivers of those variations. Only through understanding natural variation in coral reef benthic community organization can we begin to comprehensively assess the effects of human disturbance.

References

- Baird, R. W., D. L. Webster, S. D. Mahaffy, D. J. Mcsweeney, G. S. Schorr, and A. D. Ligon. 2008. Site fidelity and association patterns in a deep-water dolphin: Rough-toothed dolphins (*Steno bredanensis*) in the Hawaiian Archipelago. *Marine Mammal Science* **24**: 535-553.
- Benoit-Bird, K. J., and W. W. L. Au. 2003. Prey dynamics affect foraging by a pelagic predator (*Stenella longirostris*) over a range of spatial and temporal scales. *Behav Ecol Sociobiol* **53**: 364-373.
- . 2006. Extreme diel horizontal migrations by a tropical nearshore resident micronekton community. *Marine Ecology Progress Series* **319**: 1-14.
- Benoit-Bird, K. J., W. W. L. Au, R. E. Brainard, and M. O. Lammers. 2001. Diel horizontal migration of the Hawaiian mesopelagic boundary community observed acoustically. *Marine Ecology Progress Series* **217**: 1-14.
- Brown, B. E. 1997. Adaptations of Reef Corals to Physical Environmental Stress, p. 221-299. *In* J. H. S. Blaxter and A. J. Southward [eds.], *Advances in Marine Biology*. Academic Press.
- Caldeira, K., and M. E. Wickett. 2003. Anthropogenic carbon and ocean pH. *Nature* **425**: 365-365.
- Church, J. A., and N. J. White. 2006. A 20th century acceleration in global sea-level rise. *Geophys. Res. Lett.* **33**: L01602.
- Done, T. J. 1999. Coral community adaptability to environmental change at the scales of regions, reefs and reef zones. *American Zoologist* **39**: 66-79.
- Donner, S. D. 2009. Coping with Commitment: Projected Thermal Stress on Coral Reefs under Different Future Scenarios. *Plos One* **4**: e5712.
- Donner, S. D., T. R. Knutson, and M. Oppenheimer. 2007. Model-based assessment of the role of human-induced climate change in the 2005 Caribbean coral bleaching event. *Proceedings of the National Academy of Sciences* **104**: 5483-5488.
- Doty, M. S., and M. Oguri. 1956. The Island Mass Effect. *Journal du Conseil* **22**: 33-37.
- Duarte, C., and J. Cebrian. 1996. The fate of marine autotrophic production. *Limnol Oceanogr* **41**: 1758-1766.
- Emanuel, K. 2005. Increasing destructiveness of tropical cyclones over the past 30 years. *Nature* **436**: 686-688.
- Fabricius, K., G. De'ath, L. Mccook, E. Turak, and D. M. Williams. 2005. Changes in algal, coral and fish assemblages along water quality gradients on the inshore Great Barrier Reef. *Mar Pollut Bull* **51**: 384-398.
- Freeman, L. A., A. J. Miller, R. D. Norris, and J. E. Smith. 2012. Classification of remote Pacific coral reefs by physical oceanographic environment. *J. Geophys. Res.* **117**: C02007.
- Friedlander, A. M., E. K. Brown, P. L. Jokiel, W. R. Smith, and K. S. Rodgers. 2003. Effects of habitat, wave exposure, and marine protected area status on coral reef fish assemblages in the Hawaiian archipelago. *Coral Reefs* **22**: 291-305.
- Friedlander, A. M., and E. E. Demartini. 2002. Contrasts in density, size, and biomass of reef fishes between the northwestern and the main Hawaiian islands: the effects of fishing down apex predators. *Marine Ecology Progress Series* **230**: 253-264.
- Gove, J. M. and others in prep. The Island Mass Effect: Explaining Enhanced Phytoplankton Biomass for Island Ecosystems Across the Pacific.

- Gove, J. M., G. J. Williams, M. A. Mcmanus, J. S. Clark, J. S. Ehses, and L. M. Wedding. submitted. Intra-island gradients in physical forcings drive spatial patterning in coral reef benthic communities. *Limnol Oceanogr*.
- Gove, J. M. and others 2013. Quantifying Climatological Ranges and Anomalies for Pacific Coral Reef Ecosystems. *Plos One* **8**: e61974.
- Hamner, W. M., and I. R. Hauri. 1981. Effects of island mass: Water flow and plankton pattern around a reef in the Great Barrier Reef Lagoon, Australia. *Limnol Oceanogr* **26**: 1084-1102.
- Hernández-León, S. 1991. Accumulation of mesozooplankton in a wake area as a causative mechanism of the “island-mass effect”. *Mar Biol* **109**: 141-147.
- Hoegh-Guldberg, O. 1999. Climate change, coral bleaching and the future of the world's coral reefs. *Marine and Freshwater Research* **50**: 839-866.
- Hoegh-Guldberg, O. 2011. The Impact of Climate Change on Coral Reef Ecosystems Coral Reefs: An Ecosystem in Transition, p. 391-403. *In* Z. Dubinsky and N. Stambler [eds.]. Springer Netherlands.
- Hoegh-Guldberg, O. and others 2007. Coral reefs under rapid climate change and ocean acidification. *Science* **318**: 1737.
- Holland, K. N., R. W. Brill, and R. K. C. Chang. 1990. Horizontal and vertical movements of yellowfin and bigeye tuna associated with fish aggregating devices. *Fishery Bulletin* **88**: 493-507.
- Hughes, T. P. 1994. Catastrophies, phase-shifts, and large-scale degradation of a Caribbean coral reef. *Science* **265**: 1547-1551.
- Hughes, T. P. and others 2003. Climate change, human impacts, and the resilience of coral reefs. *Science* **301**: 929-933.
- Hughes, Terry p. and others 2012. Assembly Rules of Reef Corals Are Flexible along a Steep Climatic Gradient. *Curr. Biol.* **22**: 736-741.
- Hughes, T. P., and J. H. Connell. 1999. Multiple stressors on coral reefs: A long-term perspective. *Limnol Oceanogr* **44**: 932-940.
- Jennings, S., F. Mélin, J. L. Blanchard, R. M. Forster, N. K. Dulvy, and R. W. Wilson. 2008. Global-scale predictions of community and ecosystem properties from simple ecological theory. *Proceedings of the Royal Society B: Biological Sciences* **275**: 1375-1383.
- Kleypas, J. A., J. W. Mcmanus, and L. a. B. Menez. 1999. Environmental Limits to Coral Reef Development: Where Do We Draw the Line? *American Zoologist* **39**: 146-159.
- Knowlton, N. 2001. The future of coral reefs. *P Natl Acad Sci USA* **98**: 5419-5425.
- . 2004. Multiple “stable” states and the conservation of marine ecosystems. *Prog Oceanogr* **60**: 387-396.
- Knowlton, N., and J. B. C. Jackson. 2008. Shifting baselines, local impacts, and global change on coral reefs. *Plos Biology* **6**: 215-220.
- Leichter, J. J., G. Shellenbarger, S. J. Genovese, and S. R. Wing. 1998. Breaking internal waves on a Florida (USA) coral reef: a plankton pump at work? *Marine Ecology Progress Series* **166**: 83-97.
- Leichter, J. J., H. L. Stewart, and S. L. Miller. 2003. Episodic nutrient transport to Florida coral reefs. *Limnol Oceanogr*: 1394-1407.
- Mccook, L., J. Jompa, and G. Diaz-Pulido. 2001. Competition between corals and algae on coral reefs: a review of evidence and mechanisms. *Coral Reefs* **19**: 400-417.

- Mcmanus, M. A., K. J. Benoit-Bird, and C. Brock Woodson. 2008. Behavior exceeds physical forcing in the diel horizontal migration of the midwater sound-scattering layer in Hawaiian waters. *Marine Ecology Progress Series* **365**: 91-101.
- Musyl, M. K., R. W. Brill, C. H. Boggs, D. S. Curran, T. K. Kazama, and M. P. Seki. 2003. Vertical movements of bigeye tuna (*Thunnus obesus*) associated with islands, buoys, and seamounts near the main Hawaiian Islands from archival tagging data. *Fisheries Oceanography* **12**: 152-169.
- Norstrom, A. V., M. Nystrom, J. Lokrantz, and C. Folke. 2009. Alternative states on coral reefs: beyond coral-macroalgal phase shifts. *Marine Ecology Progress Series* **376**: 295-306.
- Nyström, M., C. Folke, and F. Moberg. 2000. Coral reef disturbance and resilience in a human-dominated environment. *Trends Ecol Evol* **15**: 413-417.
- Reid, S. B., J. Hirota, R. E. Young, and L. E. Hallacher. 1991. Mesopelagic-boundary community in Hawaii: Micronekton at the interface between neritic and oceanic ecosystems. *Mar Biol* **109**: 427-440.
- Roder, C., L. Fillinger, C. Jantzen, G. M. Schmidt, S. Khokiattiwong, and C. Richter. 2010. Trophic response of corals to large amplitude internal waves. *Marine Ecology Progress Series* **412**: 113-128.
- Sander, F. 1981. A preliminary assessment of the main causative mechanisms of the “island mass” effect of Barbados. *Mar Biol* **64**: 199-205.
- Sander, F., and D. M. Steven. 1973. Organic productivity of inshore and offshore waters of Barbados: A study of the island mass effect. *B Mar Sci* **23**: 771-792.
- Schils, T., P. S. Vroom, and A. D. Tribollet. 2013. Geographical partitioning of marine macrophyte assemblages in the tropical Pacific: a result of local and regional diversity processes. *J Biogeogr* **40**: 1266-1277.
- Smith, J. E., C. M. Smith, P. S. Vroom, K. L. Beach, and S. Miller. 2004. Nutrient and growth dynamics of *Halimeda* tuna on Conch Reef, Florida Keys: Possible influence of internal tides on nutrient status and physiology. *Limnol Oceanogr*: 1923-1936.
- Vroom, P., C. Musburger, S. Cooper, J. Maragos, K. Page-Albins, and M. V. Timmers. 2010. Marine biological community baselines in unimpacted tropical ecosystems: spatial and temporal analysis of reefs at Howland and Baker Islands. *Biodivers Conserv* **19**: 797-812.
- Vroom, P. S., and C. L. Braun. 2010. Benthic Composition of a Healthy Subtropical Reef: Baseline Species-Level Cover, with an Emphasis on Algae, in the Northwestern Hawaiian Islands. *Plos One* **5**: e9733.
- Williams, G. J., J. E. Smith, E. J. Conklin, J. M. Gove, E. Sala, and S. A. Sandin. 2013. Benthic communities at two remote Pacific coral reefs: effects of reef habitat, depth, and wave energy gradients on spatial patterns. *PeerJ* **1**: e81.
- Williams, I. D. and others 2011. Differences in Reef Fish Assemblages between Populated and Remote Reefs Spanning Multiple Archipelagos Across the Central and Western Pacific. *Journal of Marine Biology* **2011**.
- Wolanski, E., and W. Hamner. 1988. Topographically Controlled Fronts in the Ocean and Their Biological Influence. *Science* **241**: 177-181.
- Wooldridge, S. A. 2009. Water quality and coral bleaching thresholds: Formalising the linkage for the inshore reefs of the Great Barrier Reef, Australia. *Mar Pollut Bull* **58**: 745-751.
- Zgliczynski, B. J., I. D. Williams, R. E. Schroeder, M. O. Nadon, B. L. Richards, and S. A. Sandin. 2013. The IUCN Red List of Threatened Species: an assessment of coral reef fishes in the US Pacific Islands. *Coral Reefs* **32**: 637-650.